Queen Mary
University of London

Pleiotropic Effects of Erythropoietin

Sharples, Edward John

For additional information about this publication click this link.
http://qmro.qmul.ac.uk/jspui/handle/123456789/2351

Information about this research object was correct at the time of download; we occasionally make corrections to records, please therefore check the published record when citing. For more information contact scholarlycommunications@qmul.ac.uk

Barts and The London
Queen Mary's School of Medicine and Dentistry

Pleiotropic Effects of Erythropoietin

A thesis submitted to the University of London for the degree of Doctor of Philosophy

by

Edward John Sharples

Supervisor: Professor M.M. Yaqoob

Centre for Experimental Medicine, Nephrology and Critical Care

St Bartholomew's and Royal London School of Medicine and Dentistry

Declaration

I confirm that the work presented in this thesis is solely the work of the author. Assistance with techniques including histopathology is fully acknowledged in the text.

Abstract

The haematopoietic growth factor Erythropoietin (EPO) is essential for the survival of erythroid progenitors to maturation and differentiation. It has been recognised that the EPO signalling pathway is also present in other tissues including the brain and vasculature, and is integral to the physiological response to ischaemia. Exogenous EPO was found to improve the outcome in animal models of stroke. The primary aim of this thesis was to examine whether erythropoietin was protective in a model of acute kidney injury, and to determine the mechanism by which EPO exerted this effect. In vitro experiments using HK-2 cells, a human tubular epithelial cell line, showed that EPO induced dose-dependent changes in cell number, and activated a number of intra-cellular signalling pathways. EPO reduced apoptotic cell death induced by nutrient starvation through the expression of anti-apoptotic proteins. A short-term model of ischaemia reperfusion was used to determine that EPO reduced the development of acute kidney injury, with a reduction in caspase activity and apoptosis. Longer models of ischaemia were then performed to confirm these findings, and showed that a pre-conditioning regime before the onset of the insult was also effective. In order to examine the mechanism of action, EPO was used in a model of cisplatin-induced kidney injury. EPO reduced apoptosis and caspase activation through the maintenance of mitochondrial membrane potential, inhibition of stress kinase signalling, and expression of XIAP and Bcl-X_L. EPO also reduced the induction of oxidative stress and PARP-1 activity. EPO was then given to animals exposed to cisplatin and confirmed the finding that pre-treatment with EPO significantly reduced cisplatin nephrotoxicity. Finally, EPO was used in a model of myocardial infarction and heart cells in culture to confirm that EPO plays a significant physiological role in cellular protection in multiple tissues.

Table of Contents

List of Figures and Tables

Chapter 1.

Chapter 2.

Chapter 3

Chapter 4

Chapter 5

Chapter 6

Abbreviations

[…]	concentration
Ab	antibody
AKI	acute kidney injury
BFU-E	burst forming unit – erythroid
BSA	bovine serum albumin
CAPS	N-cyclohexyl-3-aminopropanesulfonic acid
cDNA	complimentary DNA
CFU-E	colony forming unit – erthyroid
CKD	chronic kidney disease
DAPI	4', 6-diamidino-2-phenylindole
DEPC	diethyl pyrocarbonate
DNA	deoxyribonucleic acid
dNTP	deoxynucleotides (e.g.adenine, dATP)
EDTA	ethanolamine diamine tetra-acetic acid
EGTA	ethylene glycol tetra-actetic acid
EIA	enzyme immunoassay
ELISA	enzyme linked immunoabsorbant assay
ESRF	end stage renal failure
EPO	erythropoietin
EPO-R	erythropoietin receptor
FCS	foetal calf serum
Hb	haemoglobin
HRP	horse radish peroxidase
IL	interleukin
iv	intravenous
JAK	janus kinase

mRNA	messenger RNA
n	number of samples or replicates
NAD	nicotinamide adenine dinucleotide
NO	nitric oxide
NS	not significant
OD	optical density
P	probability
PAGE	polyacrylamide gel electrophoresis
PBS	phosphate buffered saline
PCR	polymerase chain reaction
PMSF	phenylmethylsulfonyl fluoride
RNA	ribonucleic acid
RT-PCR	reverse transcriptase PCR
sc	sub-cutaneous
SD	standard deviation
SDS	sodium dodecyl sulphate
TBS	tris-buffered saline
TBS-T	TBS containing 0.05% Tween 20
TEMED	*N*,*N*,*N*,*N*’ – tetrametylethylenediamine
TMB	3, 3’,5, 5’-tetramethylbenzidine
TNF	tumour necrosis factor
SE	standard error of the mean
SH2	Src- homology 2 domain
STAT	signal transducer and activator of transcription
UV	ultraviolet

List of Units

Da	Daltons	
kDa	kilodaltons	10^3 Daltons
g	gram	
kg	kilogram	10^3 gram
mg	milligram	10^{-3} gram
µg	microgram	10^{-6} gram
L	litre	
dL	decilitre	0.1 litre
mL	millilitre	10^{-3} litre
µL	microlitre	10^{-6} litre
M	molar	
mM	millimolar	10^{-3} molar
µM	micromolar	10^{-6} molar
nM	nanomolar	10^{-9} molar
min	minute	
U	units	
mU	milliunits	10^{-3} Units
w/v	weight per volume	
v/v	volume per volume	
%	percent	

Publications arising from the work

1: Sharples EJ, Patel N, Brown P, Stewart K, Mota-Philipe H, Sheaff M, Kieswich J, Allen D, Harwood S, Raftery M, Thiemermann C, Yaqoob MM. Erythropoietin protects the kidney against the injury and dysfunction caused by ischemia-reperfusion.
J Am Soc Nephrol. 2004 Aug; 15(8):2115-24.

2: Abdelrahman M, Sharples EJ, McDonald MC, Collin M, Patel NS, Yaqoob MM, Thiemermann C. Erythropoietin attenuates the tissue injury associated with hemorrhagic shock and myocardial ischemia.
Shock. 2004 Jul; 22(1):63-9.

3. NS Patel, **EJ Sharples**, S Cuzzocrea, PK Chatterjee, D Britti, MM Yaqoob and C Thiemermann. Pretreatment with EPO reduces the injury and dysfunction caused by ischemia/reperfusion in the mouse kidney in vivo.
Kidney Int 66: 983-989 (2004).

4. Sepodes B, Maio R, Pinto R, **Sharples EJ,** Oliveira P, McDonald M, Yaqoob M, Thiemermann C, Mota-Filipe H. Recombinant human erythropoietin protects the liver from hepatic ischemia-reperfusion injury in the rat.
Transpl Int. 19(11):919-926 (2006).

5**. EJ Sharples**, C Thiemermann, M Yaqoob. Mechanisms of disease: Cell death in acute renal failure, and the emerging evidence for a protective role of erythropoietin.
Nature Clin Pract Nephrol 1: 87-97 (2005)

6**. Sharples EJ**, Yaqoob M. Erythropoietin in experimental acute renal failure.

Nephron Experimental Nephrology 104(3):e83-88 (2006)

7**. Sharples EJ**, Thiemermann C, Yaqoob M. Novel applications of Erythropoietin**.**

Current Opinions in Pharmacology 6: 184-189 (2006)

8**. Sharples EJ**, Yaqoob MM. Erythropoietin and acute kidney injury.

Seminars in Nephrology 26; 325-331 (2006)

9. Walden AP, **Sharples E**, Young D. Bench to bedside: A role for erythropoietin in sepsis.

Crit Care 14: 220-222 (2010)

Acknowledgements

The studies which comprise this thesis would not have been possible without the support and encouragement of my supervisor, Professor Magdi Yaqoob. I am thankful for the opportunity to work with him and his invaluable guidance over the last four years in research and in my clinical career progression. He remains an inspiration as a clinician-scientist. This work would not have been possible without the financial support from Kidney Research-UK through a clinical training fellowship.

I owe thanks to the staff at the Biological Services Unit and Professor Thiemermann's laboratory, particularly Nimesh Patel, for their considerable efforts in teaching and assisting me with the animal experiments. I would also like to thank the many people who have given their time and expertise to teach and assist me in learning the laboratory techniques described in this thesis. Particular thanks go to David Allen and Steve Harwood for unstinting advice, help, and a bountiful supply of biscuits and tea.

Finally, the time and commitment to this work has only been possible due to the forgiving and caring support from my lovely wife, Caroline, and my family.

Chapter One: General Introduction

1.1 Acute Kidney Injury

Acute kidney injury (AKI), also known as acute renal failure, is a clinical syndrome characterised by the rapid deterioration of kidney function over a period of hours or days, resulting in the failure of the kidney to excrete nitrogenous waste products, and to maintain fluid and electrolyte homeostasis. AKI can result from multiple types of insult, including decreased renal perfusion without cellular injury; an ischaemic, toxic, or obstructive insult to the renal tubular epithelium; a tubulo-interstitial process with inflammation; or a primary reduction in the filtering capacity of the glomerulus [Lameire N, 2005].

1.1.1 Epidemiology of AKI

The incidence of AKI varies greatly depending on the clinical setting, the demographics of the patient population, and, in particular, the definition of renal insufficiency utilised. It is difficult to directly compare the many studies of the epidemiology and management of AKI due to the wide variation in definition used. This weakness has recently been addressed with the universal adoption of the term acute kidney injury (AKI) in preference to acute renal failure or acute tubular necrosis (ATN), indicating that kidney damage may occur in the absence of complete loss of function, and with the consensus development of the RIFLE classification (Risk, Injury and Failure) based on the degree of change in biochemical parameters, observed urine output, and two clinical outcome scores (Loss, End-stage), through the work of the Acute Kidney Injury Network [Kellum JA, 2002].

Hou *et al* demonstrated an overall incidence of AKI of 5 % in a hospitalised population (109 of 2216 medical and surgical patients) using an increase in serum creatinine of > 44 μmol/L (0.5 mg/dl) above the measured baseline as the definition of AKI. AKI was associated with decreased renal perfusion (42 %) or major surgery (18 %) in the majority of cases. Predictors

of poor prognosis included a reduced urine output (<400 mL/ 24 hr) and relatively modest elevation in serum creatinine concentration [Hou SH, 1983]. In the late 1990s an updated study, using identical diagnostic criteria, observed that the frequency of hospital acquired AKI had increased to 7.2 % [Nash K, 2002]. In comparison, community acquired AKI present at the time of admission to hospital was identified in only 0.9 % of patients [Kaufman J, 1991].

In the modern era, the use of more stringent RIFLE classification has reduced the observed incidence of AKI. Liangos *et al* analysed data from the National Hospital Discharge survey, a nationally collected sample of approximately 330,000 inpatient admissions from 500 hospitals in the USA, and demonstrated a 1.9 % incidence of AKI in hospitalized patients. Patients with AKI were more likely to have the sepsis syndrome or other non-renal acute organ system dysfunction [Liangos O, 2006].

Sustained impairment of renal perfusion is the most common factor that predisposes patients to ischaemia-induced tubular injury, and is implicated in approximately 70 % of community acquired AKI, and 40 % of hospital-related events [Mehta RL, 2004]. Hospital acquired cases are more often multi-factorial, with an accumulation of multiple acute insults, including exposure to nephrotoxic agents such as radio-contrast agents, treatment with non-steroidal anti-inflammatory drugs (NSAIDs), and infection, often in the presence of cardiac dysfunction and reduced tissue perfusion. Mortality rates in AKI range from 7 % among patients admitted to a hospital with hypotension-related AKI, to more than 80 % in patients with post-surgical AKI [Nash K, 2002; Thakker CV, 2003].

The severity of kidney injury may determine the natural history and patient outcome in AKI. Few epidemiology studies have examined the association between small changes in serum creatinine and patient outcome. These population studies can only show an association

between AKI and mortality, especially in intensive therapy unit-based studies, because it is often part of the spectrum of multi-organ failure. However, published studies have demonstrated a consistently elevated relative risk associated with AKI despite adjustment for co-morbid conditions and severity of illness. Levy *et al.* compared 183 patients with radiocontrast-associated AKI and 174 age-matched patients who received similar radiocontrast loads without developing AKI. The mortality rate was 34% in patients with AKI *versus* 7% in those patients without AKI. Adjusting for differences in co-morbidity, the odds of death were increased 5.5-fold in the AKI group [Levy EM, 1996]. This increased relative risk of death was confirmed in a more heterogeneous cohort of patients, which may be a truer representation of the general population, from a study of 19201 admissions to a large urban hospital. This demonstrated that even a 50 % increase in serum creatinine above baseline was associated with an increased mortality adjusted odds ratio of 5.8 (4.6-7.5), with similar increases (odds ratio 4.1 (3.1-5.5) in mortality observed with only a 28 μmol/L (0.3 mg/dl) increase in serum creatinine [Chertow GM, 2005].

This increase in mortality associated with even quite small changes in renal function may directly be related to the distant effects of renal ischaemia on other organ systems. Models of AKI have shown induction of a more general systemic inflammatory response, with apoptotic cell death in the myocardium and changes in cardiac function [Grigiryev DN, 2008], vascular dysfunction [Kelly KJ, 2003], and neutrophil aggregation in the lungs with associated inflammation [Awad AS, 2009]. The observed increase in mortality may, however, be indirectly related to AKI, however, as the risk factors for AKI are also risk factors for cardiovascular disease and mortality, and AKI occurs much more commonly in those with higher co-morbidity, including pre-existing renal impairment. Patients with relatively early stage CKD (eGFR 30-45 mL/min) have a 5-fold increased odds ratio of AKI when compared to matched controls [Hsu Y, 2008].

1.2 The Pathophysiology of Ischaemic AKI

In health, the kidneys receive 25% of cardiac output, but renal blood flow is not uniformly distributed within the renal parenchyma, so that tissue perfusion and oxygen consumption are highly heterogeneous - resulting in areas susceptible to reduced oxygen tension [O'Connor PM, 2006]. Tissue oxygen tension varies between 60 -100 mm Hg (6.6 – 13.3 kPa), obtained close to the cortical surface in micro-puncture studies, and 10-20 mm Hg (1.3-2.9 kPa) in the S3 segment of the proximal tubule [Welsh WJ, 2001]. The anatomical arrangement of pre-glomerular arterial and corresponding post-capillary venous vessels suggests a structural basis for this low medullary oxygen tension. This is confirmed by studies demonstrating the large anaerobic capacity of the outer-medullary region, chronic up-regulation of hypoxia-induced gene expression, and an increased susceptibility to hypoxic insult [Brezis M, 1989].

The kidney responds to alterations in renal perfusion pressure by a feedback loop to auto-regulate pre-glomerular blood flow and hence maintain glomerular filtration rate (GFR) within fairly narrow limits, even with mean arterial pressure as low as 80 mm Hg [Dworkin LD, 2003]. When the blood pressure falls, gradual dilatation of the pre-glomerular arterioles occurs, mediated by the angiotensin stimulated generation of vasodilating products of arachidonic acid (prostaglandin I_2) and nitric oxide [Baylis C, 1978]. As perfusion pressure falls further, concomitant vasoconstriction of the postglomerular arterioles, mainly under the influence of angiotensin II, maintains a constant glomerular capillary hydrostatic pressure. The postglomerular capillary bed, which perfuses the tubules, has diminished blood flow and pressure, but the tubules remain intact. Drugs which act on the prostaglandin system, such as non-steroidal anti-inflammatory drugs, or inhibit the angiotensin pathway, can interfere with the normal autoregulatory responses and increase the risk of impaired perfusion pressure and subsequent AKI [Abuelo JG, 2007].

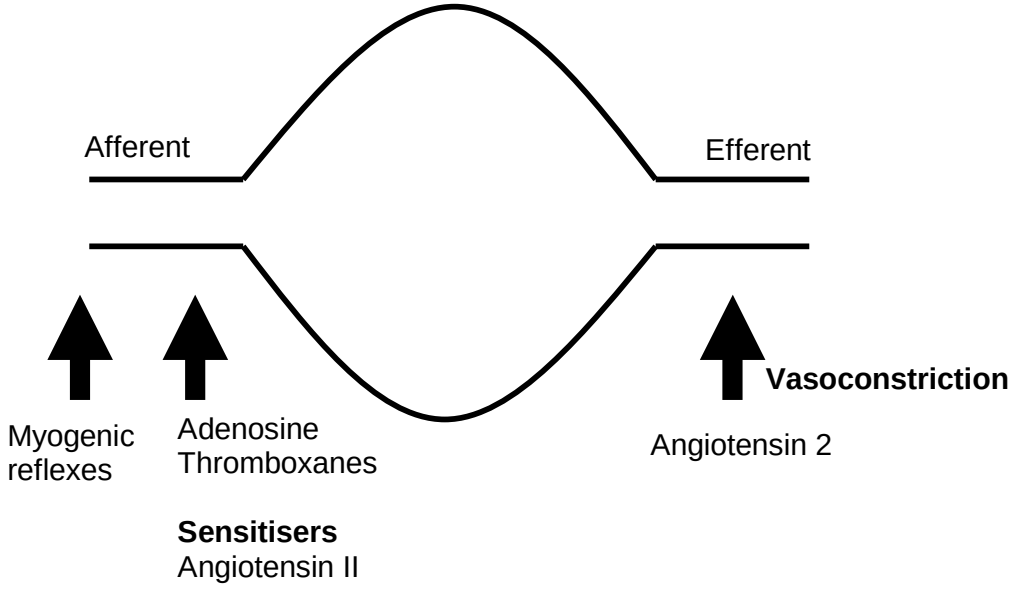

Figure 1.1 Perfusion Pressure and mechanisms to maintain GFR

Several pathways interact to maintain the relationship between systemic blood pressure and renal perfusion. Vasoconstriction of the efferent arteriole increases transglomerular resistance and hence GFR, but contributes to tubular hypo-perfusion.

Prolonged ischaemic insults, alone or in synergistic combination with nephrotoxins, overcome the autoregulatory systems in the kidney, and initiate epithelial and vascular cell injury, resulting in an extremely rapid decrease in glomerular filtration rate (GFR), appropriately referred to as the *initiation phase* of AKI [Sutton TA, 2002].

The initiation phase is immediately followed by the *extension phase* [Sutton TA, 2002], in which multiple interrelated events dependent on altered vascular function lead to worsening of epithelial and endothelial cell injury and subsequent cell death, primarily in the cortico-medullary region of the kidney. Established ischaemic AKI is associated with a reduction in renal perfusion by 30-50%, and there is evidence of selective reduction in blood supply to the outer medulla [Yamamoto T, 2002].

The *maintenance phase* represents a phase of stabilization of injury, and subsequent correcting events leading to cellular repair, division, and re-differentiation. This sets the stage for improved epithelial and endothelial cell function and recovery of GFR during the *recovery phase*. Correction of the initiating insult with appropriate therapy during the early initiation and extension phases of AKI may limit the degree of cellular injury and hence the duration of the maintenance phase, allowing more rapid onset of the recovery phase and hence preservation of kidney function.

1.2.1 Vascular dysfunction

Under physiological conditions, the oxygen tension of the kidney decreases from the outer cortex to the inner medulla [Brezis M, 1995]. After an ischaemic insult, total renal blood flow returns to normal, but marked, regional alterations occur, playing an important role in the extension phase of renal ischaemic injury [Yamamoto T, 2002]. Blood flow to the outer

medullary or cortico-medullary junction regions remains approximately 10 % of normal during early reperfusion, leading to congestion due to interstitial oedema, red blood cell trapping, leukocyte adherence and extravasation.

Several lines of evidence indicate that endothelial dysfunction is a feature of the initiation phase of ischaemic renal injury. Firstly, ischaemia results in profound loss of the vasorelaxing effect of acetylcholine [Lieberthal W, 1989]. Vasorelaxation in response to stimuli generating endothelium-derived relaxing factor was also inhibited [Conger JD, 1995]. In addition, nitric oxide production in response to bradykinin was found to be suppressed in ischaemic kidneys [Noiri E, 1996]. Loss of normal endothelial function and altered NO homeostasis alters vascular homeostasis, leading to an increased thrombotic potential and reduced response to local and systemically derived vaso-active substances.

Intra-vital video-microscopy has proved useful for the study of blood flow in peri-tubular capillaries [Yamamoto T, 2002]. Reperfusion initiates an immediate partial recovery of blood flow after release of renal artery occlusion, followed by a profound and sustained flow reduction. There is evidence of retrograde flow in some vessels, and temporary loss of vessel patency. The pattern of glomerular microcirculation is similar to that of the peri-tubular capillaries; initial brief recovery of flow is followed by ‘no flow’. Restoration of flow in these capillary beds, however, is different. Glomerular circulation is re-established initially, while return of blood flow to peri-tubular capillaries is significantly delayed. So, endothelial injury and dysfunction have major roles in the ‘no-flow–reflow’ phenomenon in the early stages of ischaemic injury. This injury manifests structurally as loss of endothelial integrity, and functionally as defective endothelium-dependent vasorelaxation.

Inflammatory activation of the endothelial cell with upregulation of adhesion molecules, as well as injury to the endothelial cells leading to cell swelling and loss of patency of the

endothelial barrier, potentiates the interaction with leukocytes and platelets causing mechanical obstruction to the small vessels [Bonventre J, 2003]. Leukocytes are activated by a number of local factors, including cytokines, chemokines, eicosanoids and reactive oxygen species, which result in further upregulation of adhesion molecules, leukocyte recruitment and inflammation [Suwa T, 2001]. Leukocyte trafficking and the differential role of lymphocytes and mono-nuclear cells in the generation of reperfusion injury remains a controversial subject [De Greef KE, 1998; Park P, 2002]. Recent studies have suggested an important role of T-lymphocytes in the development of reperfusion injury, and in particular, the systemic inflammatory response [Ascon DB, 2006; Grigoryev DN, 2008].

The reduced perfusion and hypoxic conditions lead to deprivation of nutrients and loss of ATP in the endothelium. Injection of cultured endothelial cells that constitutively express high levels of endothelial nitric oxide synthase (eNOS) into rats subjected to renal ischaemia resulted in implantation of these cells into the vasculature and reduction in ischaemic kidney injury, highlighting the important role of endothelial cells and the vasculature in the protection from renal ischaemic injury [Brodsky SV, 2002]. Permanent damage to the peritubular capillaries occurs in rats subjected to prolonged renal ischaemia, and this may be associated with the development of tubulo-interstitial fibrosis, poor urine concentrating ability, and impaired recovery in the post-ischaemic kidney [Basile DP, 2001].

1.2.2 Tubular changes

In the commonly studied vascular clamp small animal models of renal artery occlusion, the S3 segment of the proximal tubule that traverses the outer-medullary region is extremely susceptible to ischaemic injury when compared to S1 and S2 segments or distal tubule [Ventatachalam M, 1978]. The sensitivity of the outer medulla derives from a combination

of its microvascular architecture, and a relatively low glycolytic capacity to generate ATP in the setting of rapid ATP depletion resulting from impaired oxidative phosphorylation. The medullary thick ascending limb of the loop of Henle, although situated in the same region, does not undergo the same extent of cell death because there is a greater glycolytic capacity to generate ATP under ischaemic conditions [Bonventre JV, 2002].

During the maintenance phase of AKI, large areas of severe local ischaemia may no longer be present, but cell injury continues due to surrounding acute inflammation and the effects of prior insults on intrinsic cellular responses such as apoptosis. The tubular cell is also a major contributor to the local inflammatory response. Tubular epithelial cells produce a number of pro-inflammatory cytokines, including TNF α and interleukin-6, chemotactic cytokines such as RANTES and monocyte chemoattractant protein (MCP-1) in response to an ischaemic insult [Rice J, 2002]. Tubular epithelial cells also contribute to leukocyte migration through the local production of the CX3-family chemokine fractalkine (CX3CL1) [Chakravorty SJ, 2002].

The structural response to the tubular epithelium to ischaemic injury is multifaceted, and includes loss of cell polarity and brush border, cell death, de-differentiation of surviving cells, proliferation and restitution of a normal epithelium. Cellular ATP depletion leads to a rapid disruption of the apical actin cytoskeleton and redistribution from the apical domain and microvilli into the cytoplasm [Molitoris B, 1992]. The ensuing alterations in microvillar structure leads to formation of membrane-bound, free floating extracellular vesicles, or “blebs,” that are either internalised or lost into the tubular lumen. Brush border membrane components that are released into the lumen contribute to the formation of casts and tubular obstruction. These casts and vesicles that contain actin and actin depolymerising factor have been detected in the urine in animal and human acute renal failure. Disruption of the actin cytoskeleton also results in the loss of tight junctions and adherens junctions. Reduced

expression, re-distribution and abnormal aggregation of a number of key proteins that constitute these junctions have been documented after ischaemic injury, and this loss of tight junction may magnify the transtubular backleak of glomerular filtrate that is induced by tubular obstruction.

Ischaemia results in the early disruption of two basolateral polarised proteins, Na, K ATPase and adhesion molecule family of β1-integrins. The Na, K, ATPase is normally tethered to the spectrin-based basolateral cytoskeleton at the basolateral domain via the adapter protein ankyrin. The mislocated Na, K, ATPase remains bound to ankyrin but is devoid of spectrin, possibly due to either phosphorylation of spectrin or cleavage of spectrin by proteases such as calpain [Woroniecki, 2003]. The β1 integrins are normally polarised to the basal domain, where they mediate cell-substrate adhesions. Ischaemic injury leads to a redistribution of integrins to the apical membrane, with consequent detachment of viable cells from the basement membrane. There is good evidence for abnormal adhesion between these exfoliated cells within the tubular lumen, mediated by an interaction between apical integrin and the Arg-Gly-Asp (RGD) motif of integrin receptors. Administration of synthetic RGD compounds attenuates tubular obstruction and renal impairment in an animal model of renal ischaemia [Molina A, 2005].

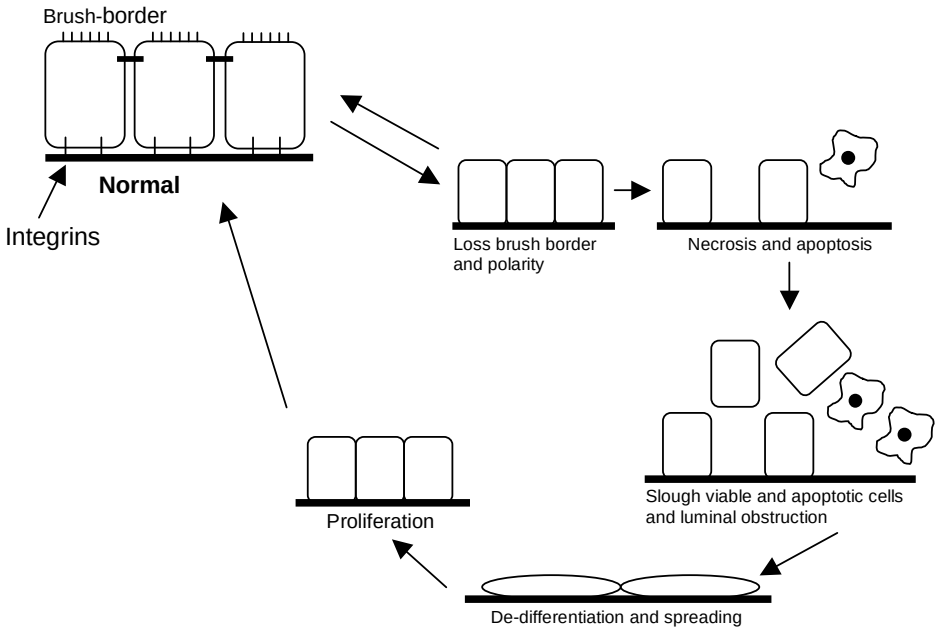

Figure 1.2 Alterations in tubular cell structure after ischaemic acute renal failure.

The initiation phase leads to sub-lethal injury, with loss of brush border and disruption of cell polarity and the cytoskeleton. If the injury is alleviated at this stage, then complete recovery ensues. If not, cell death, desquamation, luminal obstruction and an inflammatory response occurs.

1.3 Cellular Mechanisms of Tubular cellular injury following ischaemia-reperfusion

1.3.1 ATP and GTP depletion

In the absence of normal mitochondrial oxidative phosphorylation, prolonged ischaemia leads to a rapid decrease in the level of available adenine nucleotide pool (ATP, ADP and AMP). Dephosphorylation of ATP and ADP lead to further catabolism of AMP to hypoxanthine and xanthine, which contribute to the generation of reactive oxygen species. Functional recovery in rabbits after ischaemic injury was correlated to the degree of ATP depletion and xanthine accumulation [Buhl MR, 1979]. Zager *et al* demonstrated regional differences in ATP depletion after 15 minutes of ischaemia, with the outer medulla most affected, but after 45 minutes these regional differences were no longer significant due to global reduction [Zager RA, 1990]. *In vitro* studies of chemical induced ATP depletion, using inhibitors of mitochondrial oxidative phosphorylation pathway such as antimycin A, have demonstrated an association between ATP depletion and activation of pro-inflammatory and cell death pathways, including Fas and Fas ligand up-regulation and caspase-8 activation [Feldenberg, 1999]. Partial ATP depletion leads to apoptotic cell death whereas more severe or total ATP depletion causes necrosis [Leiberthal W, 1998].

GTP depletion also occurs in association with ATP depletion in both *in vitro* and *in vivo* models of ischaemic injury [Daugher P, 2000]. Preferential depletion of GTP with maintained ATP induces apoptosis in cultured renal tubular cells. Administration of guanosine before the inducement of ischaemic renal injury maintains GTP regenerative capacity, leading to a significant reduction in the number of apoptotic tubular cells, and hence improved renal function [Kelly KJ, 2001]. GTP depletion may induce apoptosis via the activation of p53, and there is *in vivo* evidence that inhibition of p53 pathway also

protects the kidney from ischaemia reperfusion injury [Kelly KJ, 2003; reviewed by Dagher PC, 2004].

1.3.2 Increased cytosolic Ca^{2+} concentrations

Renal proximal tubular cells undergo a significant increase in free cytosolic ionised calcium concentration during the initial five minutes of hypoxia. The increase in Ca^{2+} precedes hypoxic membrane damage, and is reversible if re-oxygenation occurred before the cell underwent lethal injury [Wetzels JF, 1993]. ATP depletion leads to impaired calcium sequestration in the endoplasmic reticulum, as well as diminished extrusion into the extracellular space [Edelstein CL, 1997]. Increased cytosolic Ca^{2+} leads to uptake of Ca^{2+} into the mitochondria via the Ca^{2+} uniporter. In the presence of ATP depletion, mitochondrial Ca^{2+} overload leads to opening of mitochondrial permeability transition pore (mPTP) and permeabilization of the inner mitochondrial membrane, and the release of pro-apoptotic mitochondrial proteins, including cytochrome c.

Prolonged increases in cytosolic Ca^{2+} activate the Ca^{2+}-dependent cysteine protease calpain. Calpain activity is tightly regulated by its ubiquitously expressed endogenous inhibitor calpastatin. Calpains result in the proteolysis of a broad spectrum of cellular proteins and a distinguishing feature of their activity is their ability to confer limited cleavage of protein substrates into stable fragments rather than complete proteolytic digestion. Thus, calpain-mediated proteolysis represents a major pathway of post-translational modification that influences various aspects of cell physiology, including apoptosis, cell migration and cell proliferation [Sato M, 2001].

Renal proximal tubule epithelial cells constitutively express calpains, which are activated in response to toxic and hypoxic injuries. Inhibition of calpain activity using various

pharmacological inhibitors ameliorated necrotic cell death in proximal tubule cells subjected to hypoxic injury [Harriman JF, 2000], ATP depletion [Liu X, 2001] and reduced tubular dysfunction in rats subjected to ischaemia reperfusion injury [Chatterjee PK, 2001].

1.3.3 Poly (ADP-ribose) polymerase-1 (PARP-1)

PARP-1 plays a primary role in the process of poly (ADP)-ribosylation, in which posttranslational modification of nuclear proteins is activated in response to DNA damage. Activation of PARP-1 by DNA strand breaks results in the synthesis of poly (ADP-ribose) at the expense of NAD^+ that is cleaved into ADP-ribose and nicotinamide. PARP-1 catalyzes the binding of the first ADP-ribose on acceptor proteins, primarily at glutamic residues, and subsequently catalyzes the elongation and branching reactions with additional ADP-ribose units. Decreased NAD^+ levels cause an unbalanced NAD/NADH ratio, which, in turn, affects the activation of enzymes involved in glycolysis, the pentose shunt, and the Krebs cycle. Decreased NAD^+ levels also drastically alter the redox state of cells. Because the cell attempts to restore NAD^+ pools by recycling nicotinamide with 2 ATP molecules, excessive activation of PARP-1 depletes pools of intracellular NAD^+ and ATP and, consequently, interferes with most, if not all, energy-dependent cellular processes [De Murcia J, 1997].

The switch between necrosis and apoptotic cell death may also be modulated by the degree of activation of PARP-1 since this decision seems to be determined by the cellular ATP levels. PARP-1 overactivation and poly(ADP-ribose) synthesis result in the heavy use of NAD^+ and a reduced activity of NAD^+-dependent cellular processes, including ATP synthesis. Moreover, because NAD^+ re-synthesis is done at the expense of ATP, the resulting ATP depletion is believed to induce cell death by necrosis. In apoptosis, PARP-1 is cleaved into two fragments of 89 kDa and 24 kDa (p89 and p24) by caspases-3 and -7 at the

DEVD site located in the NLS of PARP-1. The p89 fragment contains the catalytic site and the auto-modification domain, and p24 contains the DBD and zinc finger domains. The motive for PARP-1 cleavage is not yet defined, but it seems to be a key event in the execution phase of apoptosis, possibly by allowing preservation of the cellular ATP required to accomplish apoptosis, because this process is energy dependent, and therefore allows completion of apoptosis rather than necrosis.

In the kidney, PARP-1 activity contributes to ischaemia reperfusion injury in transplanted kidneys [O'Valle F, 2005], and inhibition of PARP-1 has been shown to reduce tubular cell death *in vitro* [Chatterjee PK, 1999], and in animal models of haemorrhagic shock [McDonald MC, 1999] and acute renal ischaemia [Chatterjee PK, 2000].

1.3.4 Oxidant Injury

There is now substantial evidence for the role of reactive oxygen species in the pathogenesis of AKI. During reperfusion, the conversion of accumulated hypoxanthine to xanthine, catalysed by xanthine oxidase, generates hydrogen peroxide and superoxide. In the presence of iron, hydrogen peroxide forms the highly reactive hydroxyl radical. Concomittantly, ischaemia induces nitric oxide synthase (iNOS) in tubular cells, and the NO that is generated interacts with superoxide to form peroxynitrite, which contributes to cellular injury via oxygen toxicity and nitrosative stress [Devarajan P, 2005]. Collectively, reactive oxygen species cause renal tubular epithelial cell death by oxidation of proteins, peroxidation of lipids, damage to DNA and induction of apoptosis via redox activation of the transcription factor NF-κB and the mitogen-activated stress kinase family [Finkel T, 1998].

In vitro studies have confirmed that reactive oxygen species are important mediators of necrotic cell death following ischaemic and toxic injury to tubular epithelial cells [Beckman JS, 1996]. Mitochondrial injury leads to uncoupling of oxidative phosphorylation which has two sequelae: impaired ATP production and increased superoxide generation. Lipid peroxidation of the membrane phospholipid bilayers and subcellular organelles is a major contributor to necrotic cell death. Several scavengers of reactive oxygen species, including superoxide dismutase, catalase, N-acetylcysteine) have been effective in animal models of ischaemic injury [Chatterjee PK, 2004], but human studies have failed to show similar benefit [Macedo E, 2006].

1.4 Alterations in Cell Viability and Mechanisms of cell death

Both experimental and human studies indicate that tubular epithelial cells can suffer one of three distinct fates after ischaemia. The majority of cells remain viable, suggesting that they escape injury, or are only sub-lethally injured and can undergo recovery. The remaining tubular epithelial cells display patchy, non-continuous areas of cell death that results from at least two pathological mechanisms – necrosis and apoptosis. These two forms of cell death co-exist, and the mode of individual cell death depends primarily on the severity of the insult and the resistance of the cell type.

Necrotic cell death is characterised by progressive loss of cytoplasmic membrane integrity, rapid influx of sodium and calcium ions and water, resulting in nuclear degeneration and cytoplasmic swelling. The latter feature leads to cellular fragmentation and release of lysosomal and granular contents into the extracellular space, with subsequent development of acute inflammation.

A distinction between these changes of necrotic cell death and the morphology of cells undergoing controlled non-inflammatory cell death was observed more than 50 years ago. The term apoptosis was applied to the characteristic morphological changes associated with programmed cell death [Kerr JF, 1972]. It is defined by cytoplasmic and nuclear shrinkage, chromatin margination and fragmentation, and division of the cell into multiple spherical bodies that retain membrane integrity. These apoptotic bodies are rapidly phagocytosed and degraded by macrophages and by surrounding epithelial cells [Lieberthal W, 1996]. Phagocytosis provides an efficient mechanism for the removal of dead cells without incurring any of the surrounding tissue inflammation and injury associated with necrotic cell death [Kerr JF, 1972] although in some circumstances apoptotic cells may undergo a process of secondary necrosis.

Recently, a third process resulting in cell death has also been described, and is termed autophagy [Tsujimoto Y, 2005]. Autophagy plays a role in normal tissue homeostasis and growth, but is also activated in certain circumstances, such as nutrient starvation, hypoxia and high temperatures. The cells undergo partial autodigestion that prolongs survival for a short time, but if these adverse conditions persist, the cell dies [Ohsumi Y, 2001]. Autophagosomes are double-membrane cyctoplasmic vesicles that are designed to engulf various cellular constituents, including cytoplasmic organelles. These fuse with lysosomes to become autolysosomes, where sequestered cellular components are digested. Autophagy is now recognized to play an important role in ischaemia reperfusion injury in the kidney and heart [Suzuki C, 2008; Matsui Y, 2008]

1.4.1 Apoptotic cell death in Acute Kidney Injury

There is now increasing evidence indicating that apoptosis is a major mechanism of early tubular cell death in ischaemic AKI. Several animal models have demonstrated the presence of apoptotic tubular cells [Schumer M, 1992], and this was subsequently confirmed in human studies in kidney transplantation [Oberbauer R, 1999; Castaneda MP, 2003]. Nevertheless, the mechanistic role of apoptosis in the degree of renal dysfunction observed is not fully understood.

First, most estimates place the peak incidence of apoptosis at only approximately 3-5% of tubular cells after ischaemic injury, which arguably is insufficient to explain the degree of renal insufficiency. It is likely, however, that the degree of apoptotic cell death is underestimated, because it is a rapidly occurring event that is heterogenous in distribution, and both tissue preparation and techniques to demonstrate apoptosis have limited specificity. The terminal deoxynucleotidyl transferase (TdT)-mediated dUTP-biotin nick end labeling (TUNEL) assay, which adds labelled dUTP to multiple free DNA ends generated by activated endonucleases during cell death, has been widely used to determine the extent and localisation of apoptotic cell death, but can be criticized for its lack of sensitivity and specificity in discriminating among apoptotic and necrotic mechanisms of cell death [Kelly KJ, 2003].

Secondly, apoptosis is commonly encountered in the distal tubule, whereas loss of viable cells occurs in the proximal tubule. Distal tubular cells are more resistant to cell death, with some evidence that this resistance may be determined by persistent Akt phosphorylation and activation, possibly as a protective mechanism against the osmotic and hypoxic environment, and apoptosis may appear to be the dominant cause of cell death as necrosis is therefore prevented [Kroning R, 1999].

Thirdly, apoptosis is crucial to the physiological repair processes that remove damaged cells after injury, and therefore may be beneficial to the organ and the organism. This can be reconciled by the observation that apoptosis occurs in two-waves in animal models. The first wave is detectable by six hours, peaks at 24-36 hrs and rapidly diminishes. The second wave becomes apparent after 4 days, removing hyperplastic and unwanted cells, and is likely to play a role in the remodelling of the regenerating tubule.

1.4.2 The Caspase cascade

Apoptosis is characterised by the activation of a family of cysteine proteases called caspases, which participate in enzymatic cascades that terminate in cellular disassembly. This action can be initiated through mitochondrial-dependent and -independent pathways.

The genetic analyses of apoptosis in the nematode flatworm *Caenorhabditis elegans* led to the elucidation of genes that control this cellular suicide mechanism [Driscoll M, 1992]. The central components of apoptosis machinery in *C. elegans* are a troika of ced genes: *ced-3*, *ced-4* and *ced-9*, where *ced-3* protein is a cysteine protease responsible for the execution of the apoptotic program, *ced-4* protein is a pro-apoptotic adaptor molecule, and *ced-9* protein is an inhibitor of apoptosis [Hengartner 1992; Miura M, 1993]. Homologues of these genes have been clearly shown to regulate apoptosis in higher eukaryotes, albeit utilizing much more evolved and complex mechanisms. The mammalian homologues of the inhibitor of apoptosis *ced-9*, the B cell lymphoma-2 (Bcl-2) family members, are critical regulators of the mitochondrial step in apoptosis [Gross A, 1999].

All caspases are synthesized as inactive zymogens containing an N-terminal prodomain followed by a large 20 kDa subunit, p20, and a small 10 kDa subunit, p10. Depending on the

structure of the pro-domain and their function, caspases are typically divided into three major groups. The caspases with large prodomains are referred to as inflammatory caspases (group 1: caspase-1, -4,-5, -11, -12, -13, -14), initiator caspases (Group 2: caspases-2, -8, -9, -10), while caspases with a short prodomain of 20-30 amino acids are named effector caspases (Group 3: caspase-3, -6, -7). Cleavage of a procaspase at the specific Asp-X bonds results in the formation of the mature caspase, which comprises the heterotetramer p202-p102 and causes release of the prodomain. Each heterodimer is formed by hydrophobic interactions resulting in the formation of parallel β-sheets, composed of 6 anti-parallel β-strands [Stennicke HR, 1999].

All caspases share a number of distinct features. These include the catalytic triad residues, consisting of the active site Cys_{285}, which is a part of the conserved QACXG pentapeptide sequence, His_{237} and the backbone carbonyl of residue -177 [Stennicke HR, 1999]. The striking feature of the caspases is their specificity for substrate cleavage after an asparate residue, which is unique among mammalian proteases, except for the serine protease granzyme B.

The initiator caspases form active catalytic dimers via association of their long prodomains with adapter molecules with selectivity for individual caspases. In contrast, executioner caspases become catalytically active only after cleavage by the active initiator caspases. Once activated, executioner caspases can cleave initiator caspases, which may not lead to their activation, but may serve to stabilize active initiator caspase dimers, or render them subject to regulation via cellular inhibitors of apoptosis. This hieracrchy of caspase activation generates a cascade culminating in executioner mediated cleavage of multiple substrates including PARP-1, cytoskeleton proteins such as fodrin, actin and focal adhesion kinase, an array of phenotypic characteristics including cell blebbing, condensation and

fragmentation of chromatin, and re-distribution of lipids in the outer plasma membrane, ending in controlled cell death [Lavrik IN, 2005].

1.4.3 Caspase Activation in AKI

Several studies have documented activation of caspase molecules after ischaemia reperfusion in the kidney and post-hypoxic injury in renal proximal tubule epithelium. The expression of caspases-1, -2, -3, -6, -7, -8, and -9 has been characterized in rat kidneys at the mRNA level [Kaushal GP, 1998; Singh AB, 2002]. The expression and activity of caspases-1, -2, and -6 are altered in kidneys post-I/R. LLC-PK_1 and Madin-Darby canine kidney (MDCK) cells subjected to chemical hypoxia underwent apoptosis with a marked increase in activation of caspases-3 and -8. The activation of caspase-3 is accompanied by Bax translocation from cytosol to mitochondria and cytochrome *c* release from mitochondria.

Inhibition of caspases using a pancaspase inhibitor is shown to protect kidneys from ischaemic injury. The pancaspase inhibitor Z-Val-Ala-Asp(OMe)-CH2F protected against ischaemic AKI in mice by inhibition of apoptosis and subsequent inflammation [Daemen M, 2001]. Inhibitors of specific caspases have also been demonstrated to alter the natural history of renal injury in a short-term model of I/R in the rat, although there is controversy over exact specificities [Chatterjee PK, 2005]. The results from these studies clearly demonstrate a role for caspases in I/R. However, the role of individual caspases contributing to the injury and inflammation post-renal injury cannot be discriminated from these studies because non-specific caspase inhibitors were utilized. The availability of more specific inhibitors of individual caspases will provide better clues as to the functions of individual caspases in renal I/R. RNA interference techniques have also been used to inhibit the expression and activity of specific caspases during ischaemia reperfusion injury in a murine model. RNA interference inhibition of caspase-3 and caspase-8 has been shown to reduce both

histological and biochemical markers of ischaemic injury, and significantly improved rates of animal survival [Zhang X, 2006].

Caspase-1 does not appear to play a direct role in the induction of apoptosis, but rather, is integral to the development of the acute inflammatory response and removal of pathogens [Scott AM, 2007]. The role of caspase-1 in ischaemia reperfusion injury has not been determined, as induction of injury in mice deficient for caspase-1 has furnished contrasting results. Results from one study indicated that caspase-deficient mice underwent less severe injury than their wild-type counterparts and that this was due to impaired interleukin-18 activation [Melnikov V, 2001], whereas a second group found no changes in the severity of the injury between control groups and caspase-1-deficient mice [Daemen MA, 2001].

1.4.4 Mechanism of Caspase activation: Extrinsic Pathway

Apoptosis can be initiated through several separate but interacting pathways. Extracellular signals are transmitted to the cell via the TNF superfamily of death receptors, the members of which are characterised by a conserved extracellular cysteine-rich motif, and include Fas, TNFR1, TNF-related apoptosis-inducing ligand (TRAIL). These receptors, generally composed of 3 identical polypeptide chains, have binding and signalling features in common as well as unique, individual characteristics. These death receptors have an intracellular death domain (DD) that activates cytosolic cysteine proteases by proteolysis, recruiting adapter proteins that also have death domains, including FADD and TRADD. The death effector domain of FADD binds to the prodomain of caspase-8, forming a complex termed the death-inducing signalling complex (DISC). The auto-catalytic activation of caspase-8 then activates a series of downstream caspases that result in cleavage of structural and regulatory intracellular proteins [Jin Z, 2005]. C-FLIP is a naturally occurring dominant negative antagonist of death receptor mediated caspase-8 activation, and contains two DED

and a defective caspase-like domain. C-FLIP can associate with DEDs of FADD and caspase-8, interfering with the recruitment of caspase-8.

The extrinsic pathway is activated by ischaemia reperfusion injury in the kidney. Mice treated with siRNA knockdown of caspase 8 expression were protected from ischaemic injury and had improved survival when compared to untreated animals [Zhang X, 2006].

1.4.5 Mechanism of Caspase activation: Intrinsic (mitochondrial) pathway

The apoptotic signal transduction pathways that are undertaken in response to an intrinsic signal such as DNA damage, oxidative stress and growth factor deprivation involve mitochondrial release of pro-apoptotic molecules. A critical regulatory role for the maintenance of mitochondrial membrane permeability has been suggested for proteins of the Bcl-2 family, which includes anti-apoptotic proteins Bcl-2 and Bcl-X_L [Walensky LD, 2006].

Permeabilization of the outer mitochondrial membrane is followed by release of pro-apoptotic proteins, usually present in the intermembrane space of these organelles, into the cytosol. Such effectors include cytochrome c, smac/DIABLO, HtrA2/ OMI, the flavoprotein apoptosis-inducing factor (AIF) and endonuclease G. In the cytosol, cytochrome c interacts with the adapter protein Apaf-1 and induces a conformational change that allows stable binding of dATP/ ATP, an event that drives the formation of a heptamer Apaf-1/ cytochrome c complex, the apoptosome [Acehan D, 2002], which binds procaspase-9 via their homologous caspase recruitment domains (CARDs). Caspase-9 is activated by allosteric change and dimerisation, rather than cleavage [Rodriguez J, 1999], which in turn activates the downstream effector caspase-3,-6 and -7 by proteolytic cleavage of inactive precursors.

The vital role of mitochondrial release of cytochrome c in stress induced apoptosis has been questioned. Initial reports on mice lacking either Apaf-1 [Cecconi 1998], or caspase-9 [Hakem 1998] supported the importance of cytochrome c in the intrinsic pathway: mice died near birth with enlarged brains, as do mice lacking caspase-3. Recent findings, however, rule out the essential role for Apaf-1 and caspase-9 in stress induced apoptosis in certain cell lines [Marsden VS, 2002]. Unlike Bcl-2 overexpression or loss of Bim, the absence of Apaf-1 or caspase-9 did not interfere with the development of mature lymphocytes, where programmed cell death is essential. Thus, in many cells, the apoptosome is dispensible for the initiation of stress induced apoptosis. Since the level of caspase activity is lower in Apaf-1 knockouts, the apoptosome must be an amplifier of the caspase cascade rather than a critical initiator of it [Marsden VS, 2002]. This amplification may be more important in some cell types than others, and in certain types of cellular stress leading to activation of the programmed cell death machinery.

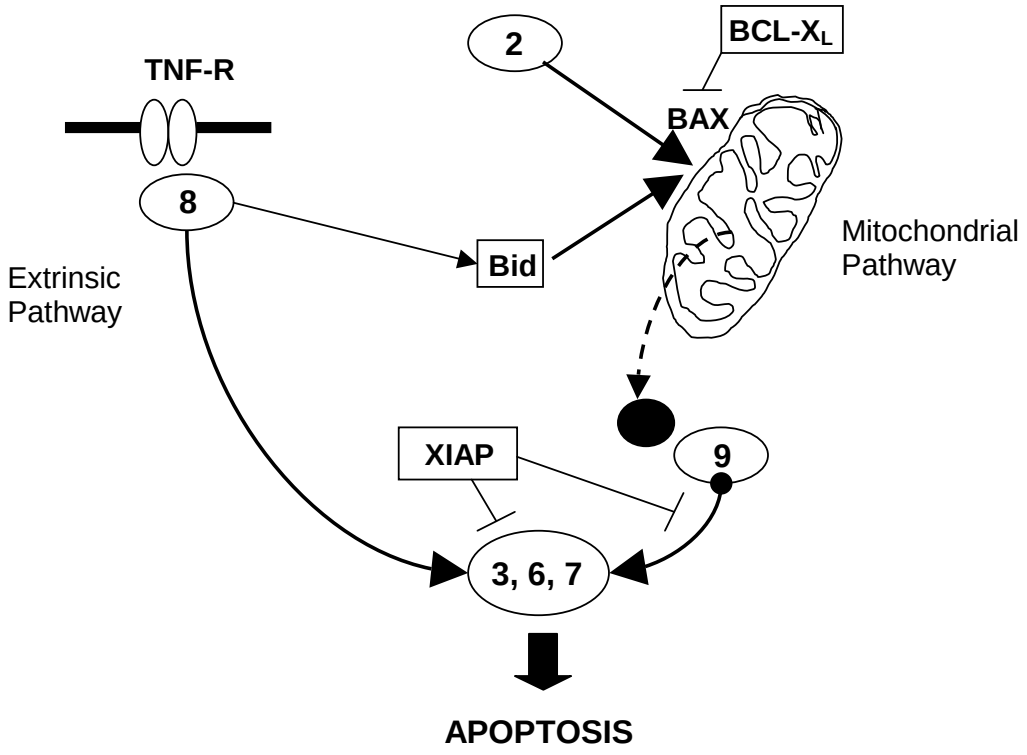

Figure 1.3 Apoptotic signalling cascade via Activation of Caspase pathways.

Apoptotic cell death is initiated by activation of a caspase cascade via two distinct but communicating pathways: receptor mediated activation of caspase-8 and mitochondrial depolarisation causing release of cytochrome c which activates caspase-9. These intermediate caspases causes activation of the effector caspases-3, -6 and -7 which causes nuclear vacuolation and shrinking, disruption to cellular membrane, and ultimately cell death.

Mitochondria participate in inducing apoptosis after I/R through multiple changes, including generation of oxygen free radicals, calcium translocations, altered permeability transitions, and release of cytochrome *c*, apoptogenic factors, and Bcl-2 family members. Renal I/R in rats can induce mitochondrial swelling, rupture of inner and outer membranes, and release of Bcl-2 post-injury. A recent study investigated the proximate events that lead to mitochondrial permeability transition and release of cytochrome *c* after hypoxia/reoxygenation injury in kidney proximal tubular cells. A persistent respiratory defect occurs in complex I-dependent substrates during reoxygenation after hypoxia, and this defect is associated with condensed mitochondrial configuration and incomplete recovery of mitochondrial membrane potential. Amelioration of impaired substrate flux through mitochondrial complex I and ATP generation by α-ketoglutarate plus greatly improved mitochondrial function and cellular recovery. The identification of these upstream pathways of anaerobic metabolism and the possibility of metabolic manipulations to improve mitochondrial functions at an early stage may help to prevent irreversible mitochondrial damage in renal ischemia [Plotnikov EY, 2007].

Ischaemic renal injury is associated with a marked increase in the expression of the antiapoptotic Bcl-2 family of proteins, Bcl-2, Bcl-X_L and the apoptotic protein Bax, in distal tubules and moderate increases in the proximal tubules [Chien CT, 2001]. The marked upregulation of the antiapoptotic proteins in the distal tubules may tip the balance in favour of cell survival, and this imbalance may be involved in its adaptive resistance to ischaemic injury. It can be hypothesised that this survival mechanism may allow the cells to produce growth factors that may aid in the protection and/or regeneration of the distal tubules by an autocrine mechanism and of the more vulnerable proximal tubules by a paracrine mechanism.

The relative expression of the Bcl-2 family of proteins in distal and proximal tubules subjected to oxidant injury in culture is similar to that seen *in vivo*. However, the expression

of Bcl-X_L is decreased in proximal tubular cells and a translocation of Bcl-X_L from the cytosol to the mitochondria is observed in the surviving distal tubule cells. No change in the sub-cellular distribution of Bax was observed in the surviving distal tubule cells, and it remained widely distributed in the cytosol. The expression of Bcl-2 or Bax was also unchanged in PTC post-oxidant injury [Chien CT, 2001]. It is unclear if the translocation of Bcl-X_L plays a role in its protection from the oxidative injury. In a separate study, proximal tubules subjected to ATP depletion induced by hypoxic injury or impaired oxidative phosphorylation are shown to translocate Bax from the cytosol to the mitochondria. It is suggested that Bax may form pores in the mitochondrial outer membrane causing the release of cytochrome *c* from the mitochondrial intermembrane space and may activate apoptotic pathways [Wei Q, 2004].

1.4.6 Cellular inhibitors of apoptosis

The inhibitors of apoptosis (IAPs) family proteins includes eight mammalian family members, including X-linked inhibitor of apoptosis (XIAP), c-IAP1, c-IAP2, and ML-IAP/livin [Deveraux QL, 1999]. They act as a last line of defence to prevent cellular disassembly by binding to caspases by their BIR (Baculovirus IAP repeat) motif, which contains a conserved cysteine and histidine core sequence Cx2Cx6Wx3Dx5Hx6C [Dereraux QL, 1997; 1999] which may lead to ubiquitination of the caspases. XIAP, X-linked inhibitor of apoptosis, contains three BIR domains and has been shown to directly inhibit caspase-3, -7 and -9, but not caspase-1, -6, -8 or -10. This caspase selectivity could be due to the presence of conserved amino acid residues found in the BIR domains and the linker regions that separate them [Sun C, 1999]. Severe hypoxia up-regulates these endogenous inhibitors of apoptosis, particularly c-IAP2, and hypoxia-resistant epithelial cells which express increased c-IAP2 and Bcl-X_L are more resistant to a second ischaemic or toxic insult [Dong Z, 2001; Dong Z, 2003].

The activity of IAPs is regulated by Smac/DIABLO, a structural homologue of the Drosophila proteins Reaper, Hid, and Grim [Du C, 2000]. Smac/DIABLO is released from mitochondria and inhibits IAPs, which facilitates caspase activation during apoptosis. Omi/ HtrA2 has been recently identified as another modulator of IAP function. Omi/HtrA2 is a mitochondrial-located serine protease, which is released in the cytosol and inhibits IAPs by a mechanism similar to Smac [Suzuki Y, 2001].

1.5 Erythropoietin

1.5.1 The cell biology of erythropoietin

Erythropoietin (EPO) is a glycoprotein hormone with a molecular weight of 30.4 kDa. The gene for EPO, situated on chromosome 7q11-22, consists of five exons and four introns, encodes a protein precursor of 193 amino acids. During post-translational modification, which consists of cleavage of a 27 amino acid sequence, glycosylation of 3 *N*-linked (at Asn-24, Asn-38 and Asn-83) and one *O*-linked (ser-126) amino acids, the removal of Arginine residue (Arg-166) from the C-terminal end yields the final circulating EPO molecule comprising of 165 amino acids. The tertiary structure of erythropoietin is defined by four anti-parallel α-helices. EPO was successfully purified from the urine of patients with aplastic anaemia [Miyake T, 1977]. From tryptic fragments of this urinary EPO, DNA probes were synthesized for the isolation and cloning of the human EPO gene [Jacobs K, 1985]. The manufacture and application of recombinant human EPO molecule (rhEPO) to treat the anaemia of chronic renal failure followed shortly thereafter [Winearls CG, 1986; Eschbach JW, 1987].

In the healthy adult, EPO secretion is primarily from the kidney, in response to hypoxia, in order to maintain an optimal red cell mass to cope with normal tissue oxygen demand. The basal level of EPO secretion in the picomolar range maintains a plasma concentration equivalent to 15-25 mU/ L, although during periods of hypoxic stimulation plasma levels may increase by 50 -100 fold [Al-Huniti NH, 2004]. In the kidney, EPO production is restricted to a population of cells in the interstitium of the cortex and outer medulla. Immunohistochemical characterization utilizing SV40 labelled erythropoietin-producing transgenic mice demonstrated that EPO is produced in a population of fibroblast-like type I interstitial cells using light and electron microscopy [Maxwell PH, 1993].

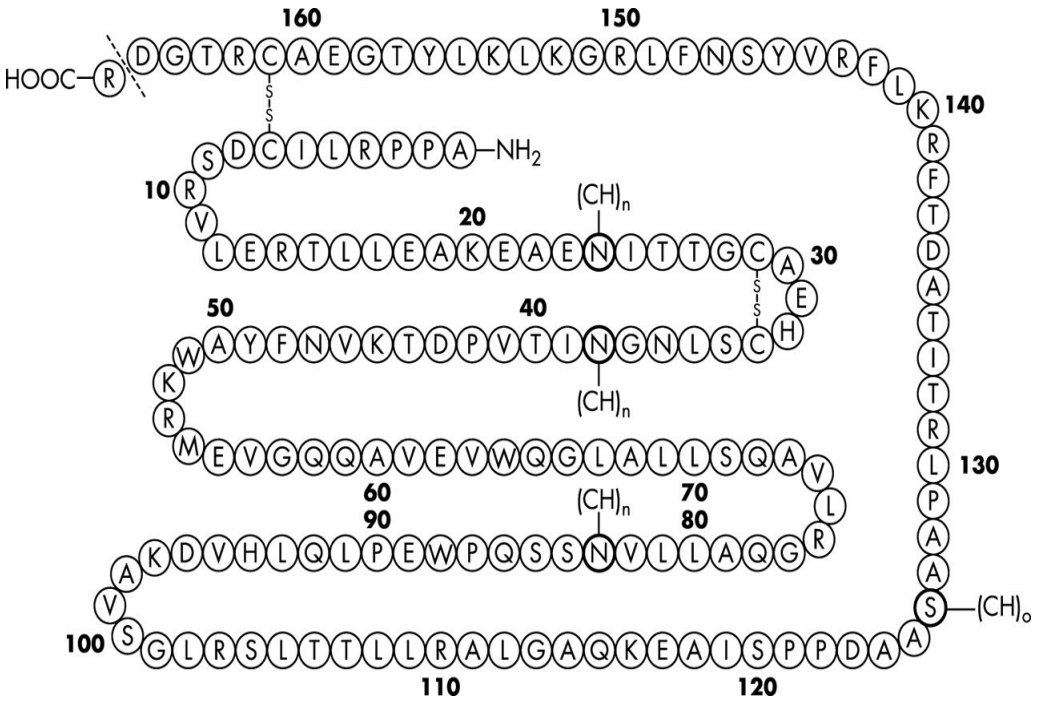

Figure 1.4 Primary structure of erythropoietin, demonstrating cysteine sulphide cross-bridges

Recently, it has been discovered that EPO is additionally produced at several other sites, including the brain [Masuda S, 1994], the endometrium [Yokomizo R, 2002] and the epididymis [Kobayashi T, 2002]. The physiological role of EPO produced in these locations remains uncertain, but foetal production at multiple sites may be essential for normal development [Juul SE, 2004].

1.5.2 Regulation of EPO production

EPO gene expression is under the control of the oxygen-sensitive transcription factor hypoxia-inducible factor (HIF), which consists of a regulatory α-sub-unit (HIF-1α, -2α, and -3α) and the constitutively expressed sub-unit HIF-1β [Wang GI, 1993]. Both subunits are members of multi-protein families and belong to the extended family of basic helix-loop-helix PAS domain transcription factors. Low oxygen tension averts enzymatic prolyl-residue hydroxylation within a region of HIF-α called the oxygen-dependent degradation domain (ODD), by a family of prolyl-4-hydroxylases (PHD 1-3). In normoxia, the hydroxyl residue serves as a target for von-Hippel-Lindau (VHL)-dependent polyubiquitination and subsequent proteosomal degradation. Hypoxia prevents HIF degradation by inhibition of this oxygen-dependent pathway, leading to nuclear accumulation of HIF and DNA binding. The VHL gene product is the recognition component of a multiprotein E3 ubiquitin-ligase complex that captures HIF-α chains that have undergone enzymatic prolyl hydroxylation [Jaakkola P, 2001].

The HIF isoform that hypoxically regulates EPO production remains controversial. Although HIF-1 was initially purified from human hepatoma (HepB3) cells as the HIF molecule that bound to the 18-nucleotide fragment of the 3’ regulatory element containing the HRE, the regulation was found to be largely dependent on HIF-2, and not HIF-1, in studies utilizing a

siRNA knockdown approach [Warnecke C, 2004]. Hepatic production of EPO is suppressed in the livers from animals with Cre-LoxP-mediated inactivation of HIF-2, and complete absence of HIF-2 further suppressed physiological EPO concentrations [Rankin EB, 2007]. This may be due to preferential binding of HIF-2 to the HRE, although the expression of HIF-2 is variable, and this observed dominance may be cell type specific [Racliffe PJ, 2007].

In addition, prolyl hydroxylation requires 2-oxoglutarate as a co-factor because the hydroxylation reaction is coupled to the decarboxylation of 2-oxoglutarate to succinate, which accepts the remaining oxygen atom [Kivirikko K, 1998]. The prolyl-4-hydroxylase requires iron as a cofactor, and cobalt administration mimics the effect of hypoxia on HIF-1α activation. Cobalt administration to rats, via up-regulation of HIF-dependent proteins including EPO, VEGF and haem-oxygenase-1 (HO-1), diminished the degree of renal injury caused by ischemia-reperfusion [Matsumoto M, 2003], suggesting the HIF-dependent production of EPO may play an important role in ischaemic pre-conditioning. Evidence supporting the importance of EPO in ischaemic pre-conditioning comes from work in transgenic heterozygotic HIF -/+ mice, which express only small amounts of constitutively expressed HIF-1, and are resistant to an ischaemic pre-conditioning protocol [Cai Z, 2003]. These animals showed increased renal production of EPO which was significantly greater than the increase in other HIF-dependent hormones VEGF and HO-1.

HIF activation leads to the altered expression of a diverse range of cytokines and mediators that mediate the adaptive response to stress and ischaemia, including pro-angiogenesis hormone vascular endothelial growth factor (VEGF), glucose transporters (GLUT1) and glycolytic enzymes, iron metabolism (transferrin), and a variety of genes involved in cellular proliferation, differentiation and viability (IGF binding proteins, p21, cyclin G2 and caspase-9) [Iyer N, 1998].

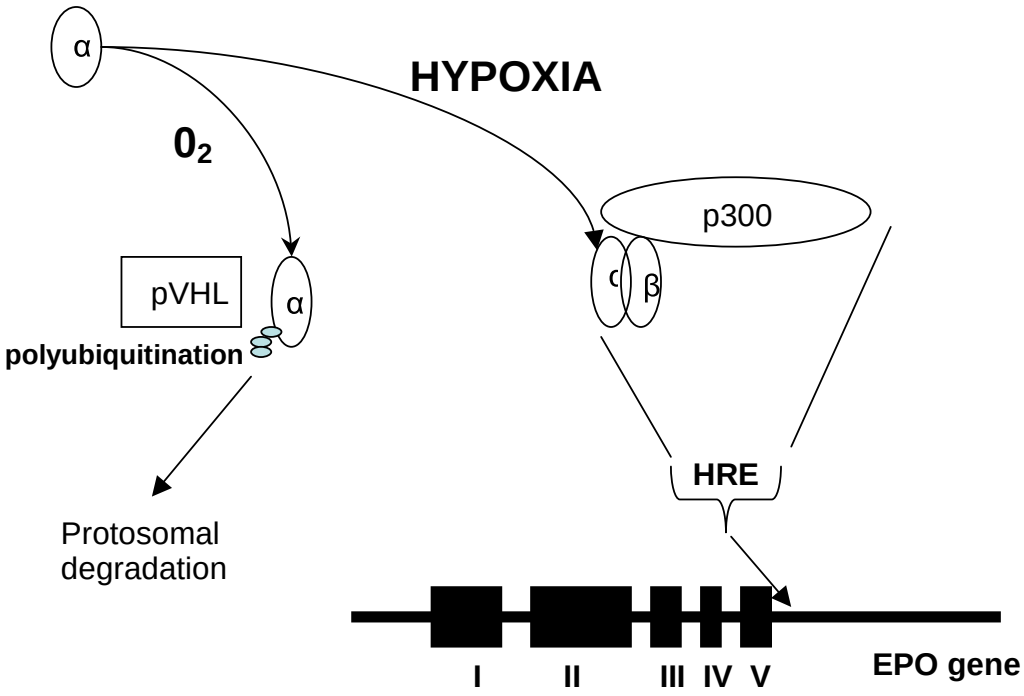

Figure 1.5 Oxygen Sensing and EPO gene transcription.

Low oxygen tension averts enzymatic prolyl-residue hydroxylation within a region of HIF-1α called the oxygen-dependent degradation domain (ODD), by a family of prolyl-4-hydroxylases (PHD 1-3), which, in normoxia, serves as a target for von-Hippel-Lindau (VHL)-dependent polyubiquitination and subsequent proteosomal degradation, thereby preventing HIF degradation, leading to nuclear accumulation of HIF-1. In the presence of c-factor p300, HIF binds to the hypoxia response element (HRE) in the EPO promoter sequence and increases gene transcription.

1.5.3 EPO in Haematopoietic Tissues

Due to the natural destruction of aging erythrocytes in the reticuloendothelial system there is a need for continual production of new red blood cells throughout life. There are several stages of erythroid cell maturation and each step is dependent on the presence of numerous growth factors for survival, proliferation and differentiation [Kaushansky K, 2006]. The effects of erythropoietin on the erythroid components of bone marrow are mediated by binding to specific EPO receptors on erythroid precursors (intermediate-stage erythroid burst-forming units (BFU-E) and the erythroid colony-forming units (CFU-E), which have already differentiated from pluri-potent stem cells. Differentiation to this stage is not dependent on EPO, as EPO-R knock-out mice are incapable of erythropoiesis but have committed BFU-E and CFU-E in foetal liver tissue [Wu H, 1995]. Thus the expression of the EPO receptor is itself an essential part of the mechanism by which erythropoiesis is controlled. The expression of the erythropoietin receptor is dependent on the specific phase of differentiation, and in the absence of EPO, the erythroid progenitors undergo apoptotic cell death [Boyer SH, 1992].

EPO can efficiently support the proliferation of murine erythroid progenitor cells ex vivo, and induce entry into the cell cycle in dormant cells [Miller CP, 1999]. Using the EPO-dependent human erythroid progenitor cell line HCD-57, Silva et al showed that erythropoietin maintained their viability via repressing apoptosis by upregulating Bcl-X_L, an anti-apoptotic protein of the Bcl-2 family [Silva M, 1996]. To further highlight the importance of this pathway, Bcl-X_L null mice exhibit fetal liver haematopoietic defects and severe anaemia during embryogenesis [Wagner KU, 2000].

1.5.4 Erythropoietin Receptor and Intracellular Signalling

Before the cloning of the EPO receptor cDNA, investigators had used radiolabelled EPO to demonstrate specific binding to cells derived from the erythroid lineage [D'Andrea D, 1990]. These studies showed that approximately 200 EPO receptors were present on the cell surface of purified normal erythroid progenitors. This relatively low expression of cell surface receptors is characteristic of other receptors of haematopoietic cytokines such as G-CSF, GM-CSF and interleukin-3 [Groopman JE, 1989]. Affinity cross-linking experiments using radiolabelled EPO revealed two cross-linked EPO receptor complexes, and subsequent crystallization studies have confirmed receptor dimerisation [Matthews DJ, 1996].

The murine EPO receptor was cloned by transfecting pools of recombinant plasmids from a MEL cDNA library in to COS cells and screening for uptake of radiolabelled EPO by transfected cells [D'Andreau AD, 1989]. The cloned EPO receptor was a 507-amino acid polypeptide with a single membrane spanning domain, with extensive homology with the interleukin 2 receptor β chain [D'Andreau AD, 1990]. The extracellular domain of the receptor possesses a conserved domain of ~200 amino acids, which derives from the duplication of a 100 amino acid subdomain with a type III fibronectin structure [Bazan JF, 1990]. The EPO receptor exhibits a WSXWS sequence in the membrane-proximal subdomain and two pairs of cysteines in the first subdomain. The two pairs of cysteine are held by disulphide bonds. The WSXWS sequence is thought to be necessary for the correct folding and cell membrane stability [Yoshimura A, 1992].

Like all the receptors in the cytokine receptor superfamily, the EPO receptor does not possess endogenous tyrosine kinase activity, but binding of EPO to the extracellular portion of the receptor induces a conformational change, which brings JAK2 kinase into proximity,

allowing autophosphorylation and activation of JAK2 kinase domain (Figure 1.5). This induces rapid tyrosine phosphorylation of a number of proteins [Witthuhn B, 1993]. Eight tyrosine residues located on the cytoplasmic domain of the EPO receptor are phosphorylated by JAK2, upon EPO stimulation, and these phosphorylated tyrosine residues are docking sites for proteins containing src-homology 2 (SH2) domains [Dusanter-Fourt I, 1992].

The STAT (signal transducer and activator of transcription) pathway plays a major role in cytokine-induced signalling. EPO activates both STAT5A and STAT5B [Damen JE, 1993; Wakeo H, 1995]. The two first tyrosine residues in the intracellular domain of the EPO receptor (Y343 and Y401) are responsible for STAT5 binding and activation [Chin H, 1996]. The precise role of STAT5 activation induced by EPO is the subject of controversy. A correlation between STAT5 activation and cellular proliferation has been observed, but STAT5 activation may also play a role in erythroid differentiation [Chretien S, 1996].

A direct association between phosphatidylinositol 3-kinase (PI 3-kinase) and the EPO receptor has been shown, which involves the SH2 domains of the p85 subunit of the PI 3-kinase and tyrosine-479 of the EPO receptor [Damen J, 1995]. An alternative pathway for the activation of PI 3-kinase has been described, which involves the tyrosine phosphorylation of the adaptor protein IRS2 and its subsequent association with PI 3-kinase, which allows for the previous finding that cells expressing a truncated EPO receptor had PI 3-kinase activity [Verdier F, 1997]. PI 3-kinase leads to phosphorylation and activation of its downstream target, the serine/ threonine kinase AKT, which in turn phosphorylates multiple targets including FKHRL1, and P70S6-kinase [Downward J, 1998]. Several studies have suggested that the PI 3-kinase/AKT pathway is the major pathway involved in the anti-apoptotic effects of EPO in erythroid progenitors [Haseyama Y, 1999] and also has a role in the proliferation and differentiation of endothelial progenitor cells [Bahlmann FH, 2003].

AKT is an important molecule in mammalian signalling to promote cell survival by inhibiting apoptotic cell death pathways. AKT is also able to induce protein synthesis pathways, and therefore is a key signalling step in general tissue growth. AKT regulates the cellular survival and metabolism pathways by binding and regulating many downstream effectors both directly and indirectly, including BAD, a pro-apoptotic protein of the Bcl-2 family. AKT phosphorylates BAD on Ser^{136}, which makes BAD dissociate from the Bcl-2/ Bcl-X_L complex and lose the pro-apoptotic function [Chong Z, 2005]. AKT also activates NF-κB via regulating IκB kinase (IKK), thus result in transcription of pro-survival genes which are up-regulated by NF-kB [Terrangi J, 2008].

Erythropoietin receptor signalling is terminated through receptor internalisation and proteosomal degradation [Verdier F, 2000], after 30-60 minutes of stimulation. Receptor activation and signalling causes the activation of protein tyrosine phosphatases, which de-phosphorylates JAK2 and inactivates its kinase function, with inactivation of STAT pathways [Klingmuller U, 1995]. Mutations in the EPO receptor that lead to decreased or absent de-phosphorylase activity, prolonging the stimulation signal produced by ligand binder are associated with familial erythrocytosis syndromes [Arcisoy MO, 1999].

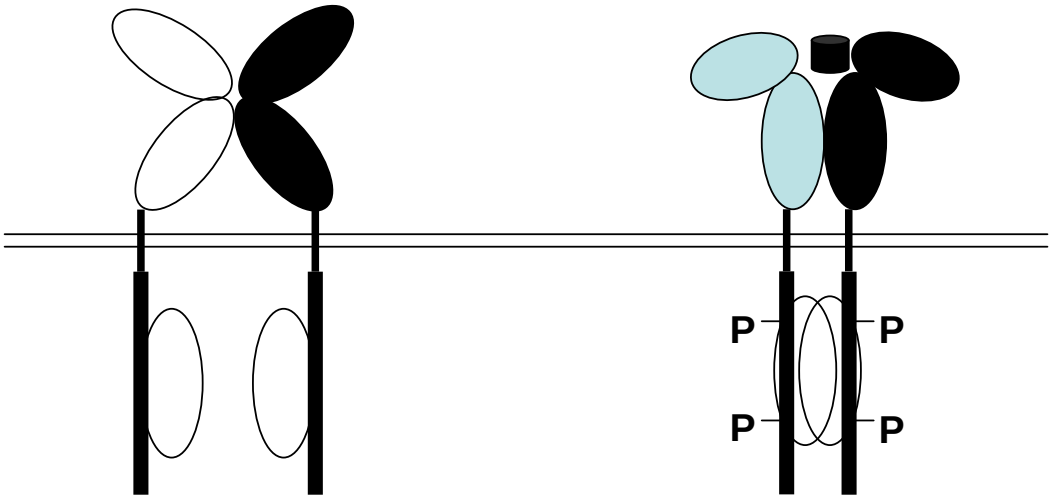

Figure 1.6 Conformational change on ligand binding allows activation

EPO binds to the extracellular portion of the receptor, leading to structural rearrangement which allows proximity-dependent autophosphorylation of receptor associated JAK2 kinases, which phosphorylate tyrosine residues on the intracellular portion of the receptor, allowing SH-2 domain containing mediators, activating STAT5. The activated STAT5 homodimer translocates to the nucleus.

Studies of the tissue distribution of EPO and the EPO receptor in the developing human foetus have demonstrated the presence of mRNA for EPO and the receptor in virtually all major organs in the first two trimesters [Juul SE, 1998]. This leads to speculation that EPO acts in concert with somatic growth and developmental factors during early foetal life. Although mice with EPO gene knock-down were found to be neurologically normal [Maxwell PH, 1994], subsequent studies have demonstrated defects in cardiac structure and reduction in the expression of neuronal stem cells [Chen ZY 2007] in these animals. Latent expression in adult tissues may be up-regulated in disease states, particularly in the development of cancer. Indeed, an increasing number of cancer cell types have been shown to express a functional EPO receptor [Westenfelder C, 2000; Kumar SM, 2005], which may have implications for the therapeutic use of erythropoietin in certain clinical situations. Further work is required to fully answer the questions raised by these observations.

Mature endothelial cells also express EPO receptors (Epo-Rs) and EPO induces a proangiogenic response in cultivated mature endothelial cells, as evidenced by stimulation of endothelial cell proliferation, migration, endothelin-1 release, and increase in cytosolic-free calcium concentration [Chong Z, 2002]. A physiologic significance for the EPO-EPO-R signaling pathway has been demonstrated for the oestrogen-dependent cyclical angiogenesis in the uterus [Yasuda Y, 1998].

1.5.5 Use of EPO in Anaemia associated with end-stage renal failure

Anaemia develops in most patients with CKD because less erythropoietin is produced by the diseased kidneys [Erslev AJ, 1997]. The decline in haemoglobin (Hb) concentration may start at levels of creatinine clearance of around 70 mL/min among men and 50 mL/min among women, and progresses relentlessly. The management of anaemia before the

introduction of recombinant human erythropoietin was a struggle, with a combination of "good dialysis", minimizing blood loss, parenteral iron and androgens, together with avoidance of excess blood tests, achieving average haemoglobins of approximately 8 g/ dl. This left about 10% of patients dependent on blood transfusions and susceptible to the complications of iron overload. Following successful cloning of EPO, pilot studies followed very rapidly [Winearls C, 1986], leading to a number of successful multi-centre trials [Eschback JW 1989]. The doses required to reverse anaemia and maintain haemoglobin were found to be similar in American and UK studies [Bommer J, 1988; Eschbach JW, 1989].

The erythrokinetic studies performed on the first dialysis patients treated with r-HuEPO showed that the total red cell volume was below normal before treatment and increased after treatment. These increases in red cell volume were accompanied by reciprocal changes in plasma volume, so that total blood volume was not altered by treatment. Red cell survival in non-transfused patients was only modestly shortened before treatment and was not altered by treatment. Studies of the response of bone marrow erythroid progenitors to r-HuEPO treatment showed that after treatment, the number of bone marrow BFU-E had fallen to a mean of 24% of pre-treatment values, but there was no significant change in the number of CFU-E. The failure to change the number of CFU-E would have to be explained by self-renewal and replenishment from the BFU-E, keeping the size of this compartment constant [Reid CDL, 1988].

The best marker of benefit of the introduction of erythropoietin to clinical practice is the reduction in the need for regular blood transfusions [Sundal E, 1991]. The improvement in symptoms attributable to anaemia, and hence quality of life, is unequivocal, and confirmed in several randomised, placebo controlled trials [Auer J, 1990]. Associated improvements in

haemodynamic status due to correction of anaemia lead to reduction in progression of left ventricular hypertrophy, with a concomitant reduction in mortality.

The therapeutic use of EPO in these patients led to the identification of systemic and vascular effects that caused significant complications. EPO administration results in an increase in diastolic blood pressure of up to 10 mmHg in 10-20% of patients [Smith KJ, 2003]. The underlying mechanism of this effect is unclear, but a number of possibilities have been studied, including the induction of the vaso-constrictor endothelin-1 [Carlini RG, 1993], altered intracellular calcium concentration and a diminished response to NO [Marrero MB, 1998].

1.5.6 The novel role of Erythropoietin in the Nervous System

Both erythropoietin and the EPO receptor are functionally expressed in the nervous system of rodents, primates and humans. In the mouse, EPO is present in the hippocampus, capsula interna, cortex and mid-brain areas [Digicaylioglu, 1995]. In cultured rat cortical neurones, the expression of the EPO receptor has been demonstrated by immunostaining and RT-PCR [Morishita, 1997]. In humans, EPO and the EPO receptor are present in both astrocytes and neurones, although the level of expression varies according to gestation age, with reduced production after birth [Juul, 1999].

Hypoxia results in the induction of EPO in brain tissues. Accumulation of EPO mRNA and the EPO protein in response to hypoxia has been observed in cultured astrocytes [Marti HH, 1996]. EPO and the EPO receptor are also inducible in the hippocampal neurones, although *in vivo* models demonstrate a broader up-regulation during hypoxia [Bernaudin M, 1999].

Initial experiments have therefore examined the potential role of EPO in the nervous system during cerebral ischaemia. Infusion of EPO into the lateral ventricle of gerbils subjected to the occlusion of the common carotid arteries prevented ischaemia-induced learning disability and resuced hippocampal neurones from degeneration [Sakanaka M, 1998]. Multiple studies have now confirmed the beneficial effects of EPO administration in the course of ischaemic brain injury in vivo, using systemic administration to overcome the impracticalities of ventricular delivery systems [Sadamoto Y, 1998; Matsushita H, 2003; Grasso G, 2002].

Ischaemia-related investigations examining the potential of erythropoietin to prevent neuronal injury have also been extended to the spinal cord, peripheral nervous system and visual system, summarized in table 1.1.

Animal studies		
Focal and global cerebral ischemia ***Sakanaka M, 1998***	25–100 U i.p. or 0.2–25 U day-1 i.c.v. applied either pretreatment or post-treatment with injury in rats, mice or gerbils	Infarct volume, brain edema and neuronal apoptosis decreased; neuronal survival increased
Retinal ischemia ***Junk AK, 2002***	5000 U kg i.p. or 2 ml intravitreal applied imm. or posttreatment	Photoreceptor and retinal ganglion cell apoptosis decreased
Neonatal hypoxic–ischemic brain injury ***Aydin A, 2003***	1000–5000 U/Kg i.p. applied pre-treatment with injury in mice	Infarct volume and neuronal apoptosis decreased; caspase-3 activity decreased
Spinal cord injury ***Gorio A, 2002; Celik M, 2002***	100–5000 U/kg i.p. with injury in rats	Motor neuron apoptosis, inflammation and lipid peroxidation decreased; functional recovery improved
Subarachnoid hemorrhage ***Buemi M, 2000***	1000 U/kg i.p. applied 5 min after injury in rabbits	Neuronal death decreased; functional recovery and blood flow autoregulation improved
Peripheral nerve injury ***Campana W, 2003***	1000–5000 U/kg s.c. applied pre-treatment with injury in rats	Dorsal and ventral root ganglion cell injury decreased; recovery from mechanical allodynia improved
Tissue culture studies		
Anoxic injury ***Chong ZZ, 2003***	10 ng/mL applied pre-treatment with injury in ECs or hippocampal neurons	DNA fragmentation and PtdSer exposure decreased; cell survival increased
NO injury ***Yamasaki M, 2005; Sakanaka M, 1998***	10 ng/ml or 20 U/ml applied pre-treatment or imm. with injury in ECs or hippocampal neurons	DNA fragmentation, PtdSer exposure and NO production decreased; cell survival increased
Glutamate toxicity ***Yamasaki M, 2005***	50 ng/ml or 3–300 pM/ml pre-treatment with injury in hippocampal, cortical and cerebellar neurons	Glutamate release decreased; neuronal survival increased

Table 1.1 Therapeutic use of EPO in experimental models of brain injury

1.6 Aims

The evidence presented in the introduction has led to the hypothesis that the haematopoietic growth hormone Erythropoietin is functional in tissues outside the bone marrow, and that it exerts physiological effects to lessen injury induce by exposure to ischaemia, and to inititate the tissue healing process.

In order to test this hypothesis, the primary aim of this thesis is to establish the role and effects of the haematopoietic growth factor erythropoietin (EPO) on the course of ischaemia reperfusion injury in the kidney. In order to fully achieve this, it is essential to study the direct *in vitro* effects of EPO on proximal tubular epithelial cells, and examine the intracellular mechanisms which underpin the protective effects of EPO in these models. Finally this thesis will aim to extend the examination of the effects of EPO into different types of injury model, including other *in vivo* organ systems.

Chapter Two:

In vitro effects of Erythropoietin in a Human Proximal tubular epithelial cell line

2.1 Introduction

In erythroid precursor cells at the CFU-E stage, EPO activates a number of signalling pathways via engagement of its cell surface receptor, which reduce growth factor withdrawal-induced cell death, and hence allow proliferation and differentiation, as discussed in detail in section 1.5.4.

A direct effect of EPO on the viability and resistance to cell death of tubular epithelial cells would require cell surface expression of a functional EPO-R on this cell population. The identification of a functional EPO/ EPO-R system in the nervous system led to a range of studies demonstrating signalling effects and beneficial responses in a range of injury models, including hypoxia and toxic insults, described in section 1.5.7. At the time of starting the body of work described in this thesis, experiments utilizing both polyermase chain reaction mRNA expression and immunoblotting techniques had demonstrated that the EPO-R is present on human, mouse and rat proximal tubular epithelial cells, and that, in cultured proximal tubular epithelial cells, EPO binds to its cell surface receptor, and exerts effects on cellular proliferation in culture [Westenfelder C, 1999].

2.2 Aims

The aim of the experiments in this chapter was to examine the signalling pathways activated by EPO in a human proximal tubular epithelial cell line, concentrating on the pathways known to be EPO-responsive in erythroid progenitor cells, and determine the effects of EPO on cell survival in a basic *in vitro* injury model.

2.3 Materials and Methods

2.3.1 Proximal Tubule epithelial cell lines

HK-2 cells, a proximal tubule epithelial cell line (PTEC) derived from normal human kidney, were obtained from the ECACC (European collection of cell cultures). HK-2 cells were immortalised by transduction with human papilloma virus 16 (HPV-16) E6/E7 genes. The recombinant retrovirus vector pLXSN 16 E6/E7 containing these genes was used to transfect the ectotropic packaging cell line Psi-2. Subsequent viruses produced by the Psi-2 cells were used to transfect the amphotropic packaging cell line PA317. Viruses obtained from the PA317 cells were used to transduce primary proximal tubule epithelial cells. The pLXSN 16 E6/E7 confers resistance to neomycin. The cells retain a phenotype indicative of well differentiated proximal tubular epithelium, and express alkaline phosphatase, gamma glutyltranspeptidase, leucine aminopeptidase, α3, β1-integrins and fibronectin [Ryan MJ, 1994].

2.3.2 Cell Culture

HK-2 cells were cultured in Dulbecco's Modified Eagles Medium Ham's F12 with 10% v/v fetal calf serum (FCS) and antibiotics (benzylpencillin 100 U/ mL, streptomycin 10 μg/ mL, amphotericin 2.5 μg/ mL (all Sigma-Aldrich Chemical Co., UK) [hereafter called standard medium] in sterile $T75^3$ culture flasks (VWR, UK) and incubated at 37˚C in a humidified atmosphere comprising of 95% air and 5% CO_2. When confluent, the cells were sub-cultured; the medium was removed and the cells washed with 10 mL of Phosphate Buffered Saline pH 7.4 (PBS). PBS was removed before the addition of 10 mL of 0.05% Trypsin (Sigma), which was then incubated at 37˚ for approximately 10 minutes until the cells had

detached from the culture flask. The cells were then harvested by centrifugation at 800rpm for 5 minutes. The supernatant was removed with care to avoid disturbing the pelleted cells, which were re-suspended in 10 mL culture medium for a wash step. The cells were again harvested by centrifugation at 800 rpm for 5 minutes. The supernatant was removed and the pellet was resuspended in culture medium and aliquoted into fresh culture flasks at a cell to medium ratio of 1: 3. Cells were used for all experiments between passage three and six, and fresh batches of cultured cells were developed at all times to maintain optimum cell conditions for experiments. Foetal calf serum contains a variety of growth hormones, at very small concentrations, and may include EPO, although the amount is not specified in the manfacturer's information.

2.3.3 Cell Count

After being harvested, an aliquot of pelleted cells was resuspended in 10 mL of culture medium and a 1:1 dilution of the cell suspension made with 0.1% v/v of Trypan Blue. 100 μL of cell suspension-trypan blue mixture was transferred to a haemocytometer chamber over which a cover slip was placed. Using one chamber of the haemocytometer, the numbers of dead and viable cells were counted in the middle $1mm^2$ square and at least two of the four corner squares. Each square on the haemocytometer (with the cover slip in place) represents a total volume of $0.1mm^3$ (10^{-4} mm^3). Therefore,

Live cells per mL = mean number of unstained cells per square x 10^4 x 2

Total cells = cells per mL x volume

Cell viability = $\frac{\text{number of unstained cells x 100}}{\text{Total number of cells}}$

2.3.4 Cell freezing

After being harvested by centrifugation, pelleted cells were resuspended in 100 µL of cell culture medium, and then aliquots were added to cell culture freezing medium (10 % DMSO, 90% culture medium) and transferred to a cryovial, which was placed in a polystyrene container at -80˚ C for 2 hours before being transferred to liquid nitrogen for long term storage.

2.3.5 Quantification of protein by BCA assay

The BCA assay is a detergent-compatible formulation, based on bicinchoninic acid (BCA), for the colorimetric detection and quantification of total protein. This method combines the well-known reduction of Cu^{2+} to Cu^{1+} by protein in an alkaline medium (the biuret reaction) with the highly sensitive and selective colorimetric detection of the cuprous cation (Cu^{1+}) using a reagent containing bicinchoninic acid [Smith PK, 1985]. The purple colour reaction product of this assay is formed by the chelation of two molecules of BCA with one cuprous cation. This water-soluble complex exhibits a strong absorbance at 562 nm that is nearly linear with increasing protein concentrations over a broad working range (20-2,000 µg/ ml).

Protein concentrations are determined with reference to a standard curve of known protein concentrations made up with bovine serum albumin. 100 µL of each known dilution of the standard curve was added to duplicate wells on a 96 well plate (8 wells). 100 µL from each protein sample was added to the plate. The assay reagent buffer was added to each well (200 µL), and the plate incubated at 37 ˚C for 30 minutes. Absorbance at 562 nm was measured in a plate reader and corrected for a blank well measurement.

2.3.6 Western Immunoblotting

Sub-confluent cells were incubated in culture medium with and without experimental factors for varying time points. At the end of the experiment, the incubation was stopped by washing the cells with ice-cold PBS. Cells were removed after scraping the flasks with a Teflon coated cell scraper, followed by centrifugation for 5 minutes at 1200 x *g*. Cell pellets were then lysed by the addition of ice-cold lysis buffer:

Standard Lysis buffer

20 nM Tris (pH 7.4)

150 mM NaCl

1% NP-40

0.5 % w/v Na deoxycholate

0.1 % SDS (Promega)

Protease inhibitors were added immediately prior to cell lysis at the following concentrations:

1 mM PMSF (10 mg/mL stock solution in isopropanol)

1 mM Na orthovanadate (100 mM stock solution)

30 μL of a 5-19 U/mL solution of aprotinin from bovine lung

For 1-5 x 10^6 cells, 100 μL of lysis buffer was typically used. This was left on ice for 15-20 minutes with regular vortexing and then centrifuged at 15000 x *g* for 15 minutes at 4˚C. The protein content of the supernatant was measured using the bicinchoninic acid (BCA) protein quantification assay (Pierce) in a 96-well plate format, described in 2.3.5.

2.3.7 SDS-PAGE

For each individual gel, 20 - 40 μg of protein from each sample was electrophoresed on a polyacrylamide gel in the presence of SDS. The composition of the solutions for SDS-PAGE is shown below:

Stacking gel	
Protogel (30 % w/v acrylamide; 0.8% w/v bis-acrylamide)	0.33 mL
Resolving buffer (1.44 M Tris-HCl; 0.384% SDS, pH 8.8)	0.63 mL
10 % Ammonium persulfate (APS)	12.5 μL
H_20	1.54 mL
TEMED	2.5 μL

Resolving gel	
Protogel	1.67 mL
Resolving buffer (0.5M Tris-HCl; 0.4% SDS, pH 6.8)	1.30 mL
10 % APS	50 μL
H_20	1.98 mL
TEMED	5 μL

Samples were mixed with sample buffer (0.125M Tris-HCl (pH 6.8), 4% SDS, 20 % glycerol, 10% 2-mercaptoethanol), heated to 95˚C for 5 minutes and placed on ice. 20 - 40 μL (corresponding to 20 - 40 μg of protein, equalised for the lowest protein content) per well was loaded onto the gel. Electrophoresis was carried out at 25 mA per gel for approximately 45 minutes at room temperature in a buffer containing 0.025 M Tris (pH 8.3), 0.192 M glycine, 0.1 % SDS.

In later experiments, the Invitrogen *XCell* mini-cell electrophoresis system was used for all immunoblotting. Pre-cast NuPAGE Bis-Tris gels were used (10% or graduated 4-12%), and gels were run at 200 V constant, in running buffer (MOPS 50 mM, Tris-HCl 50 mM, 0.1% SDS, EDTA 1mM (pH 7.7).

2.3.8 Immunoblotting and detection of target proteins

Acrylamide gels were carefully removed from the electrophoresis apparatus and laid on top of a piece of polyvinyldifluoride (PVDF) membrane (Immobilon P; Millipore, Sigma) which had been cut to size and pre-soaked in 100% methanol and dH_20. Air bubbles were smoothed out with a sterile glass rod and the gel and membrane sandwiched between two sponges soaked in transfer buffer (10 mM CAPS, pH 11.0; 10% methanol in dH_20). The sandwich was then placed in the transfer apparatus with the membrane facing the anode and electroblotting carried out at 400 mA for 1 hour at room temperature. Following electroblotting, the membrane was separated from the gel and any residual acrylamide washed off by soaking in TBS-T for 2 minutes. Non-specific sites on the membrane were blocked by incubation with 5% BSA in TBS-T overnight at 4˚C. After washing in TBS-T for 5 minutes at room temperature, the membrane was probed with specific primary antibody (1:400- 1:2000 v/v in TBS-T + 1% BSA) for 2 hours at room temperature with constant agitation.

The membrane was then washed in TBS-T 3 times for 5 minutes each. The membrane was then incubated with polyclonal secondary IgG antibody conjugated to horse-radish peroxidase (1:2000 in TBS-T + 1% BSA) for 1 hour at room temperature with constant agitation. The membrane was washed as before. The protein band of interest was visualised by chemiluminescence (ECL chemiluminescence Detection system, Amersham, UK). Equal

volumes (~2 mL) of ECL solutions (A+B) were mixed and gently pipetted onto the membrane and left for 30 seconds without agitation. The solutions were then drained off and the membrane placed on a lint-free tissue to remove any excess solution. The membrane was immediately covered in cling-film and exposed to light-sensitive film (Kodak Biomax Light) for various times in the dark room. The film was developed using an X-ray developer.

2.3.9 Quantification of cell viability and proliferation with MTS assay

Cell viability and proliferation experiments were performed utilizing the novel tetrazolium compound (3-(4, 5-dimethylthiazol-2-yl)-5-(3-carboxymethoxyphenyl)-2-(4-sulfophenyl)-2H-tetrazolium, inner salt; MTS) and the electron coupling reagent, phenazine methosulfate (PMS). In the presence of PMS, MTS is chemically reduced by live cells into formazan, which is soluble in tissue culture medium, and the formation of formazan is directly proportional to the number of viable, metabolizing cells. Experiments were carried out in clear 96-well microplates, using 100 μL of phenol-red free standard culture medium per well. At the end of the experiment, 20 μL of the MTS reagent (CellTiter 96® Assay, Promega) was added to each well and gently mixed. The plate was returned to the incubator for 30 minutes at 37˚C.

The absorbance of the formazan at was read at 492nm, and expressed as a percentage of absorbance from control cells. Values over 100 % were taken as to be a measure of increased cell proliferation over control, although this could be confounded by experimental conditions that alter cellular metabolism.

2.3.10 Quantification of cell death by DNA fragmentation assay

Cell death was detected by a DNA fragmentation enzyme linked immunosorbent assay (ELISA), which quantifies the mono- and oligo-nucleosomes in the cytoplasmic fraction of cell lysates (Cell Death Detection ELISA ^{PLUS}; Roche Diagnostics, Lewes, UK). Cytosolic lysates extracted using digitonin buffer (10 μM Digitonin in PBS (pH 7.4)) were diluted 6-fold in kit lysate buffer. 20 μL of the diluted cell lysate per well was added to a streptavidin coated microplate. 80 μL of a mixture of anti-histone-biotin and anti-DNA-POD were added and the plate incubated for 2 hours at room temperature with gentle mixing on a microplate stirrer (300 rpm). During the incubation period, the anti-histone antibody binds to the histone component of the nucleosomes and simultaneously captures the immunocomplex to the streptavidin coated microplate via its biotinylation. Additionally, the anti-DNA-POD antibody reacts with the DNA content of the nucleosomes. The plate is then washed 3 times with incubation buffer (250 μL/ well) before 100 μL of 2, 2'-azino-bis(3-ethylbenzthiazoline-6-sulphonic acid (ABTS) solution is added to each well and the plate incubated at room temperature for 5-10 minutes on a plate-shaker (300 rpm).

The plate is read at 405 nm on a Dynex MRX II plate reader. DNA fragmentation is expressed as an enrichment factor from a time 0 control sample per mg of total cell lysate protein.

2.3.11 Transcription factor DNA- binding Assay by ELISA

Families of closely related homo- and hetero-dimer complexes that bind to DNA (transcription factors) regulate many of the global signalling pathways and are widely studied as disease targets. Traditionally, translocation of transcription factors was

determined by electrophoretic mobility shift assay (EMSA) using labeled specific oligonucleotides, but this technique is time-consuming and only semi-quantitative in nature. The DNA binding ELISA uses binding of a specific antibody and labeled secondary antibody to give more sensitive, highly quantitative data.

10 μg of nuclear protein extract was added to each well on a 96-well plate coated with an immobilized oligonucleotide containing a transcription factor-specific consensus sequence,

STAT family (5'-TTCCCGGAA-3')

with 30 μL buffer, and the plate was incubated at room temperature with gentle agitation for one hr. After washing, buffer containing a transcription factor-specific primary antibody (1/10000 dilution) was added to each well, and the plate incubated without agitation for one hour. The plate was washed 3 times, and then a HRP-conjugated secondary antibody was added. The plate was incubated for one hour, and then washed four times. 100 μL of developing buffer was then added to each well for up to 10 min, and absorbance read on a Dynax MRX II (450 nm with reference 650 nm). Values were expressed as optical density (n=3 for 3 independent experiments).

2.3.12 Cell Transfection and transfection of siRNA

RNA-mediated interference (RNAi) is a well-recognised pathway employed by most eukaryotes as a cellular line of defence directed against invading viral genomes or as a method to clear a cell of aberrant transcription products [Hamilton AJ, 1999]. Whilst the exact mechanism of successful RNAi-mediated gene silencing remains to be fully elucidated, this method has become an invaluable tool for analysis of gene function and

target validation. Cellular uptake of long double stranded RNA (dsRNA) has been shown to induce RNA interference in a diverse group of lower eukaryotic organisms. In 2001, Dr Tuschl *et al* showed that when short RNA duplexes (21-23 bases in length) were introduced into mammalian cells *in vitro*, sequence-specific inhibition of target mRNA was effected without inducing an interferon response [Elbashir SM, 2001].

2.3.13 Optimisation of siRNA transfection protocol for HK-2 cells

In order to determine the most effective protocol for siRNA transfection in HK-2 cells, a series of optimization experiments were performed. HK-2 cells were seeded in low density (50% confluence) into 6-well plates 24 hours before transfection. Control non-targeted siRNA labelled with fluorescein was used to assess transfection by fluorescent microscopy. Standard medium was removed from each well and replaced by 800 μL standard media without antibiotics. Three μL control siRNA (final concentration 100 nM) was mixed with serum-free medium and incubated at room temperature for 7 minutes. 3 μL Oligofectamine (Invitrogen), GeneJuice, Dimrie-C, RNAifect, and NEB reagent were mixed with serum-free medium and kept. The two reagents were then gently mixed by inversion and incubated at room temperature for 20 minutes. The volume was made up to 1200 μL with medium, and 200 μL per well was added gently and mixed by swirling.

The plate was incubated in the incubator overnight. The medium was removed and 2 drops of antifade reagent (plus DAPI nuclear stain) was added dropwise to each well and placed in a dark box. Fluorescence was examined under a microscope, and percentage of cells showing green fluorescence was calculated by counting total cell number by positive nuclear DAPI staining on two random high powered fields. The highest efficiency of transfection

achieved over a number of experiments was with the transfection reagent oligofectamine, illustrated in Figure 2.1, and this was adopted for all subsequent transfection experiments.

2.3.14 Statistical Analysis of Experiments

All experiments were performed in identical passaged cells in triplicate unless stated in the methods. All values described in the text and figures are expressed as the mean ± standard error for *n* (number of) observations. Each data point representing biochemical measurements was obtained from up to 10-12 separate animals. For histological scoring, caspase activity assays and apoptosis scoring, each data point represents analysis of kidneys taken from six individual animals.

All statistical analysis was performed using GraphPad Prism 3.01/ Instat 1.1 (GraphPad Software, San Diego, USA). Data for multiple group comparisons were analysed using one-way ANOVA followed by Dunnett post-hoc test, or Kruskal-Wallis ANOVA for non-parametric data. A *P* value of less than 0.05 was considered significant.

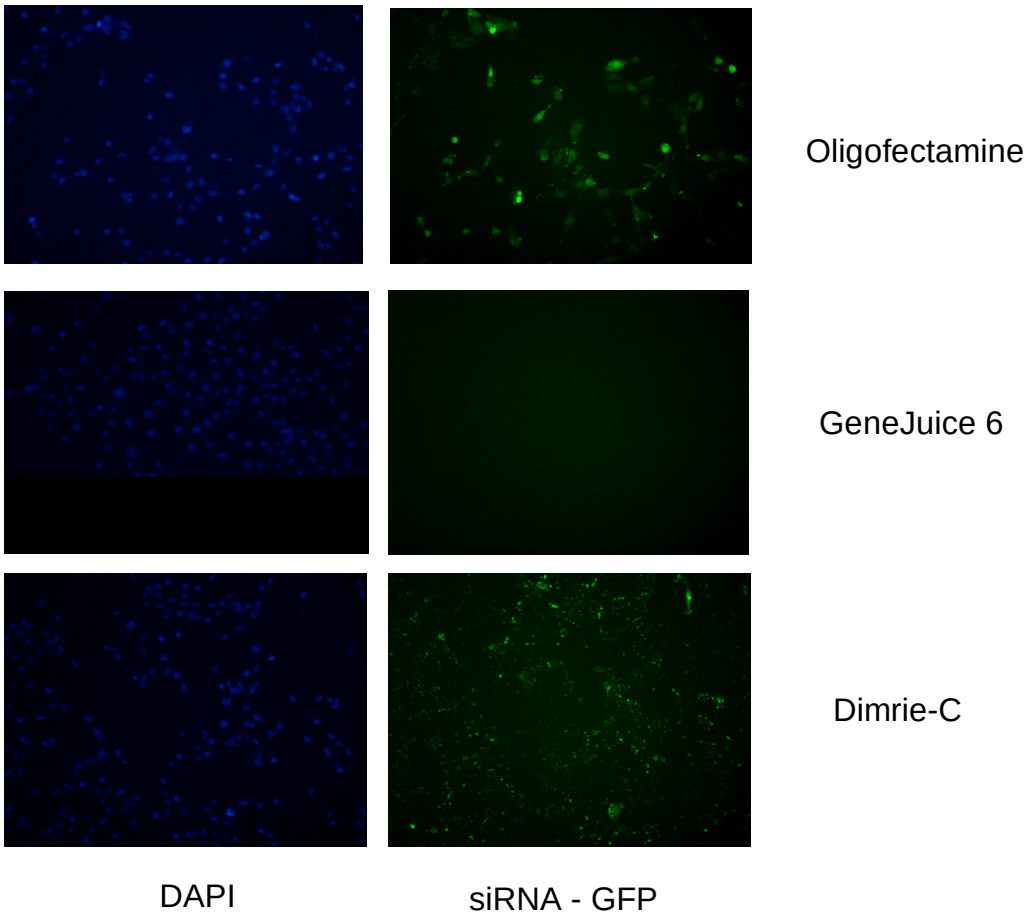

Figure 2.1 Quantification of siRNA transfection rate by fluororescent microscopy for labelled non-targeted control siRNA. Comparison was made with DAPI nuclear staining to calculate percentage transfection and amount of expression by fluorescence. All slides were analysed in a single session without adjustment of microscope settings. Images were downloaded from the PC and have not been altered.

2.4 Results

2.4.1 Expression of EPO receptor on HK-2 cells

The detection of the EPO-R in whole cell lysates was performed by immunoblotting with a validated specific polyclonal rabbit antibody to the C-terminal (Santa Cruz C-20) of the EPO-R, the specificity of which is not affected by ligand binding. Lysates were prepared from serum-starved UT-7 cells, a growth-factor dependent human erythroleukaemic cell line, known to widely express the EPO-R, to act as a positive control for immunoblotting [Dusanter-Fourt I, 1992].

Figure 2.2 shows a representative western blot, from three individual experiments, of whole cell lysates from HK-2 cells, showing two bands at approximately 68 and 55 kDa, corresponding to the EPO-R, with similarly sized bands identified in the UT-7 cell lane**.**

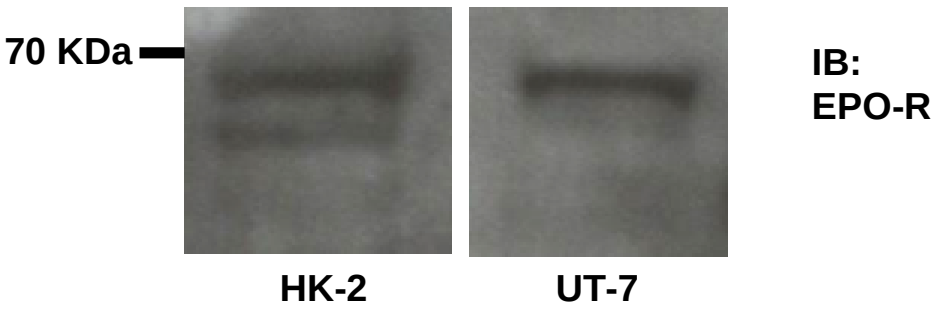

Figure 2.2 Immunoblot of EPO-R in Two cell lines shows similar bands sized approximately 65-69 kDa. Representative images are shown from 3 separate experiments. Protein loading was confirmed by reprobing membrane for actin.

2.4.2 EPO induces proliferation in HK-2 cells which is dependent on presence of EPO receptor

HK-cells were seeded at 1 x 10^5/ mL in a 96 well plate in standard medium containing 10% FCS and incubated overnight. The medium was removed and stimulated with phenol-red free standard medium containing different concentrations of EPO (1-100 U/ mL), and an MTS assay was performed after 24 hrs incubation. Experiments were repeated on three individual occasions, with 12 wells per experimental group.

At 24 hrs, administration of EPO caused a dose-dependent increase in cell number over control levels in the range of concentrations 1 - 50 U/ mL (when compared to control cell, EPO 1 U/mL + 19 % ± 0.5, EPO 10 U/mL + 33 % ± 1, EPO 50 U/mL + 45 % ± 1, ***P***<0.01), shown in Figure 2.3.

To confirm that these effects of EPO on cellular proliferation were dependent on receptor-mediated cell signalling, expression of the EPO-R was inhibited by transfection of an EPO-R specific siRNA (Dharmacon). Cells were seeded in 96 well plates and transfected with EPO-R siRNA or a control, non-targeted siRNA using the established protocol described in 4.2.3. The medium was removed 24 hrs after addition of the transfection solution or control, and then refreshed with phenol-red free standard medium with and without EPO at maximal effective concentration determined from the previous experiment (50 U/ mL). The plate was then incubated for 24 hrs, followed by a MTS assay. Control cells unstimulated by EPO demonstrated that there was no significant effect of the transfection process on cell viability (P=ns), and normal response to 24 hr incubation with EPO (when compared to un-stimulated cells, EPO 50 U/mL +17 % ± 7; ***P***<0.01). However, cells transfected with EPO-R siRNA showed a significant reduction in the response to EPO at 24 hrs when compared to non-transfected cells (*P*<0.01), shown in Figure 2.4.

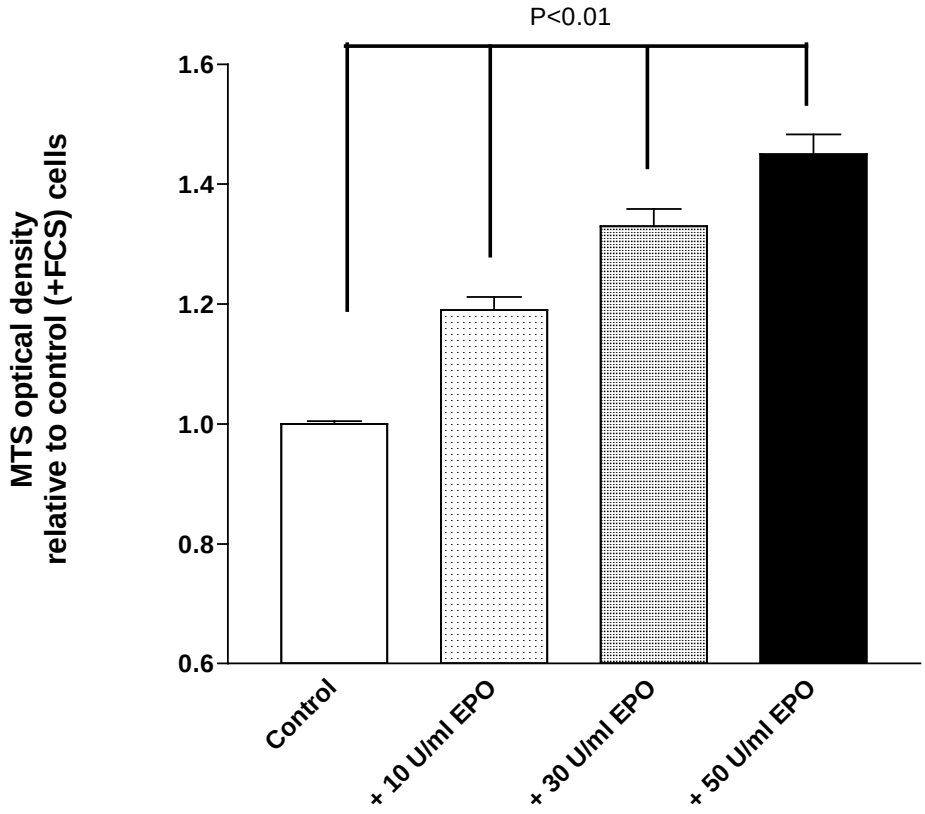

Figure 2.3 MTS value for n=12 wells expressed as relative value to control cells. EPO induced proliferation in HK-2 cells is dose-dependent (P<0.001).

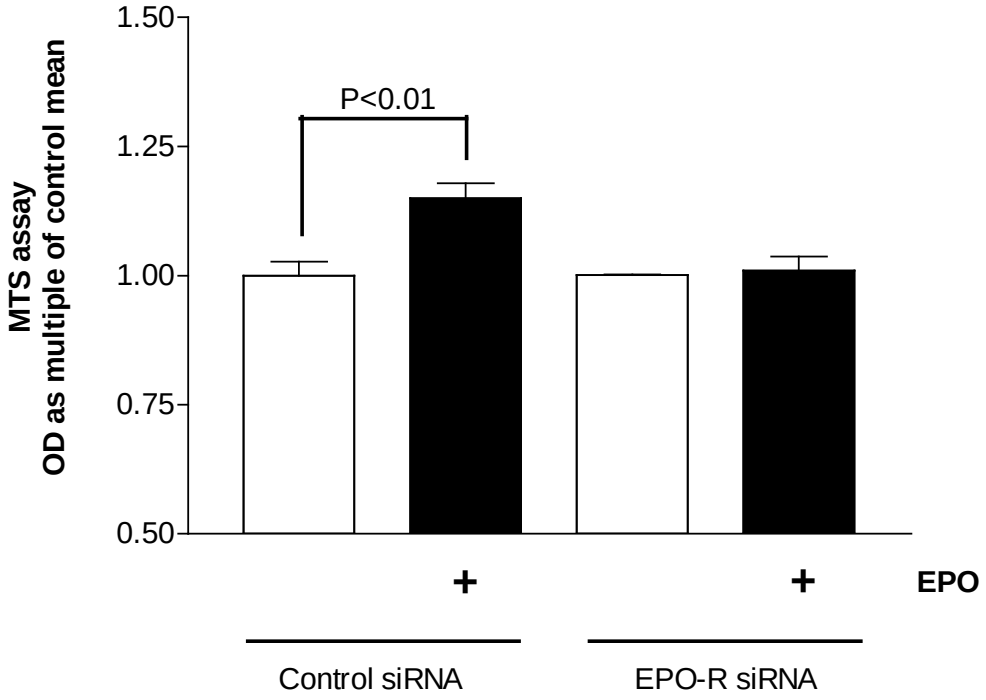

Figure 2.4 Loss of proliferation response to EPO in the absence of EPO-R following siRNA knockdown. MTS calculated for n=8 wells (3 separate experiments) and expressed as relative to control cells (P<0.01 EPO treatment in control cells).

2.4.3 EPO induces STAT activation and DNA binding

HK-2 cells were seeded at 50-75 % confluence in standard medium in 6-well plates and placed in an incubator overnight. The medium was removed, and the cells re-fed with standard medium without FCS. The cells were incubated for 6 hours, and then the medium was removed. Cells were stimulated with 1mL standard medium without FCS containing EPO (50 U/ mL) for 10 minutes. At the end of each experiment (n=6 wells for three separate experiments), cells were washed with ice-cold PBS, scraped with a Teflon cell scraper, and centrifuged at 600*g* at 4˚C for 5 minutes. The supernatant was discarded and the cell pellet was snap-frozen in liquid nitrogen.

Protein extraction was performed, and 10 µg of fractional lysates, corrected by volume for assay determined protein concentration, were used to determine STAT activation in a commercial transcription factor DNA binding ELISA assay (TransAM, Active Motif, France). The activation for STAT3 and STAT5A was determined. All results were expressed as increase in DNA binding over the value obtained for control un-stimulated cells for three experiments.

After stimulation with EPO (50 U/ mL) for ten minutes, there was significant increase in activation of STAT3 and STAT5A (STAT3 expression + 47 ± 3 % $P<0.01$, STAT5A + 52 ± 2 % $P<0.01$ when compared to time zero controls), shown in Figure 2.5 and 2.6.

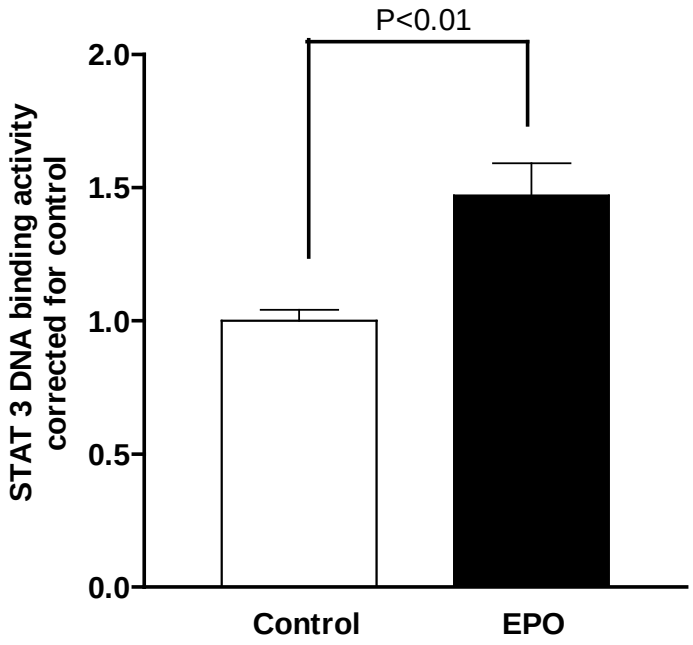

Figure 2.5 STAT3 activation by EPO at 10 minutes in HK-2 cells was measured by ELISA. DNA binding was expressed as multiple of control cells for n=3 experiments. EPO caused increase in STAT3 DNA binding (P<0.01).

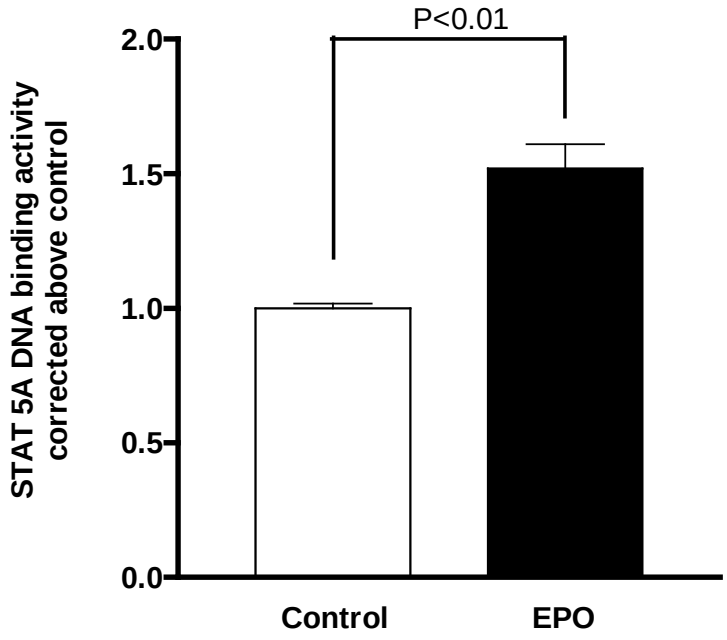

Figure 2.6 STAT5A activation at ten minutes by EPO in HK-2 cells was measured by ELISA. DNA binding was expressed as multiple of control cells for n=3 experiments. EPO caused increase in STAT5A DNA binding (P<0.01).

2.4.4 EPO Phosphorylates key Intracellular Pathways

HK-2 cells were incubated overnight in serum free medium followed by stimulation with EPO (50 U/mL) for varying lengths of time, or EPO plus either UO126 (10 μM), AG490 (10 μM), or LY294002 (10 μM). Following lysis with Phospho-safe lysis buffer (Pearce Inc), equal amounts of protein were run on a 4-12% graduated SDS gel.

Membranes were probed with specific polyclonal antibodies for phosphorylated ERK1/2. Incubation with EPO caused increased phosphorylation of ERK 1/2 which was maximal at 15 minutes. The observed phosphorylation of ERK by EPO was completed abrogated by co-incubation with the MEKK1 inhibitor UO126.

Membranes were also probed with specific polyclonal antibodies for serine-473 phosphorylated AKT. Membranes were stripped and re-probed for total AKT. Incubation with EPO caused increased serine phosphorylation of AKT which was maximal at 60 minutes. The observed phosphorylation of AKT by EPO was completed abrogated by co-incubation with LY294002, confirming the role of PI-3 Kinase. AG490, a JAK2 inhibitor, also reduced the phosphorylation of AKT by EPO at 60 minutes. This confirms the dependence of EPO signalling pathways on JAK2 activity.

The previous experiment demonstrated that AG490, an inhibitor of JAK2 kinase activity, reduced the phosphorylation of AKT in response to EPO stimulation in HK-2 cells. In order to confirm this finding was due to the inhibition of EPO-R / JAK2 interaction, a similar experiment was performed 24 hours following transfection of JAK2 siRNA, according to established protocol described in 3.3.2.2. Inhibition of JAK2 expression completely abrogated the phosphorylation of AKT following EPO stimulation (Figure 2.9)

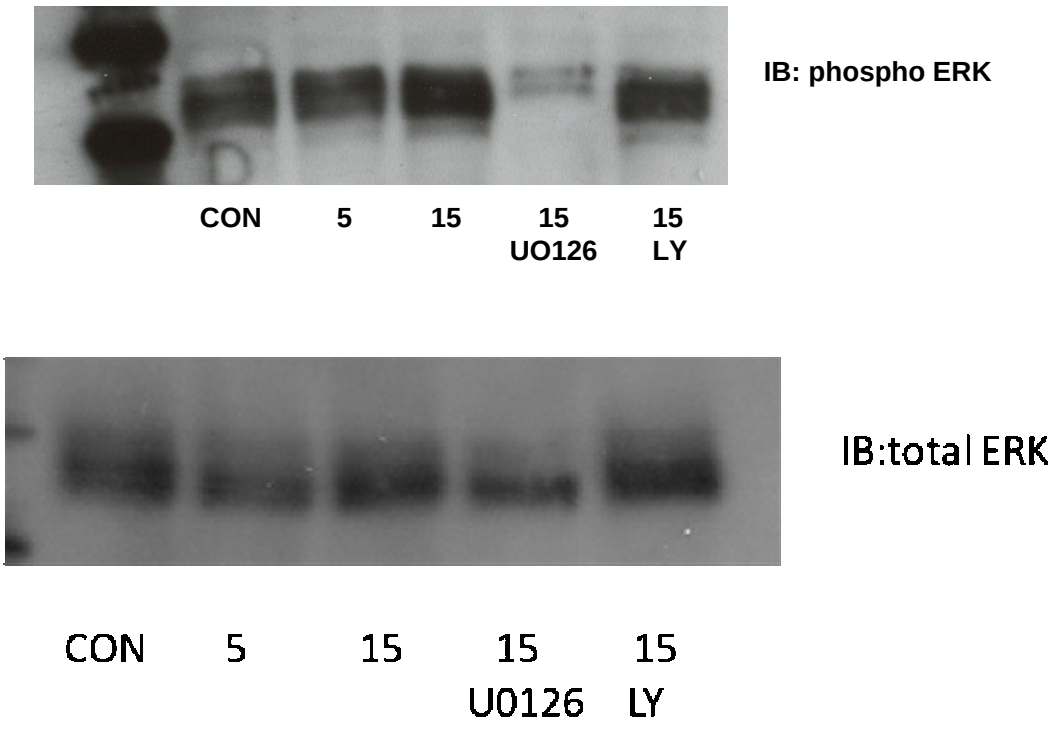

Figure 2.7 Immunoblot for Phospho-ERK 1/2

Serum-starved cells were stimulated with EPO for 5-15 minutes and then scraped on ice and underwent protein extraction. Immunoblots with a specific primary antibody for phospho-ERK were performed. (Figure is presentative of three separate experiments). Inhibiting MEK1 with pre-administration of UO126 markedly reduced ERK phosphorylation by EPO.

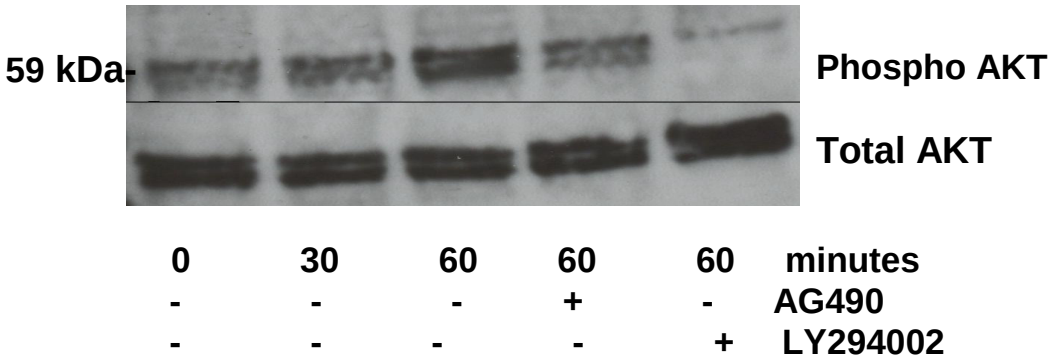

Figure 2.8 AKT activation by EPO

Immunoblots for phospho-AKT (serine 478) in HK-2 cells stimulated with EPO for 30-60 minutes. Maximum band density was observed in cells stimulated for 60 minutes. This increase in phosphorylation was reduced by the addition of a JAK2 inhibitor, confirming the dependence of EPO-R signalling on JAK2 activity, and completely prevented by LY294002, a reversible inhibitor of PI3-kinase.

Figure 2.9 Loss of AKT activation following inhibition of JAK2 expression

AKT phosphorylation (serine 473) in response to EPO stimulation is prevented in cells transfected with JAK2 siRNA. All groups exposed to EPO 50 U/mL for 30 minutes. Representative blot shown from three separate experiments.

2.4.6 EPO attenuates Apoptosis following Serum Starvation

Deprivation of FCS from the standard medium causes a progressive loss of cell viability over time in HK-2 cells. HK-2 cells were plated out in standard medium in 96-well plate. After 24 hr, the standard medium was removed, and 100 µL of phenol-red free medium was replaced without FCS except in control wells. EPO was added in a range of final concentrations to experimental groups. The cells were incubated in normal conditions for 30 hrs and an MTS assay was performed. Serum deprivation caused a significant reduction in cell viability ($P< 0.01$). Dose-response experiments (EPO 1 -100 U/ mL) reversed the reduction in cell viability caused by 30 hrs incubation in serum-deprived conditions (EPO 1 U/L $P<0.01$; EPO 10 $P< 0.01$; EPO 20 U/mL $P< 0.001$; EPO 50 U/mL, $P< 0.001$), shown in Figure 2.10.

In parallel, extracted cell pellets from the end of experimental procedures were lysed in digitonin buffer and a DNA fragmentation ELISA was performed. Serum starvation induced a significant increase in DNA fragmentation (control 1.0 ± 0.1; starvation 1.93 ± 0.48, $P<0.01$). EPO treatment reduced the increase in DNA fragmentation (+ EPO 1.13 ± 0.33, $P<0.05$), shown in Figure 2.11. The lysates in which DNA fragmentation was measured were also used to examine the expression of proteins that regulate apoptotic signalling by immunoblotting. Serum starvation for 24 hrs was associated with a reduction in the expression of anti-apoptotic proteins XIAP and Bcl-X_L. EPO treatment was associated with increased expression of XIAP and Bcl-X_L. Representative blots from these experiments are shown in Figure 2.12.

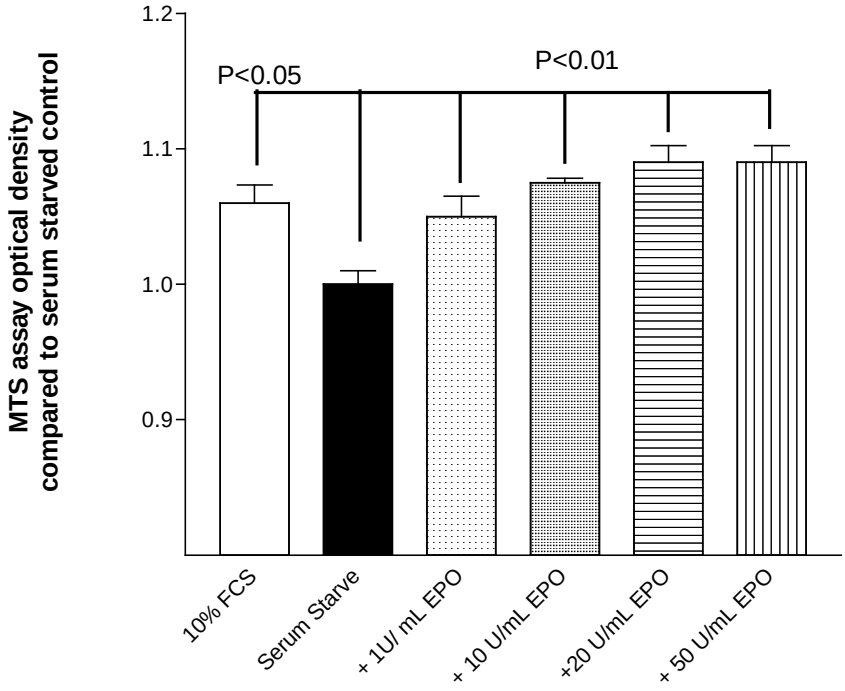

Figure 2.10 Cell viability following serum starvation with different concentrations of EPO was measured by MTS assay. At 30 hours, MTS values for treatment groups were expressed relative to cells exposed to serum starvation. Groups were compared by ANOVA.

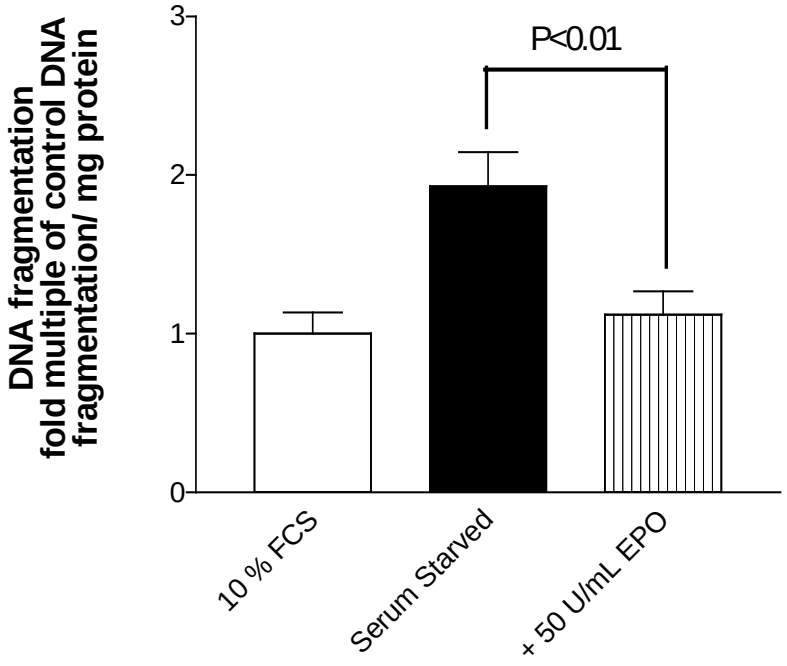

Figure 2.11 EPO reduces serum deprivation induced DNA fragmentation, measured by ELISA. Values for three experiments were expressed relative to control cells cultured with standard FCS. EPO significantly reduced DNA fragmentation (P<0.01 by ANOVA).

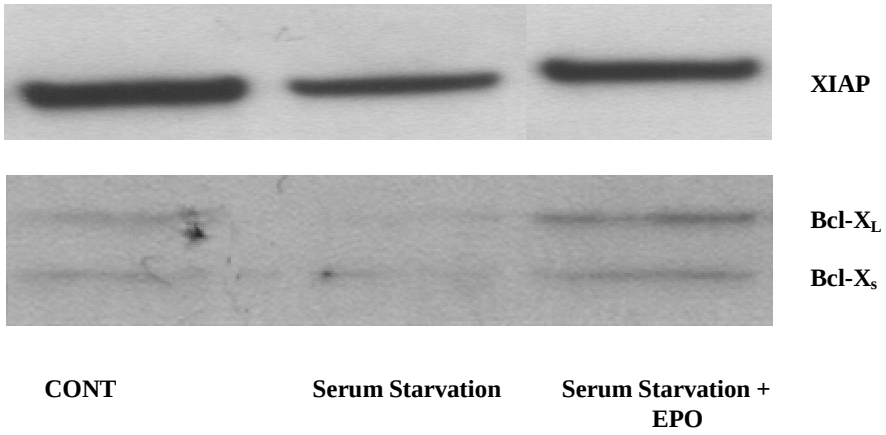

Figure 2.12 EPO maintains expression of XIAP and Bcl-X_L

Western blots on lysates from cells deprived of serum for 24 hours and cells deprived of serum for 24 hrs treated with EPO (50 IU/mL) were probed with primary antibodies for XIAP and Bcl-X_L. Serum starvation reduced the expression of both anti-apoptotic proteins, but administration of EPO caused maintenance of expression associated with a reduction in apoptotic cell death.

2.5 Discussion

The data presented in this chapter demonstrate the signalling processes initiated by the engagement of EPO with its cell surface receptor in human proximal tubular epithelial cells. The presence of the receptor on the particular cell line studied in these experiments was confirmed by the presence of an appropriately-sized strong band by immunoblotting, and also, independently, by the observation that knockdown of EPO-R expression by RNA interference completely abrogated the cellular response previously observed upon EPO stimulation.

Two bands were observed in the western blot for the EPO-R, at 59 and 68 kDA approximately. The 68-kDa band was similar in size to that observed from the erythroblastic cell line UT-7, known to highly express the EPO-R. There has been some debate concerning the size of the human EPO-R protein, which undergoes post-translational modification. Westenfelder *et al,* using the same commercial antibody, detected two EPO-R immunoreactive proteins in murine proximal tubular cells of approximately 68 and 90 kDa, respectively, and the 68 kDa protein was not observed in non-anaemic murine spleen suggesting that this represented the EPO-R [Westenfelder C, 1999]. The cloned murine EPO-R cDNA encodes a 55 kDa polypeptide, and the EPO-R is post-translationally modified by N-linked glycosylayion and phosphorylation, increasing its mass to approximately 76 kDa [Sawyer ST, 1993].

The ability of EPO-R siRNA to reduce intracellular signalling molecules and abrogate cell proliferation in the experiments described is strong evidence that these cells express a functional EPO-R. Recently, the specificity of the EPO-R antibody used in these

experiments has been questioned [Elliot S, 2006], as a dominant band at approximately 70 kDa was observed in cells which do not express the EPO-R, and the observed band could be abrogated by knockdown of HSP70 expression by RNA interference. Further studies have confirmed that the C-20 antibody does identify the EPO-R, but may show cross-reactivity with other proteins. EPO-R expression should be confirmed by either mRNA studies or functional studies with RNA interference, as was performed in these experiments [Verdner F, 2005]. The development of more specific commercial antibodies against the EPO-R is urgently required.

The described experiments demonstrated that EPO did have direct effects on the proliferation and survival of tubular cells in a cellular injury model. The protection from injury afforded by EPO in proximal tubule epithelial cells was dependent on the activation of EPO-receptor induced signalling. In neuronal cells, studies utilizing soluble EPO receptors and anti-EPO antibodies as competitive inhibitors of EPO receptor activation have confirmed that the effects of EPO *in vitro* are mediated via the EPO receptor [Ruscher K, 2002]. However, the recent development of a carbamylated erythropoietin molecule, CEPO, that does not stimulate erythropoiesis but retain a neuronal protective capacity, has questioned the uniqueness of the erythropoietin/ erythropoietin receptor interaction [Leist M, 2004]. These authors have suggested that EPO signalling in neuronal cells may be mediated through the interaction between the EPO receptor and a common β-subunit heteroreceptor [Brines M, 2004], although this observation has yet to be confirmed, and EPO retains its anti-apoptotic properties in cell lines that do not express the common β-subunit heteroreceptor [Um M, 2007].

Activation of JAK2 by EPO has been shown, in endothelial cells and neuronal cells, to lead to the activation of phosphatidylinositol-3 kinase (PI 3-kinase) and Akt phosphorylation. Once activated, Akt activates multiple targets with anti-apoptotic effects, including

phosphorylation of Bad, Bax, caspase-9 and GSK-3β, maintenance of mitochondrial membrane potential and preservation of glycolysis and ATP synthesis. Inhibition of PI 3-kinase inhibited the specific serine-473 phosphorylation of AKT induced by EPO. Therefore, one major mechanism by which EPO protects proximal tubule cells against injury is through the induction the EPO receptor-dependent activation of PI 3-kinase leading to phosphorylation and activation of its target Akt, and subsequent downstream pathways.

EPO inhibits apoptotic cell death in proximal tubule epithelial cells (as determined by DNA-fragmentation assay), and in higher doses, causes significant proliferation even in serum-free conditions. EPO administration was associated with the up-regulation of Bcl-X_L and XIAP. Bcl-$X_{L,}$ a member of the B cell lymphoma-2 family, has been shown to determine resistance to hypoxic insults *in vitro* [Dong Z, 2003]. Taken together, these *in vitro* findings support the conclusion that EPO directly protects proximal tubule epithelial cells by (i) binding to the EPO receptor and inducing JAK-2 kinase activity, (ii) with PI3K leading to phosphorylation of Akt and its downstream mediators, and (iii) up-regulation of a series of anti-apoptotic proteins including Bcl-X_L and XIAP. These experiments have demonstrated that EPO is functional in human proximal tubule cells, and led to the hypothesis that EPO would reduce tubular cell death in an animal model of kidney injury.

Chapter Three:

Effect of Erythropoietin Administration on a Short term model of ischaemia reperfusion in the rat

3.1 Introduction

As discussed in section 1.2, the outcome of AKI is a function of the interaction of multiple cell types in the tubular and vascular compartments of the kidney that must ultimately be understood at the whole tissue level, and is not predictable from the study of the behaviour of a single cell type.

This complexity necessitates an approach utilizing whole animal studies to unravel the mechanisms of injury and develop therapeutic modalities. This has led to the development of "single insult" models of renal injury induced by ischaemia, toxins and radiocontrast agents. An established animal model of ischaemia-reperfusion injury, which as far as possible mimics the type of renal injury observed in clinical medicine, in particular kidney transplantation, has been developed in the laboratory. This short-term model of ischaemia-reperfusion injury in the rat has been intimately characterised and is highly reproducible [Williams P, 1997; Chatterjee PK, 2003].

This model of bilateral renal artery occlusion in the rat is characterized histologically by widespread necrosis of proximal tubules, the distribution and extent of which vary with the ischaemic interval. The distal nephron is less affected, with mild damage in thick limbs of the loops of Henle and focal apoptosis rather than widespread necrosis in the distal convoluted tubules and collecting ducts. The S3 segment of the proximal tubule, which has the lowest oxygen tension in health, is most severely affected with between 20-90% of these segments showing lethal injury [Shanley PF, 1985]. In human AKI, morphological injury is usually more subtle and focal, affecting both proximal and distal tubules, although comprehensive biopsy series from patients with ischaemic AKI are lacking [Rosen S, 2008].

However, there are some important similarities between the rat model of ischemia and human AKI, with loss of the brush border, a predilection for the most severe injury to occur in the proximal straight tubules (S3 segments), prominent apoptotic cell death in the early phase, and the presence of luminal cast formation. Functional similarities between human ischaemic AKI and the renal artery occlusion model of AKI include the severe reduction in GFR and the reversibility, in most cases, of tubular injury with recovery of renal function.

3.2 Aims

The aim of this study was to determine whether EPO would have a protective effect in a model of ischaemia reperfusion injury in the kidney, an organ which is prone to ischaemic damage, and which expresses the EPO-receptor [Westenfelder C, 1999]. EPO had been used in a study in the management of anaemia in AKI in rats. Although there was no benefit in that study with regard renal function, mortality was significantly lower in the EPO treated animals [Nemato T, 2001].

A protocol of bolus administration of a single dose of EPO was devised from the design of studies of EPO cellular protection in models of cerebral ischaemic injury [Sakanaka S, 1998]. The aims of the experiment were to discover the biochemical and histological effects of EPO in an *in vivo* setting, and whether EPO was effective if administered at different timings relative to the initiation of tissue reperfusion.

3.3 Methods

3.3.1 *In vivo* rat model of ischaemia reperfusion (Short term)

Male Wistar rats (200-300g) were used in this procedure. Rats were kept in normal day/ night conditions and receive standard chow and water *ad libitum*. The protocol described has been approved by the U.K. Home Office and the care and use of animals is in accordance with the *Guidelines in the Operation of the Animals (Scientific Procedures) Act 1986*.

All rats were anesthetised with sodium thiopentone (Intraval® Sodium, 85 mg/kg i.p; Rhone Merieux Ltd., Essex, U.K.) and anaesthesia was maintained by supplementary infusions of sodium thiopentone. The fully anaesthetised rat is placed, on its back, onto a thermostatically controlled heating mat (Harvard Apparatus Ltd, Kent, UK) and body temperature was maintained at 38±1^{o}C by means of a rectal probe attached to a homeothermic blanket. A tracheotomy was performed to maintain airway patency and to facilitate spontaneous respiration. The right carotid artery was cannulated (PP50, I.D. 0.58mm, Portex, Kent, U.K.) and connected to a pressure transducer (Senso-Nor 840, Horten, Norway) for the measurement of mean arterial blood pressure (MAP) and derivation of the heart rate (HR) from the pulse waveform. The right jugular vein was cannulated (PP25, I.D. 0.40mm; Portex) for the administration of drugs. A midline laparotomy was performed and the bladder was cannulated (PP90, I.D. 0.76mm; Portex). 0.5 mL of normal saline was administered via the venous line to replace lost fluid. The venous line was connected to a constant-rate infuser pump and saline administered at a rate of 8 mL/Kg/ hr throughout the experimental period.

Animals were allowed to stabilize for 30 minutes after completion of preparatory surgery. Using a cotton bud to carefully move away the spleen and small intestine on the right hand side of the abdomen, the right kidney and the pedicle (containing renal artery and vein) was exposed. The pedicle was isolated and clamped using a Differenbach's bulldog artery clip. The intestine is replaced and the left kidney isolated and the pedicle clamped in the same way. Occlusion was verified visually by a change in the colour of the kidney to a paler shade and then to a darker (cyanotic) colour within minutes. The intestine was replaced into the peritoneum and the peritoneum closed with a small clip and covered with saline-soaked gauze. A total ischaemia time of 45 minutes was used for all experiments. The kidneys were carefully exposed, and the artery clamps removed with the aid of forceps to prevent tearing or localised injury to the renal pedicle. Reperfusion was confirmed by an immediate colour change in the kidney. The peritoneum was closed with a small clip and covered with saline-soaked gauze.

3.3.2 Biochemical analysis

At the end of the reperfusion period (6 hrs in all groups unless stated), blood (1 mL) samples were collected via the carotid artery into tubes containing serum gel. The samples were centrifuged (6000 *g* for 3 minutes) to separate the serum from which biochemical parameters, including creatinine, sodium and asparate transaminase (AST), a marker of tubular injury, were measured. All serum samples were analyzed within 24 hours of collection (Vetlab Services, Sussex, UK). Urine was collected throughout the reperfusion period and the volume recorded. Activity of urinary N-acetyl-β-D-glucosaminidase (NAG), a specific indicator of tubular damage [Bosomworth MP, 1999; Kotanko P, 2000] was also measured on snap frozen urine aliquots, performed by Dr Joaquim Chaves at the Clinica Medica e Diagnostico, Lisbon, Portugal.

3.3.3 Histological Evaluation

Kidneys were removed from rats at the end of the experimental period and were cut in sagittal section into two halves, which were fixed in immersion in 10% (wt/ vol) formaldehyde in phosphate buffered saline (PBS; 0.01M; pH 7.4) at room temperature for 24 hours. After dehydration using graded ethanol, pieces of kidney were embedded in Paraplast (Sherwood Medical, Mahwah, NJ) and cut in fine (8 μm) sections and mounted on glass slides. Sections were then deparaffinized with xylene, counterstained with hematoxylin and eosin, and viewed under a light microscope (Dialux 22, Leitz, Milan, Italy).

100 intersections were examined for each kidney and score from 0-3 was given for each tubular profile: 0 normal histology; 1, tubular cell swelling, brush border loss and nuclear condensation with up to 1/3 nuclear loss; 2, as for score 1, but greater than 1/3 and less than 2/3 tubular profiles showing nuclear loss; and 3, greater than 2/3 tubular profile shows nuclear loss. The histological score for each kidney was calculated by addition of all scores with a maximum score of 300, by two blinded histopathologists [Chatterjee PK, 2000]. Deparaffinized sections were also used for immunohistochemical analysis. Sections were incubated overnight with primary anti-caspase-3 antibody (1 in 10,000) in blocking buffer. After washing, secondary antibody was added for 30 minutes at 25˚C, followed by washing. A HRP containing buffer was added for a further 30 minute incubation before the slides were counterstained with haematoxylin, dehydrated and mounted for review by a blinded pathologist and the author.

In addition randomly picked sections were quantitatively assessed for apoptotic nuclei, and graded for severity, extent of nuclear changes, and the presence of nuclear debris and

apoptotic blobs**.** These were scored by a blinded pathologist and the author for three high-powered fields per animal.

3.3.4 Preparation of tissue Homeogenate for protein Analysis

Sections of experimental kidneys that had been snap-frozen in liquid nitrogen immediately after dissection, were weighed and approximately equal tissue samples by weight were used for homogenisation. The tissue block was cut into small pieces and placed in a sterile glass tissue homogeniser.

Buffer containing 25 mmol/L EDTA, 20 mmol/L EGTA, 10 mmol/L sodium hydroxide (pH 7.3) and Imidazole: HCl buffer containing 10 mmol/L mercaptoethanol (pH 7.3) was added according to dry tissue weight (1 mL / 250 mg tissue) and the tissue was homogenised with twenty equal strokes of the glass rod over 2 minutes. The suspension was aspirated by pipette into an eppendorff tube and then the samples were centrifuged at 14000*g* for 15 min at 4˚C. The resulting supernatant was aspirated into pre-chilled 1 mL Eppendorff tubes. Each sample was aliquotted into several tubes to avoid repeated thaw/ freeze cycles, and samples were kept on ice throughout the procedure.

3.3.5 End-point Caspase Activity Assay

The activity of caspase-3 was measured using the substrate Ac-DEVD linked to a fluorogenic 7-amino, 4-methylcoumarin (AMC) molecule. For *in vivo* experiments, frozen samples of harvested kidneys were washed in ice-cold PBS, and homogenized in ice-cold buffer containing 25 mmol/L EDTA, 20 mmol/L EGTA, 63.2 mmol/ L imadazole-HCl, 10 mmol/L 2-mercaptoethanol (pH 7.3). After centrifugation at 16000*g* for 15 minutes at 4˚C, the supernatant was aspirated and the amount of protein quantified using the BCA assay.

50 μg cellular protein was incubated with 50 μM substrate in caspase assay buffer (213.5 mM HEPES, pH 7.5, 31.25% sucrose, and 0.3125% CHAPS) for 1 hour, and fluorescence was measured on a microplate reader (Fluostar Galaxy, BMG Laboratory Technologies, Aylesbury, UK), with excitation at 380 nm and emission set at 460 nm. For each sample, four replicates were assayed, with two replicates containing 50 μM of the caspase-3 inhibitor (Ac-DEVD-CHO), and the remaining pair of replicates containing similar volume of vehicle (DMSO).

The activities of caspase-8 and caspase-9 were determined in the same way, using

Caspase 8: substrate **Ac-IETD-AMC** inhibitor: **Ac-IETD-CHO**
Caspase 9: substrate **Ac-LEHD-AFC** inhibitor: **Ac-LEHD-CHO**

Fluorescence readings from wells containing inhibitor were subtracted from total fluorescence, and results calculated as nmol AMC/ min/ per mg protein.

3.3.6 Experimental Design

The short term model of ischaemia reperfusion injury in the anaesthetised rat was used for all experiments described in this chapter. Experimental design was as below:

(1) Sham-operated rats (n=8)
(2) Sham-operated rats, EPO 300 U/Kg administered 30 minutes prior to sham clipping (n=8)
(3) Ischaemia-reperfusion (I/R) , animals subjected to 45 minutes bilateral renal pedicle clamping, followed by 6 hours reperfusion. (n=12)
(4) I/R, EPO administered 30 minutes prior to bilateral renal pedicle clamping. (n=12)

(5) I/R, EPO administered 5 minutes prior to reperfusion. (n=13)

(6) I/R, EPO administered 30 minutes into the reperfusion period. (n=12).

3.4 Results

3.4.1 Effect of Ischaemia reperfusion and EPO on Haemodynamic Parameters

Continuous arterial blood pressure was recorded throughout the experimental process in all animals. Hourly mean blood pressure was calculated for all experimental groups to determine whether EPO had any adverse or beneficial effect on haemodynamic parameters.

Resting mean arterial blood pressure in all experimental groups after stabilization was 130-140 mm Hg (*P*=ns). There was no significant effect on EPO administration on mean arterial blood pressure in sham operated animals. Ischemia reperfusion was associated with a non-significant fall in blood pressure in early reperfusion (Figure 3.1). When comparing each group as a series of BP measurements, there was no significant difference between I/R and EPO treated animals (ANOVA with bonferrari).

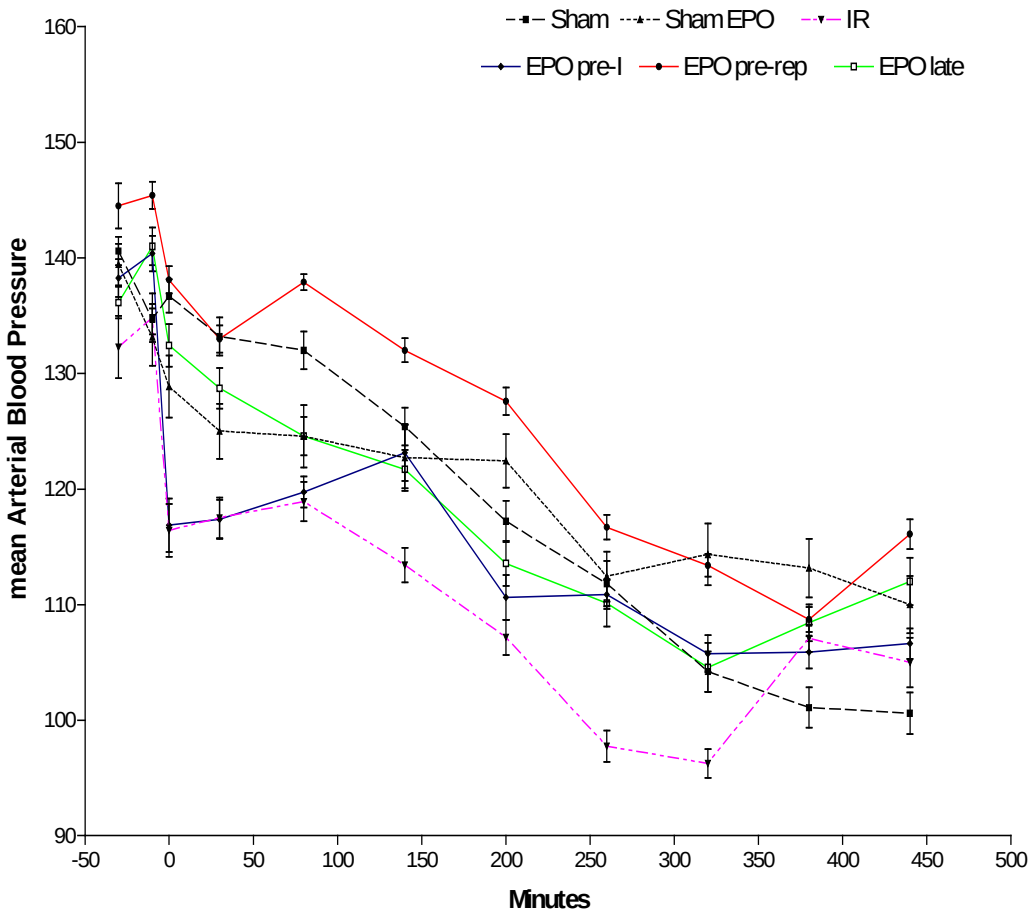

Figure 3.1 Mean arterial Blood Pressure during the Experimental Period in all experiments groups. Mean BP was calculated from the arterial pressure trasducer measurements and recorded every 30 minutes. Mean BP over the whole experimental period was similar in all groups (P=ns, ANOVA).

3.4.2 Effect of EPO on Renal Dysfunction caused by I/R

Routine biochemical parameters of kidney function were analysed in all experimental groups, including serum and urine creatinine and sodium. In comparison with sham animals, 45 minutes of ischaemia led to significant increases in serum, urinary and histological markers of renal dysfunction and injury after 6 hours reperfusion.

Administration of EPO to sham-operated animals did not have any effect on markers of renal function despite an increase in urine flow rate (Figure 3.4). Rats that underwent renal I/R exhibited significant increases in the serum concentrations of creatinine compared with sham-operated animals (serum creatinine: sham 53 ± 2 μmol/L; I/R 217 ± 7, P<0.001) (figure 3.2) and decreases in urine flow (sham animals 0.01 ± 0.0001 mL/hr; I/R 0.006 ± 0.001, ***P***<0.001) (figure 3.3) and creatinine clearance (sham animals 1.3 ± 0.1 mL/min; I/R 0.053 ± 0.016, ***P***<0.001) (figure 3.4), suggesting a significant degree of glomerular dysfunction.

In comparison with I/R animals, the administration of a single intravenous bolus of EPO (300 U/ kg), either pre-ischemia or just prior to the onset of reperfusion, produced a significant reduction in serum levels of creatinine (EPO pre I 144 ± 6; EPO post R 143 ± 7; EPO late 183 ± 8; ***P***<0.01) associated with maintenance of improved urine flow rate (EPO pre 0.022 ± 0.002; EPO post R 0.02 ± 0.002; EPO late 0.01 ± 0.007, ***P***<0.01) and creatinine clearance (EPO pre I 0.28 ± 0.05, EPO post-R 0.31 ± 0.05, ***P***<0.01). EPO administration 30 minutes after the onset of reperfusion still afforded renoprotection by attenuating the fall in glomerular filtration rate, and hence calculated creatinine clearance (figure 3.4).

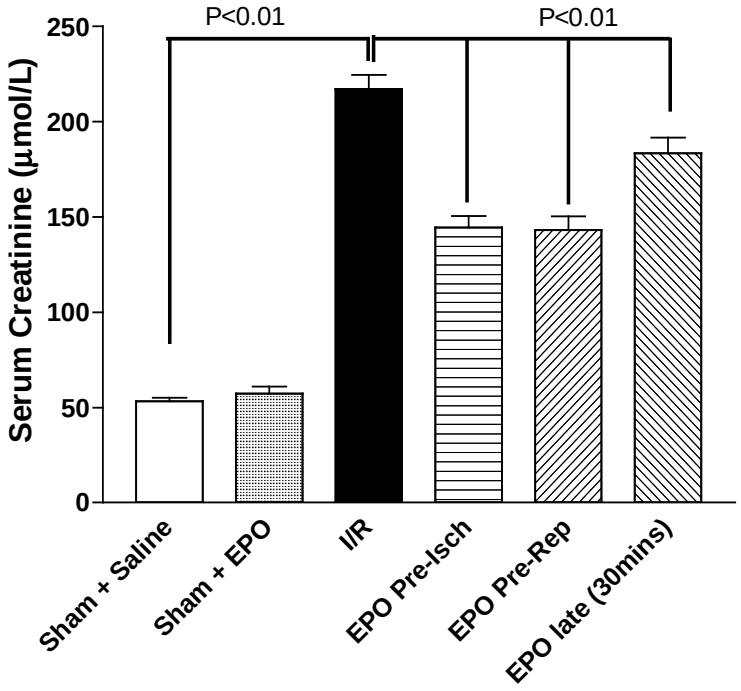

Figure 3.2 Serum Creatinine after six hours Reperfusion in all experimental groups. Creatinine in the I/R group was compared with all treatment groups by ANOVA.

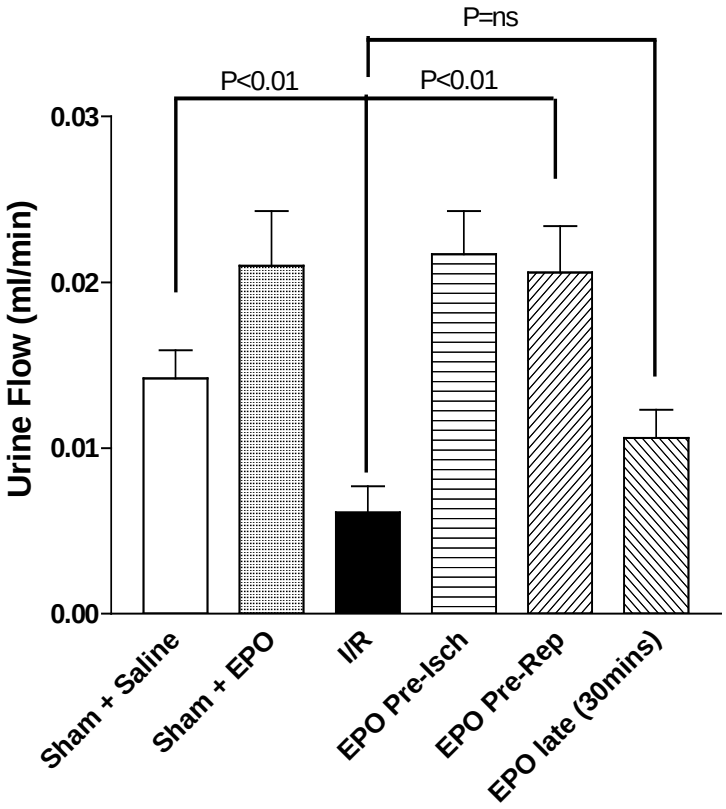

Figure 3.3 Urine Flow rates following Ischaemia-Reperfusion were measured in all experimental groups. When compared with I/R injury, urine flow was significantly maintained in EPO treated animals (P<0.01 by ANOVA).

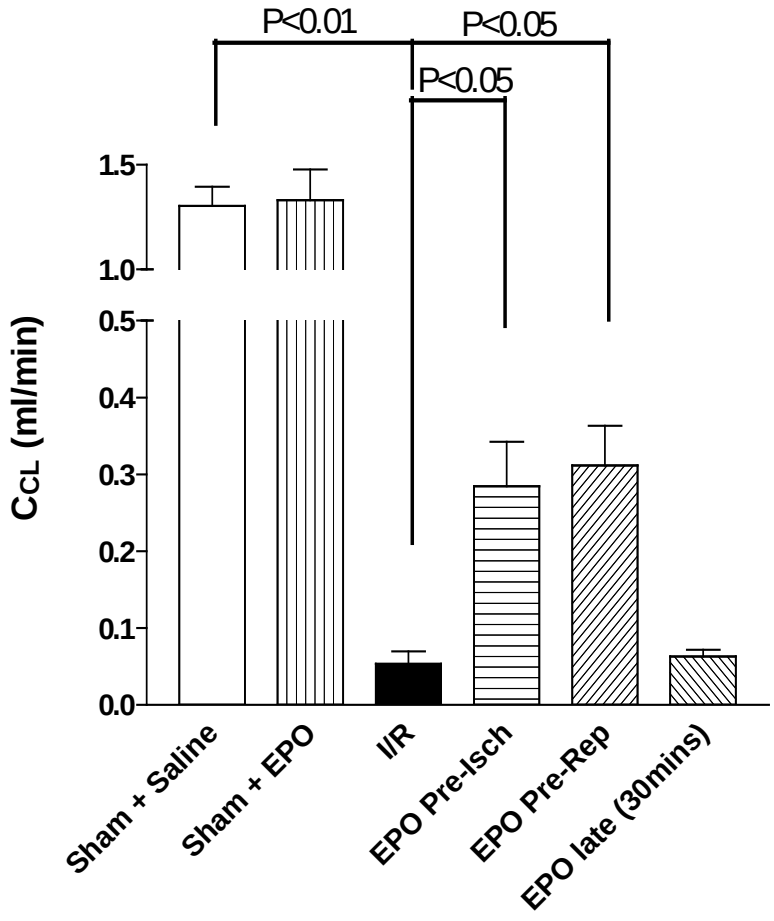

Figure 3.4 Calculated Creatinine Clearance following Reperfusion was calculated from urinary creatinine and urine flow in all experimental groups. Effect of treatment with EPO was compared against I/R by ANOVA. Pre-treatment and Pre-reperfusion treatment significantly maintained creatinine clearance (P>0.05 by ANOVA).

3.4.3 Effect of EPO on Biomarkers of Ischaemia-Reperfusion induced Tubular Injury

In comparison with values obtained from sham-operated animals, renal I/R produced a significant increase in urinary N-acetyl-β-D-glucosaminidase (NAG) activity (sham 8 ±2, I/R 22.7 ± 5.6, **P**<0.05), a specific marker of tubular dysfunction, corrected for urine volume. Serum concentrations of the enzyme asparate transamininase (AST) was analysed as a marker of tubular injury induced by reperfusion [Chatterjee PK, 2000]. Fractional excretion of sodium, as a quantitative marker of tubular function was calculated from the formula:

$$FE_{Na}(\%) = uNa\ [\mu mol/\ L] \times urine\ flow\ [mL/\ min]/\ C_{CL}\ [mL/min] \times sNa\ [\mu mol/\ L] \times 100),$$

I/R injury significantly increased sodium excretion (sham 1.3 ± 0.18 %; I/R 19.9 ± 5.9, *P*<0.01), demonstrating a reduction in tubular conservation of sodium. EPO administration was associated with a significant reduction in urinary NAG activity (sham 8 ± 2, I/R 22 ± 5.6, EPO pre 9.9 ± 3.0, EPO post 7.9 ± 0.8, P<0.01), shown in Figure 3.5, and preservation of tubular function, measured by maintenance of sodium excretion (EPO pre-reperfusion 7 ± 0.5 %, ***P***<0.05) shown in figure 3.6. There was insufficient sample to measure sodium excretin in the EPO late (30 mins) group.

Renal I/R also produced a significant increase in serum AST (sham 200 ± 30, I/R 1864 ± 232, P<0.01). Administration of EPO caused a significant reduction in serum AST levels (EPO pre 522 ± 40, EPO post 607 ± 64, EPO late 1130 ± 177, P<0.01), shown in Figure 3.7, suggesting a marked reduction in tubular injury and hence preserved tubular function post reperfusion-injury.

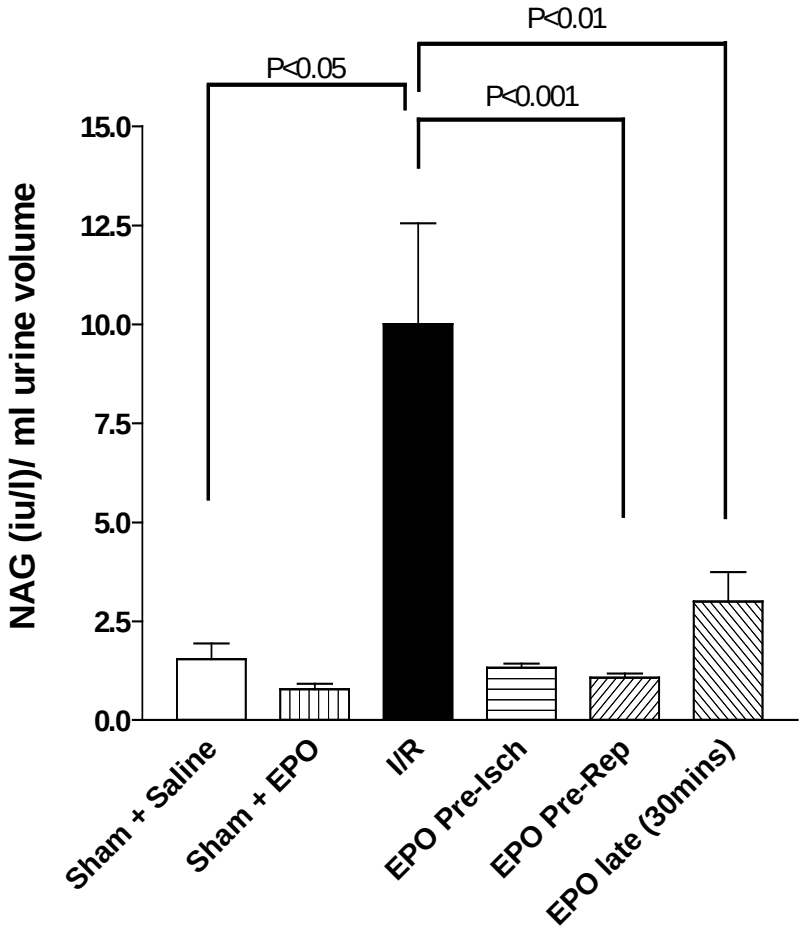

Figure 3.5 Tubular injury measured by urinary NAG concentration following renal I/R injury in the rat. Measurements were corrected to urine volume. Treatment groups were compared to I/R by ANOVA. EPO treatment was associated with significantly lower urine NAG (P<0.001 by ANOVA).

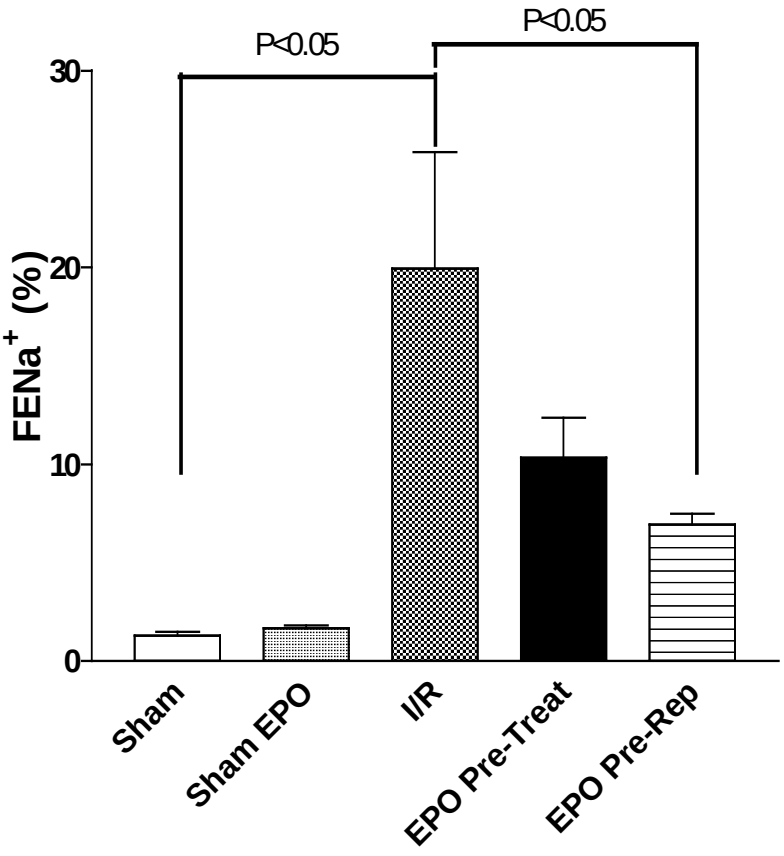

Figure 3.6 Tubular Functional reserve by Fractional Sodium Excretion following Reperfusion Injury. When compared with I/R injury, there was a significant decrease in the change in sodium excretion in EPO treated animals (P<0.05 by ANOVA).

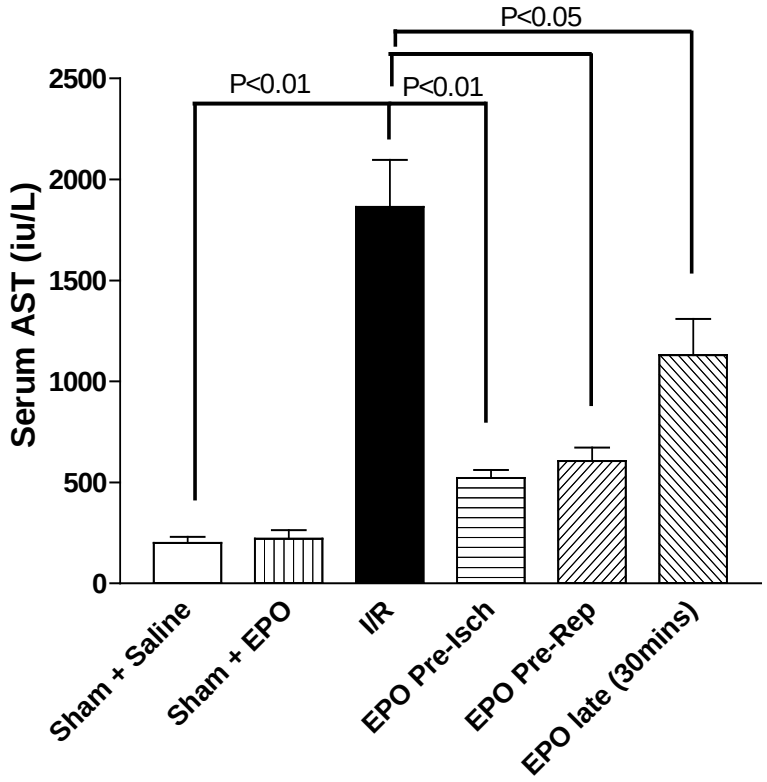

Figure 3.7 AST, a marker of Tubular Reperfusion Injury at Six Hours in all Experimental Groups. Comparision with I/R injury, by ANOVA, showed a significant reduction in tubular injury with early EPO treatment (P<0.01 by ANOVA).

3.4.4 Effects of EPO on Histological Alterations Caused by Renal I/R

Renal I/R caused marked alterations in renal histology when compared with kidneys taken from sham-operated animals. Specifically, this included widespread degeneration of tubular architecture, tubular dilatation, cell swelling and necrosis, luminal congestion with loss of brush border and infiltration of polymorphonuclear neutrophils (PMNs) (Figure 3.7 A and B). In contrast, renal sections obtained from animals treated with EPO pre ischaemia, or pre-reperfusion, demonstrated marked reduction of the histological features of renal injury. EPO administration 30 minutes after the onset of reperfusion was still associated with a significant reduction in injury, but this reduction was less marked than in the other treatment groups (Figure 3.7 C and D). Scoring of histological changes is shown in Figure 3.9.

Initially, TUNEL staining was attempted to gain a qualitative score for apoptotic cell death. Unfortunately, there was very high background staining which did not allow adequate discrimination of positive staining. In view of this, proximal tubular cell apoptosis was examined on serial sections under high power field, randomly selected by a blinded pathologist and then scored by the author and the pathologist and scores combined.

Kidneys from animals subjected to renal I/R showed extensive nuclear changes consistent with apoptotic cell death (Figure 3.10). In comparison, kidneys from sham-operated animals had no evidence of apoptosis. EPO administration prior to ischaemia, and pre-reperfusion significantly reduced the extent of apoptotic cell death ($p<0.05$). EPO administration 30 minutes after the onset of reperfusion caused only a small reduction in the number of apoptotic cells, but there was a reduction in the incidence of necrotic cell death.

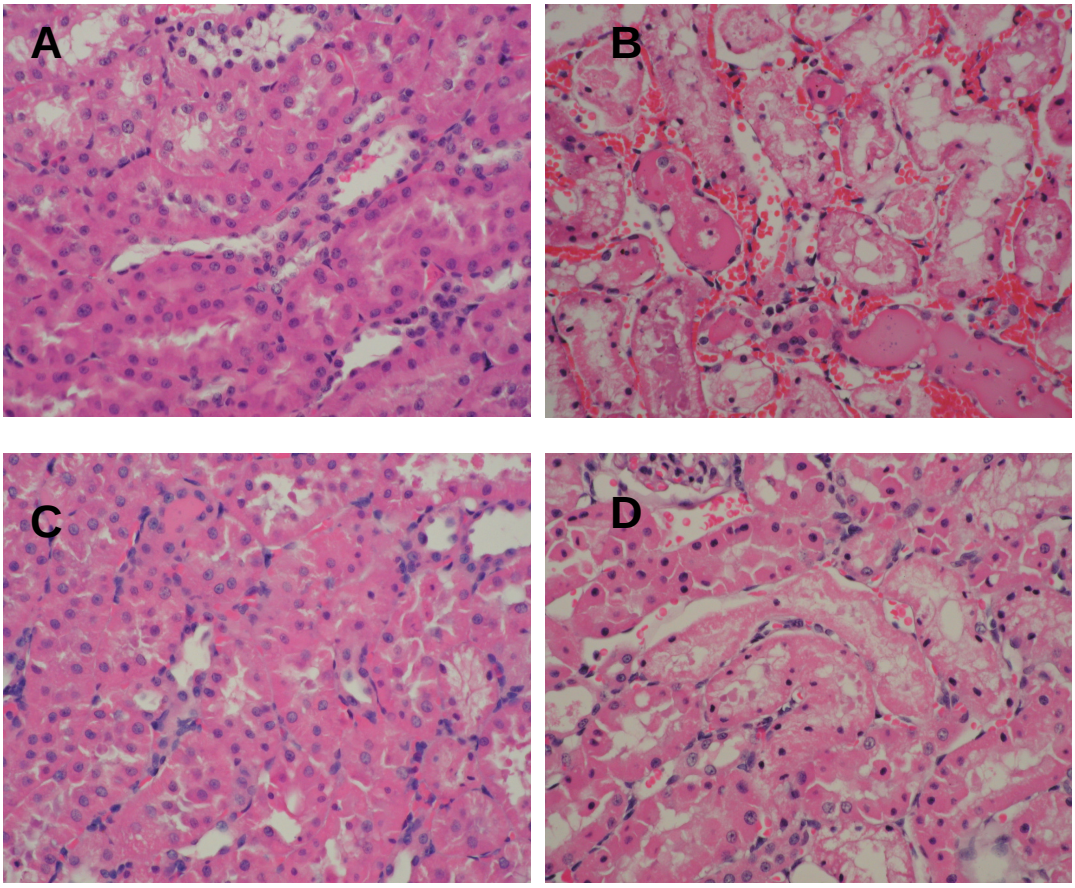

Figure 4.8 Histological Assessment of Renal Injury

Kidney sections taken from:

(A) sham operated rat

(B) renal ischemia-reperfusion. Renal sections from a rat subjected to renal I/R after administration of

(C) EPO pre-ischemia (30 min), and

(D) EPO post reperfusion (30 min)

Haematoxylin and eosin-stained kidney sections (magnification x150).

Figures are representative of at least three animals (n=5 for all groups).

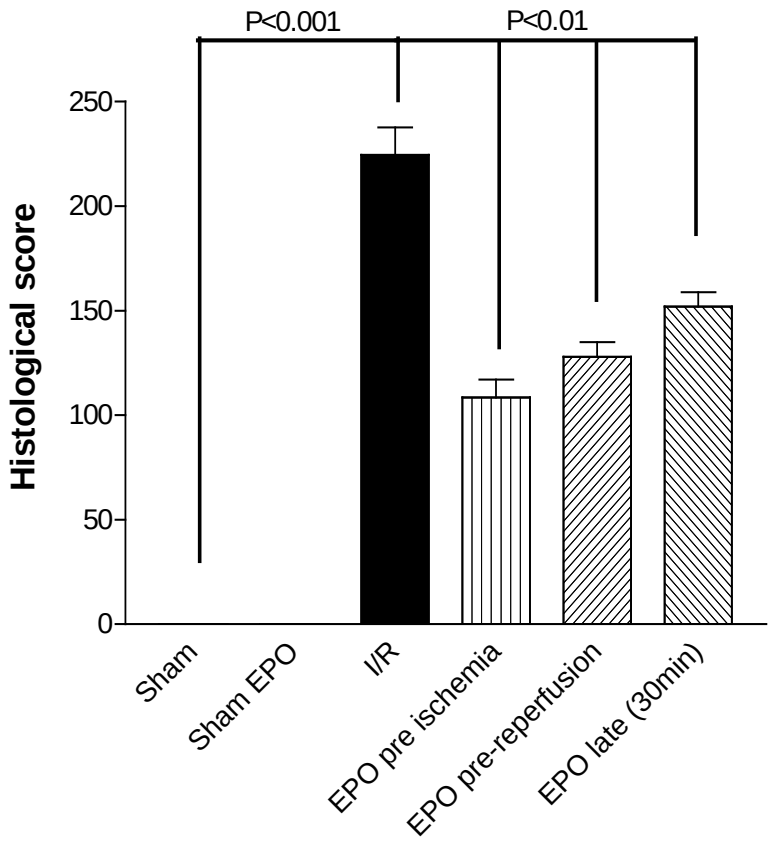

Figure 3.9 Histological assessment of Renal Injury following Reperfusion (method described in section 3.3.3). Scores for treatment groups were compared with I/R by ANOVA.

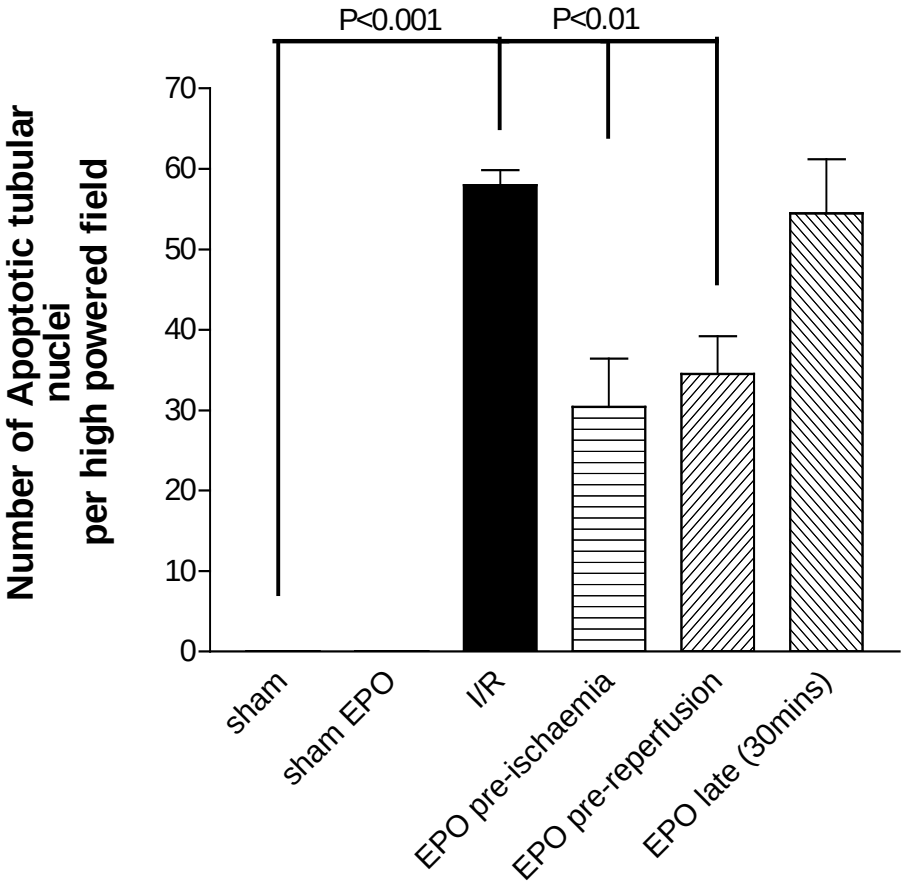

Figure 3.10. Quantitative scoring of apoptotic nuclei in high-powered fields was used to determine the extent of apoptotic cell death. Measurements were combined from the author and a blinded pathologist. Four fields were examined for each specimen, and an average score taken. Scores were analysed by ANOVA.

3.4.5 Effect of EPO on Caspase-3 activity *in vivo*

Animals subjected to ischaemia reperfusion were sacrificed during the reperfusion period after two, four and six hours respectively. Kidney tissue was harvested and then snap-frozen in liquid nitrogen. Tissue samples (n=6) for each group were homogenised and caspase activity measured. When compared to immediately pre-reperfusion, there was a significant time-dependent increase in caspase-3 activity (0hr 118 ± 28, 4 hr 239 ± 21 $P<0.01$, 6 hr 282 ± 40 $P<0.001$), shown in figure 3.11.

Caspase-3 activity (nmol/ min/ mg total protein at 37ºC) was significantly increased in the homogenates of kidneys at 6 hours in kidneys subjected to renal I/R, when compared with sham-operated animals ($p<0.01$). The elevation in caspase-3 activity was significantly reduced by EPO administration, both pre-ischaemia ($p<0.05$) or just prior to reperfusion ($p<0.05$). EPO treatment 30 min after reperfusion was associated with a non-significant reduction in caspase-3 activity, consistent with the higher levels of apoptosis observed in these kidneys (figure 3.12).

Immunohistochemical staining, described in 3.3.3, using a specific antibody to the cleaved active fragment of caspase-3 confirmed these observations. There was widespread positive cytoplasmic and perinuclear staining in both cortical and medullary tubules following I/R (Figure 3.13 B, representative image (n=4 for all groups)), when compared to sham animals (Figure 3.13 A). The severity and distribution of staining was greatly reduced in animals receiving EPO either pre-ischemia (Figure 3.13 C) or pre-reperfusion, but only partially when EPO was administered later in reperfusion (Figure 3.13 D).

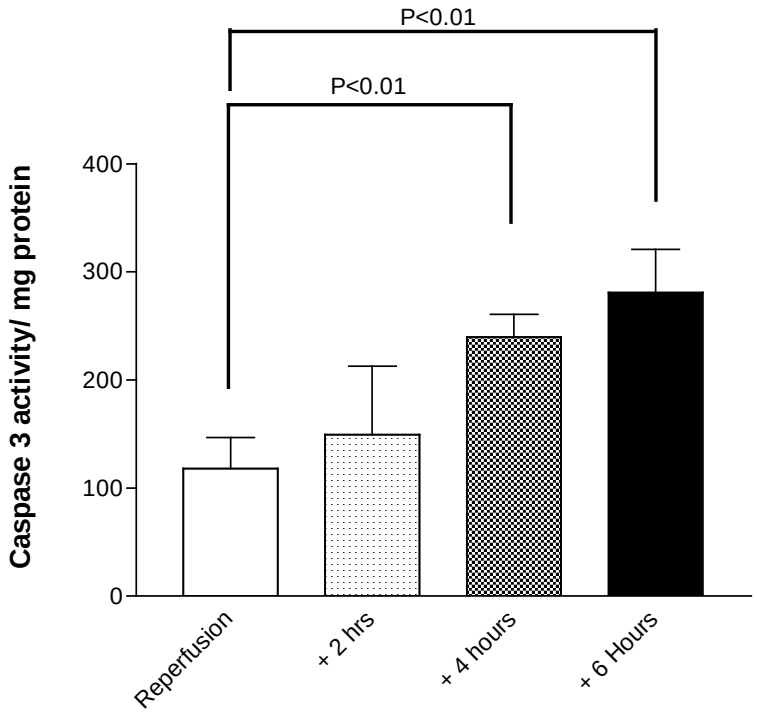

Figure 3.11 Time course of Caspase-3 activity following reperfusion from kidneys snap-frozen at time points after reperfusion. Six kidneys were analysed for caspase activity for each time point. There was a significant increase in caspase-3 activity in later time points (P<0.01 by ANOVA).

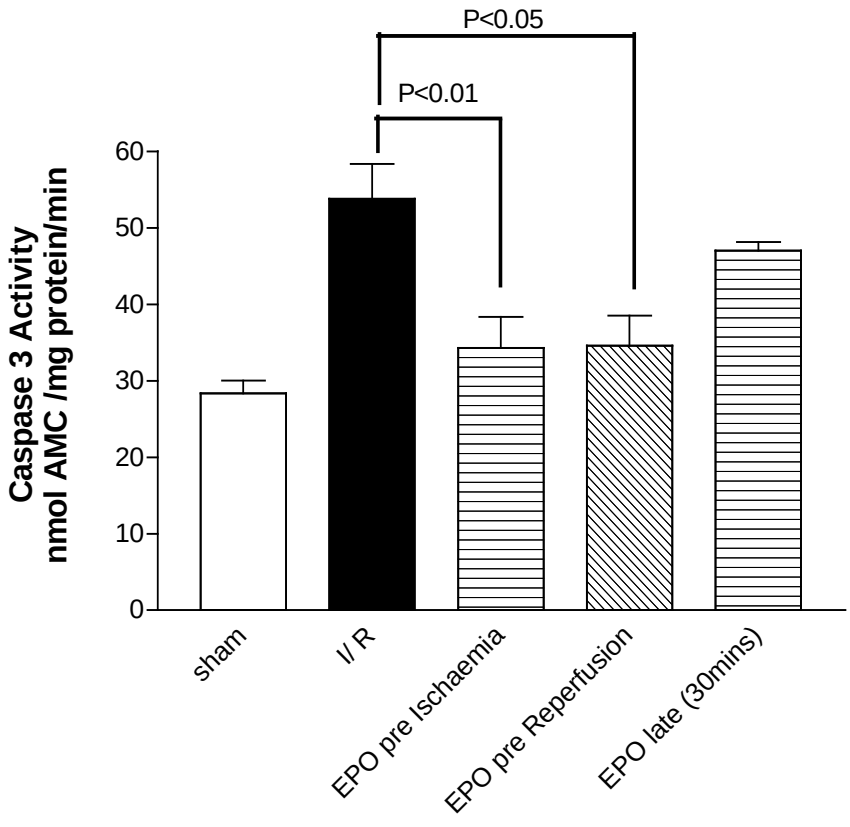

Figure 3.12 Tissue Caspase Activity following Six hours reperfusion in all Experimental groups. Kidneys from each group (n=6) were homogenised and caspase-3 activity measured. EPO treatment caused a significant decrease in caspase-3 activity at six hours (P<0.01 by ANOVA).

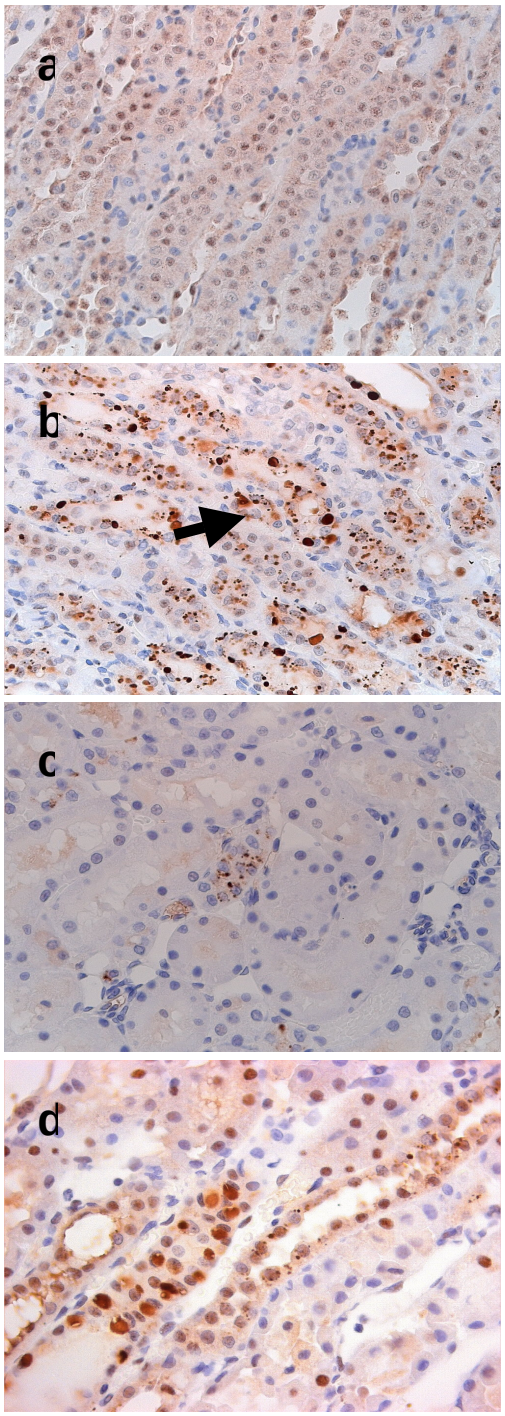

Figure 3.13 Immunohistochemistry for active caspase-3 in Representative Specimens in Experimental Groups – a. Sham, b. I/R, c. EPO pre-ischaemia, and d. EPO re-reperfusion (representative image from n=5 kidneys each group). Arrow shows cytoplasmic positive caspase-3 fragments in proximal tubule.

3.4.6 Effect of EPO on Caspase-9 and Caspase-8 activity *in vivo*

Having demonstrated that apoptotic cell death was reduced, and that this was mirrored by a significant decrease in the activation of the executioner caspase-3, the relative contributions of the extrinsic and intrinsic (mitochondrial) pathways in the activation of caspases-3 were examined. Both pathways have been shown to participate in ischaemia-reperfusion injury. Caspase-8 and caspase-9 activity was assayed in tissue homogenates from all experimental groups.

Following I/R, activity of caspase-9 was significantly increased when compared to sham-operated animals (sham 218 ± 20, I/R 300 ± 21, $P<0.01$). The increase caspase-9 was attenuated by EPO treatment (EPO pre-reperfusion 230 ± 7, $P<0.05$), shown in Figure 3.14.

When compared sham-operated animals, ischaemia reperfusion caused an increase in the activity of caspase-8 at six hours (sham 38 ± 5, I/R 144 ± 48, $P<0.01$). Treatment with EPO as a pre-treatment, or just prior to reperfusion significantly reduced the increase observed (EPO pre-ischaemia 48 ± 17, $P<0.01$; EPO pre-reperfusion 56 ± 38, $P<0.01$), shown in Figure 3.15.

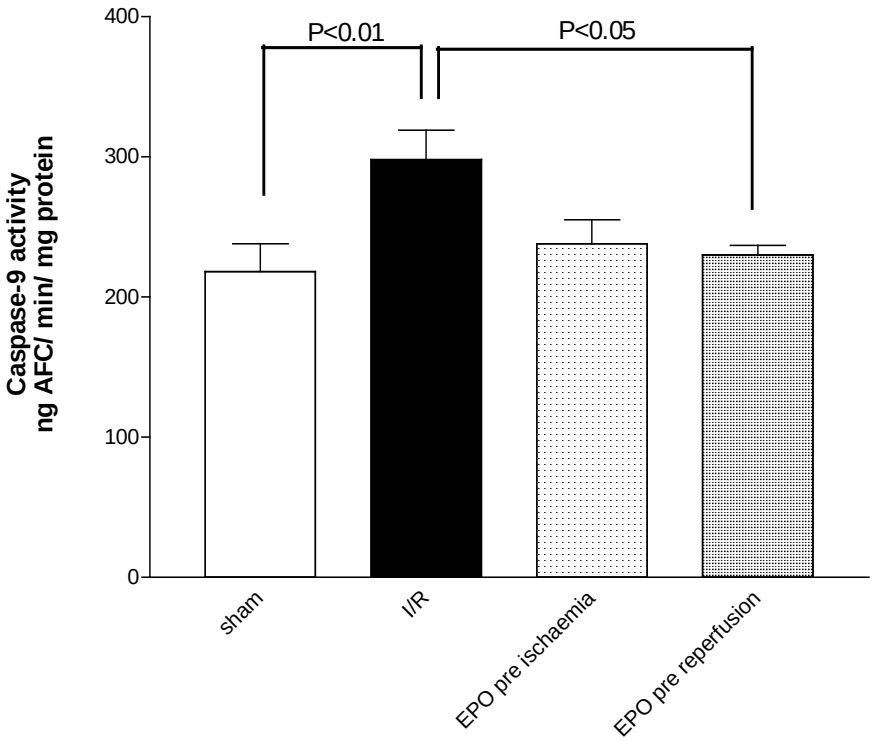

Figure 3.14 Caspase 9 Activity in kidney tissue homogenates following I/R injury was analysed as described in 3.3.5. EPO treatment was associated with significantly lower caspase-9 activity following I/R (P<0.05 by ANOVA).

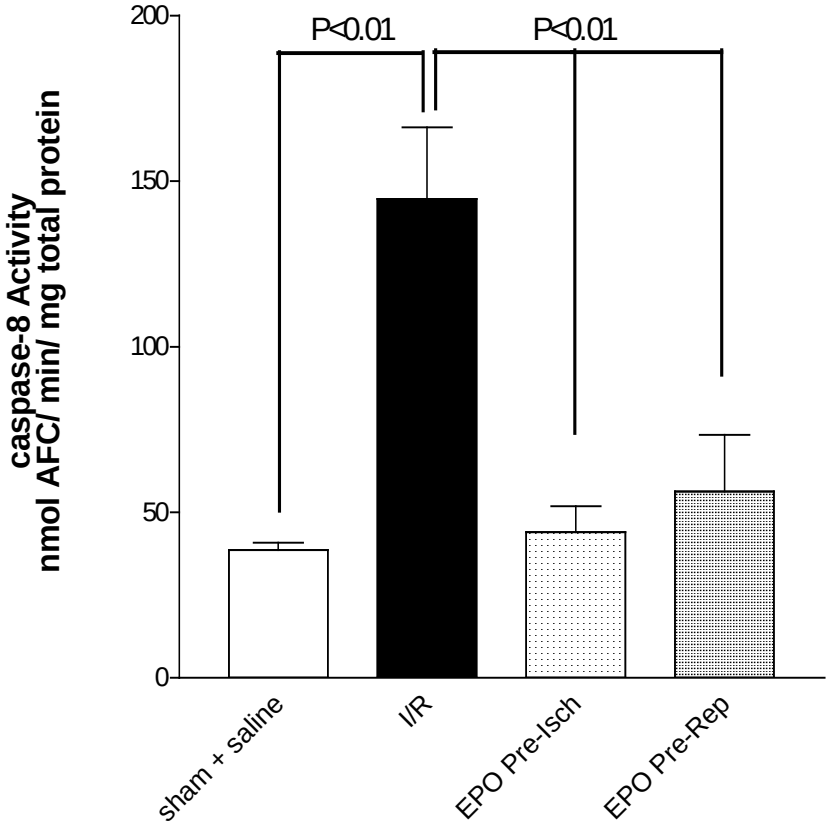

Figure 3.15 Caspase-8 Activity in kidney tissue homogenates following I/R injury showed a reduction in activity in EPO treated animals when compared to I/R (P<0.05 by ANOVA).

3.5 Discussion

Following from the results in chapter two, which showed direct effects of EPO on tubular epithelial cells in culture, the studies described in this chapter demonstrate that recombinant human EPO is able to reduce the degree of injury in the kidney following ischaemia-reperfusion (I/R) injury.

EPO reduced both the glomerular and tubular injury and dysfunction, assessed by both biochemical and histological parameters, caused by severe bilateral renal ischaemia and reperfusion in the rat. EPO reduced I/R injury when administered as a single intravenous bolus injection, either prior to the onset of ischaemia (30 min pre-treatment) or when given immediately before release of clamps (pre-reperfusion). Most notably for its potential use as a therapeutic agent in clinical settings, EPO even partially protected kidney function against I/R injury when given 30 min after the onset of reperfusion, although there was more severe histological damage and more apoptotic cells.

The degree and extent of injury induced by ischaemia in control animals in this model was consistent with previously published work [Chatterjee PK, 2000]. Morphological studies have clearly demonstrated the existence of both necrosis and apoptosis in animal models of AKI [Rana A, 2001], and there is recognition of the importance of apoptosis in the initiation phase of renal injury, and the presence of apoptotic tubular epithelial cells has been demonstrated in kidneys of humans with ischaemic AKI [Castaneda MP, 2003]. Chemical inhibition of the caspase cascade has been shown to protect the kidney in a similar model of ischaemia-reperfusion in the mouse [Daemen MA, 1999]. The reduction in renal injury by EPO was associated with a significant decrease in the number of apoptotic tubular epithelial cells, and a reduction in caspase-3 activity, which suggest that EPO may partially mediate its effects by acting directly on tubular epithelial cell resistance to cell death through the up-

regulation of anti-apoptotic mechanisms. The use of immunohistochemical techniques to determine tubular localisation of the active fragment of caspase-3 was good specific evidence to confirm the quantitative assessment of tubular apoptosis used in the absence of TUNEL staining. There was also a reduction in the activities of caspase-8 and caspase-9 at six hours post-reperfusion. I/R causes the upregulation of inflammatory cytokines including TNF-α which lead to cell death through the receptor-mediated caspase-8 pathway. A reduction in cell death and hence a reduction in inflammation and cytokine release following EPO treatment may limit the pathways that induce further apoptosis by preventing cytokine-dependent amphification of cellular injury.

A number of potential beneficial effects of EPO in the kidney may account for the organ protection observed, which may not require direct effects on tubular cell death. An increase in renal blood flow might contribute to or even account for the observed protective effects of EPO. This is, however, unlikely, as there was no significant haemodynamic effect of acute administration of EPO on the systemic circulation. Although EPO increased urine flow rate in sham-operated rats, suggestive of a possible effect on cortical perfusion and intra-glomerular pressure, creatinine clearances were similar between the sham operated groups, and there was no difference in tubular function measured by fractional sodium excretion induced by EPO in sham animals. This observation is consistent with the study by Huang *et al*, which demonstrated no immediate effect on isolated cortical and papillary perfusion in normal rats following acute EPO administration [Huang C, 1992].

Chapter Four:

Effect of Erythropoietin Administration on Recovery Models of Ischaemia-Reperfusion Injury

4.1 Introduction

The experiments described in chapter three showed that EPO given at the time of reperfusion, or as an immediate pre-treatment 30 minutes before ischaemia, was effective in attenuating the degree of renal injury observed at six hours. In this model, the extent of injury at six hours is predictive of the maximum renal dysfunction at 24 hours, and the natural history of the model shows progressive recovery of function after 24 hours, although histological recovery occurs more slowly with the development of fibrosis [Williams P, 1997].

It was recognized in 1986 that brief periods of ischaemia render an organ resistant to subsequent more prolonged ischaemic period, known as ischaemic preconditioning. Four cycles of five minutes of coronary artery occlusion prior to 40 minutes occlusion reduced infarction size by 75% [Murry CE, 1986]. This protective effect was lost when three hours occlusion was applied, reinforcing the vital need for timely reperfusion to limit damage. Ischaemic preconditioning offers two "windows" of protection in time - "early" or "classical" providing protection immediately after the preconditioning stimulus, and "late" or "delayed" preconditioning being effective for up to 24 hours. Activation of HIF-dependent signaling pathways, including EPO, has been shown to play an important role in ischaemic preconditioning in the heart and kidney [Cai Z, 2003; Hill P, 2008]. Cobalt administration to rats, via up-regulation of HIF-dependent proteins including EPO, VEGF and haem-oxygenase-1 (HO-1), diminished the degree of renal injury caused by ischemia-reperfusion [Matsumoto M, 2003].

A pre-conditioning therapy would be attractive in clinical scenarios where renal dysfunction is predictable, such as cardiac surgery, repair of aortic aneurysm or organ transplantation. The mechanism of renal protection from pre-conditioning therapy is potentially different from that observed in the short term model with EPO administered at the time of

reperfusion. Preconditioning may allow the synthesis of new anti-apoptotic signalling molecules which mediate organ protection, and there is evidence that endogenous nitric oxide (NO), possibly derived from endothelial NO synthase, plays an important role in delayed conditioning [Bolli R, 1997]. When renal tubular epithelial cells are exposed to repeated hypoxic insults, a clone of more resistant cells are selected, which show increased expression of anti-apoptotic proteins, including Bcl-2 and particularly Bcl-X_L [Brooks C, 2007]. Induced Bcl-X_L overexpression reduces apoptosis in animal model of ischaemia-reperfusion [Chien CT, 2007], and the pre-conditioning expression of this anti-apoptotic pattern might be HIF-dependent [Chen N, 2008].

4.2 Aims

The aim of this study was to determine whether EPO would also have a protective effect in a longer, recovery model of ischaemia reperfusion injury in the kidney. The aims of the experiments were to confirm that the biochemical and histological effects of EPO observed in the early phase post-reperfusion, as described in chapter three, were still present during the maintenance and recovery phase of AKI. The recovery model also was used to determine the relative effects of a pre-conditioning regime during which EPO was administered for 3 days before ischaemic injury.

4.3 Methods and Materials

4.3.1 Recovery Model of Ischaemia Reperfusion in the anaethetised Rat

When compared to the short-term model used in chapter three, the recovery model requires that the incision is closed and the animal recovers and survives during the period of experimentation. Experience in the laboratory had previously shown that the large abdominal wound used in the short term model was associated with wound breakdown and infection leading to reduced animal survival. A dorsal approach leaves a sutured wound that is virtually impossible for the animal to disrupt with its teeth or claws. Metallic surgical staples were used rather than sutures for closure of the skin incision to avoid any potential for loosening or cutting.

Male Wistar rats (200-300g) were used in this procedure. Rats were kept in normal night/ day conditions and receive standard chow and water *ad libitum*. The protocol described has been approved by the U.K. Home Office and the care and use of animals is in accordance with the *Guidelines in the Operation of the Animals (Scientific Procedures) Act 1986.* Animals were anaesthetised with halothane, and placed on a sterile mat headed by an overhead lamp. Fur was shaved over the dorsal spine bilaterally, and an incision in the skin and fascia was made. The abdominal wall was identified and opened with a small (< 1.0 cm incision). Each kidney was identified and mobilised on its pedicle by blunt dissection of the peri-renal fat and connective tissue. Once fully mobilised, the renal pedicle was clamped with a Differenbach's bulldog artery clip. Cessation of renal perfusion was confirmed by the development of colour change in the kidney. The kidney was replaced in the abdominal cavity, and the incision temporarily closed with a clamp. At 45 minutes, the kidney was mobilized and the clamp removed. Immediate "pinking-up" of the kidney confirmed adequate reperfusion. Animals were given 5 mls intrabdominal saline and subcutaneous

analgesia (pethidine). The abdominal wall incision was closed with interrupted sutures and the skin was closed with staples. Animals were placed in a cage under a heating lamp and observed until anaesthetic had worn completely off. Animals were anaethetized for terminal venesection, and then sacrificed at 24 hrs, 48 hrs and 72 hrs after the onset of reperfusion.

4.3.2 Murine Model of ischaemia-reperfusion Injury

Male C57BL/6J mice (Charles River, Milan, Italy) weighing 25 to 30 g were used to assess the role of EPO in the pathogenesis of renal I/R in the mouse. Mice were allowed access to food and water *ad libitum* and were cared for in compliance with Italian regulations on protection of animals used for experimental and other scientific purposes (D.M. 116192), as well as with the European Economic Community regulations (O.J. of E.C. L358/1 12/18/1986). These experiments were performed with the technical assistance of Dr. N. Patel.

Mice were anesthetized using chloral hydrate (125 mg/kg, intraperitoneally) and core body temperature maintained at 37°C using a homoeothermic blanket. Mice were maintained under anaesthesia for the duration of ischaemia (i.e., 30 minutes). After performing a midline laparotomy, mice in I/R groups were subjected to bilateral renal ischemia for 30 minutes, during which the renal arteries and veins were occluded using microaneurysm clamps. The time of ischaemia chosen was based on that found to maximize reproducibility of renal functional impairment, while minimizing mortality in these animals. After the renal clamps were removed, the kidneys were observed for a further 5 minutes to ensure reflow after which 1 mL saline at 37°C was injected into the abdomen and the incision was sutured in two layers. Mice were then returned to their cages where they were allowed to recover from anaesthesia and observed for 24 hours. Sham-operated mice underwent identical surgical procedures to I/R mice except that microaneurysm clamps were not applied.

4.3.3 Experimental Design

The recovery model of ischaemia reperfusion was performed in the following experimental groups:

(1) Sham operated (n=8)

(2) Ischaemia reperfusion (n=12)

(3) Ischaemia reperfusion – administered EPO 1000 U/Kg at reperfusion (n=10)

(4) Ischaemia reperfusion – administered EPO 1000U / Kg two hours post-reperfusion (n=8)

Mice were divided into the following four groups in experiments involving the acute administration of EPO:

(1) I/R group in which control mice underwent renal ischemia for 30 minutes followed by reperfusion for 24 hours (N = 11)

(2) I/R EPO prereperfusion group included mice that were administered EPO (1000 IU/kg subcutaneously bolus) 5 minutes prior to reperfusion (N = 10)

(3) sham group were sham-operated mice, which were subjected to the surgical procedures described above, but were not subjected to renal I/R (N = 4)

(4) sham EPO prereperfusion group were mice that were treated identical to sham mice except for the administration of EPO (1000 IU/kg subcutaneously) 5 minutes prior to sham reperfusion (N = 4).

In the above experiments, the route of administration and dose of EPO were based on that of a previously reported experiment in the mouse. Mice, which did not receive EPO, were administered 8 mL/kg saline (vehicle for EPO) at equivalent time points (5 minutes prior to reperfusion). In experiments involving the chronic administration of EPO, mice were divided into the following four groups:

(1) I/R group included control mice, which underwent renal ischemia for 30 minutes followed by reperfusion for 24 hours (N = 6)

(2) I/R EPO pretreatment group mice were administered EPO (1000 IU/kg/day subcutaneously) for 3 days prior to I/R (N = 6)

(3) sham group were sham-operated mice, which were subjected to the surgical procedures described above, but were not subjected to renal I/R (N = 4)

(4) sham EPO pretreatment-group were mice that were treated identical to sham mice except for the administration of EPO (1000 IU/kg/day subcutaneously) for 3 days prior to sham I/R (N = 4).

Mice, which did not receive EPO, were administered 8 mL/kg/day saline (vehicle for EPO) at equivalent time points (72, 48, and 24 hours before operation).

4.3.4 Measurement of Tissue Myeloperoxidase Activity

Myeloperoxidase (MPO) activity in kidney samples was determined as an index of polymorphonuclear (PMN) leukocyte accmulation. Kidneys were homogenized in a solution containing 0.5% hexa-decyl-trimethyl-ammonium bromide and 10 mmol/L 3-(N-morpholino)-propane-sulfonic acid dissolved in 80 mmol/L sodium phosphate buffer (pH 7), and centrifuged for 30 minutes at 20,000*g* at 4°C. An aliquot of the supernatant was then allowed to react with a solution of tetra-methyl-benzidine (16 mmol/L) and 1 mmol/L hydrogen peroxide.

The rate of change in absorbance was measured by a spectrophotometer at 650 nm. MPO activity was defined as the quantity of enzyme degrading 1 μmol peroxide/min at 37°C and was expressed in units per gram weight of wet tissue.

4.4 Results

4.4.1 Effect of EPO administration in a recovery model of ischaemia reperfusion injury.

Biochemical parameters were studied in animals subjected to I/R injury and groups were sacrificed at different time points between 24 – 72 hrs following recovery.

The natural history of I/R in this model showed a peak in serum creatinine at 24 hrs (sham animals (n=8) creatinine 34 ± 3, I/R (n=12) 193 ± 74, $\boldsymbol{P}<0.01$), which had returned to near normal levels by 96 hrs (Figure 4.1). EPO was administered as a single sub-cutaneous injection (1000 U/ Kg). EPO administered at the time of reperfusion significantly attenuated the rise in creatinine at 24 and 48 hrs (creatinine in EPO treated animals 24 hrs 65 ± 31, $\boldsymbol{P}<0.001$). When administered two hours after reperfusion, EPO therapy was associated with a similar reduction in the rise in creatinine (creatinine at 24 hrs 90 ± 35, $\boldsymbol{P}<0.01$), when compared to control animals.

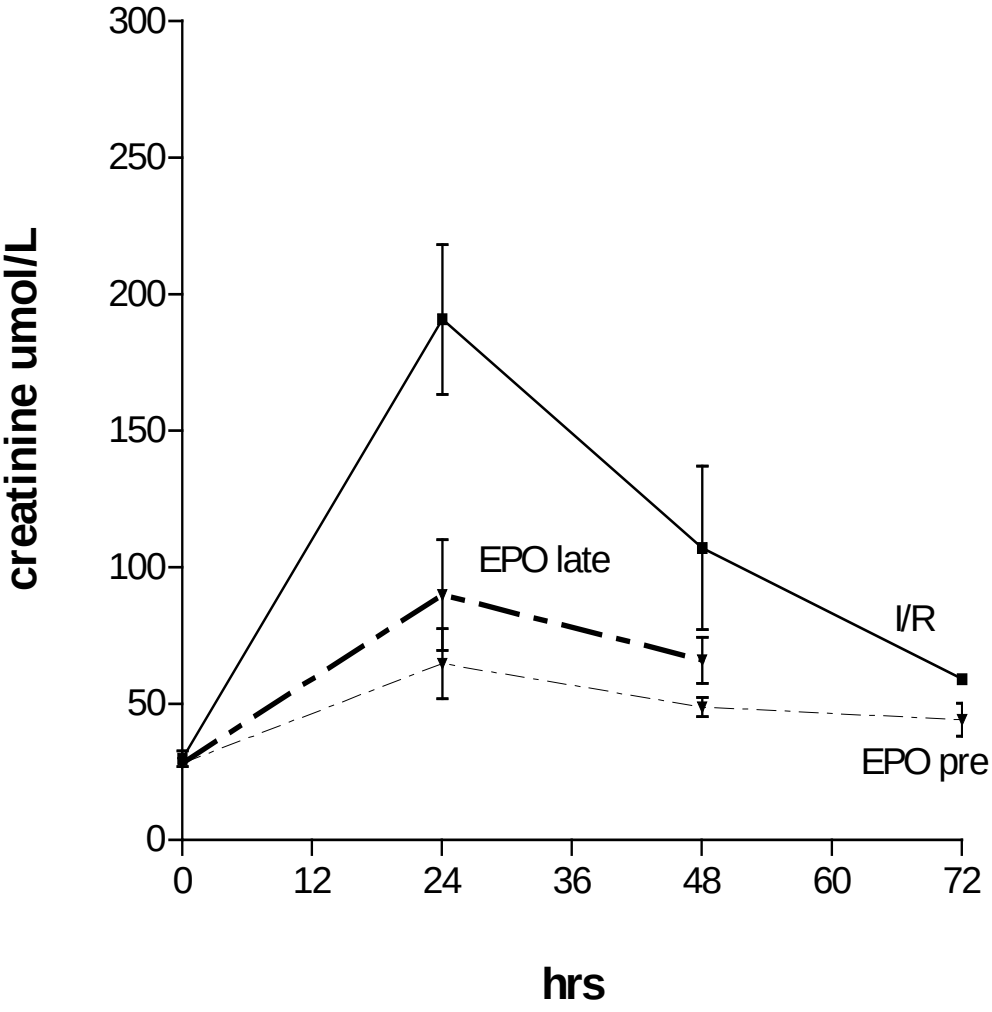

Figure 4.1 Serum Creatinine following I/R injury in the Recovery Model was measured at 24, 48 and 72 hours. I/R caused a significant increase at 24 hours when compared to sham animals (P<0.01). EPO treatment prevented this increase (dashed line), and there was a significant reduction in creatinine at 24 hours even when EPO was administered 2 hours into reperfusion (P<0.05)

4.4.2 Effect of Administration of EPO on renal dysfunction in the Mouse

When compared to sham-operated mice, I/R caused a significant increase in the plasma levels of creatinine in control mice (serum creatinine: sham 18 ± 7 μmol/L; I/R 170 ± 6, ***P***<0.001), suggesting a significant degree of renal dysfunction. Administration of EPO, at reperfusion (1000 IU/kg) or, as pre-conditioning (1000 IU/kg/day for 3 days prior to I/R), attenuated the rise in serum creatinine observed by I/R in control mice (EPO at reperfusion 128 ± 9; EPO pre-conditioning 70 ± 22, ***P***<0.01) (Figure 4.2).

Histological examination of kidneys obtained from control mice subjected to I/R demonstrated a significant degree of renal injury. Specifically, kidneys obtained from these animals exhibited degeneration of tubular structure, tubular dilatation, swelling and necrosis, luminal congestion, and eosinophil infiltration. In contrast, renal sections obtained from mice treated with EPO acutely (1000 IU/kg prior to reperfusion) and chronically (1000 IU/kg/day prior to I/R) demonstrated a marked reduction in the severity of these histological features of renal injury, when compared with kidneys obtained from control mice subjected to I/R only (Figure 4.3).

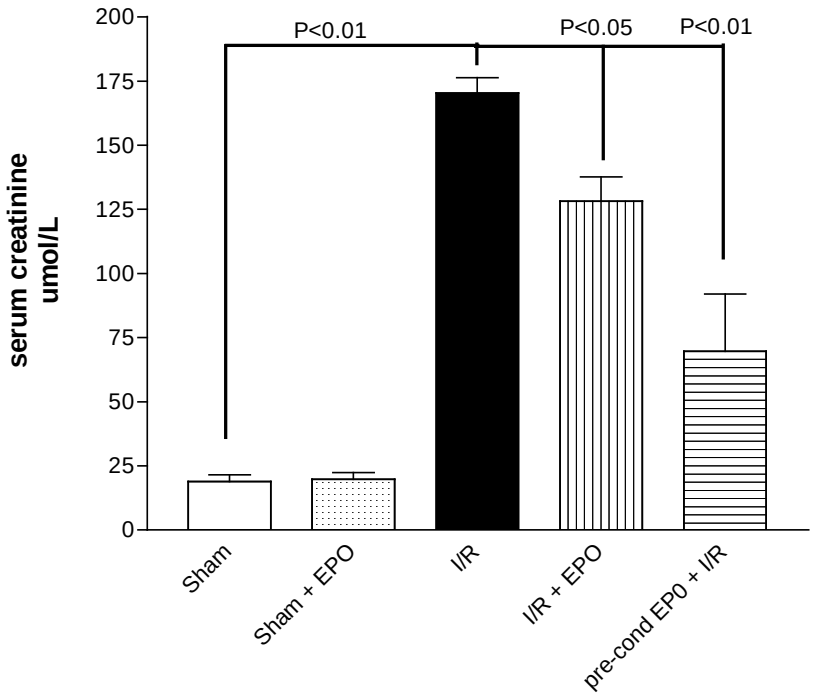

Figure 4.2 Renal function at 24 hours in Mice subjected to I/R injury was significantly preserved in animals treated with EPO (P<0.05) at reperfusion, with greater protection with pre-conditioning regime (P<0.01, by ANOVA).

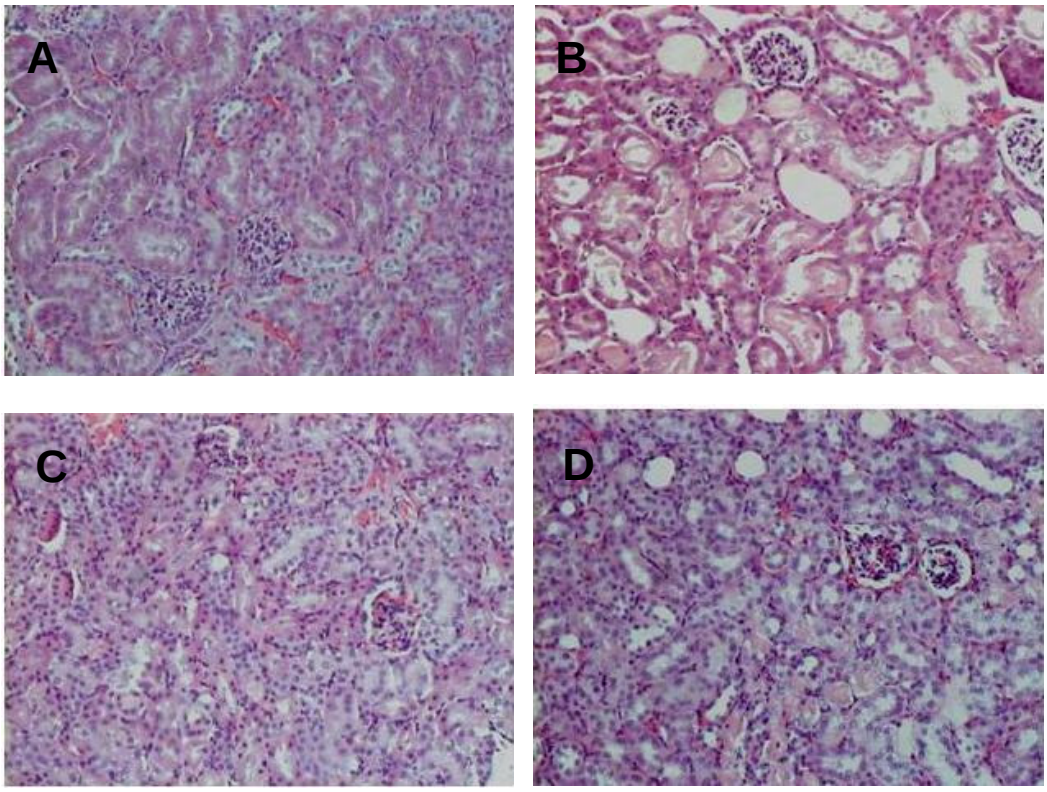

Figure 4.3 Histological Analysis of Mouse kidneys subjected to I/R Injury

Representative sections of kidney tissue from mice sacrificed 24 hours following I/R injury.

A Sham operated animal

B I/R injury

C I/R injury with EPO administered at reperfusion

D I/R injury after 3 days pre-conditioning with EPO (1000 U/ Kg)

4.4.3 Effect of EPO on renal inflammation caused by Ischaemia-Reperfusion

When compared to sham-operated mice, the kidneys obtained from control mice subjected to I/R demonstrated a significant increase in MPO activity (sham animals 3 ± 0.3; I/R 66 ± 9.8, ***P***<0.001), suggesting increased PMN infiltration into renal tissues. The increase in the tissue level of MPO seen in mice administered EPO, either acutely (1000 IU/kg prior to reperfusion) or chronically (1000 IU/kg/day prior to I/R) was significantly smaller than those seen in control mice subjected to I/R (EPO pre-reperfusion 15.2 ± 8; EPO pre-conditioning 5.5 ± 1.7, both ***P***<0.01), which in the case of chronic EPO treatment were similar to values obtained from sham-operated mice (figure 3.5). It should be noted that the chronic administration of EPO reduced the MPO levels to levels which were not different from those observed in sham-operated animals.

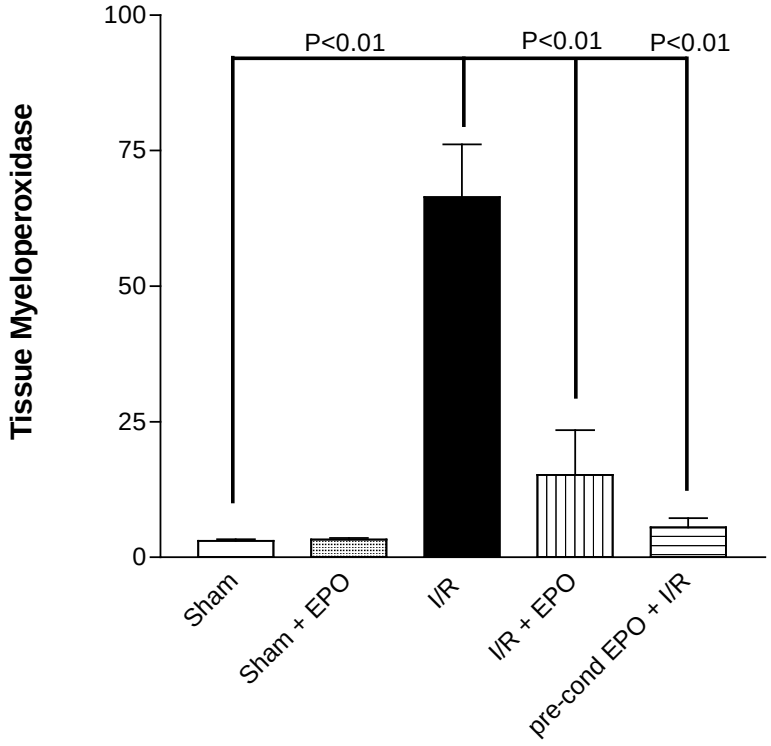

Figure 4.4 Tissue Myeloperoxidase Concentration following I/R Injury in the Mouse was measured as a marker of inflammation. I/R induced a significant rise in tissue MPO (P<0.01). EPO treatment prevented the development of inflammation following I/R (P<0.01 by ANOVA).

4.5 Discussion

In this series of experiments, EPO reduced the renal dysfunction and degree of injury caused by bilateral occlusion and reperfusion observed both at 24 and 48 hours after organ reperfusion. This beneficial response to EPO administration was observed in both rat and mouse models of ischaemia-reperfusion injury.

In mice subjected to renal I/R, EPO (1000 IU/kg given 5 minutes prior to reperfusion) significantly attenuated the renal dysfunction (increases in plasma creatinine) and characteristic histological signs of marked tubular injury. A significant reduction in polymorphonuclear neutrophil accumulation, measured by MPO assay was also observed. All this data confirmed a well-known pattern of renal dysfunction and injury caused by I/R of the kidney. Moreover, our findings are in agreement with the notion that renal ischaemia causes both renal and tubular dysfunction, as well as secondary inflammation.

Pre-conditioning pre-treatment of mice with EPO (1000 IU/kg/day for 3 days) also reduced the renal injury, dysfunction, and inflammation caused by bilateral renal artery occlusion in the mouse. Interestingly, the degree of protection afforded by this regimen with EPO was greater than the one afforded by the acute administration of a single dose of EPO at the time of reperfusion. There are several potential explanations for this finding. First, one could argue that the pre-treatment protocol has resulted in favourable systemic or local renal hemodynamic effects. However, although acute administration of EPO (in the rat) has no effect on blood pressure or cortical and pyramidal perfusion, repetitive administration of EPO for up to 1 week caused a small reduction in cortical blood flow [Huang C, 2001]. This would argue against EPO induced haemodynamic changes in glomerular filtration rate, but might contribute to the induction of delayed pre-conditioning pathways.

Secondly, as the half-life of EPO is 10 hours in the rodent, it is possible and likely that the repetitive administration of 1000 IU/kg subcutaneously per day for 3 days (pre-treatment protocol) resulted in a higher steady-state plasma concentration, when compared to the peak concentration achieved from a single dose administration prior to reperfusion (1000 IU/kg prior to reperfusion).

Thirdly, pre-treatment of mice with EPO for 3 days may well have resulted in the up-regulation of protective genes, including endothelial nitric oxide synthase (eNOS), maganese superoxide dismutase (Mn-SOD) and heat shock protein 70 (HSP70), which in turn could have contributed to the observed protective effect, mimicking the effects of delayed ischaemic preconditioning, which is protective in animal models of ischaemic myocardial and brain injury, and is mediated by the up-regulation of multiple factors, including EPO, vascular endothelial growth factor and haem-oxygenase-1, which improve tissue performance in response to metabolic stress under the control of the oxygen sensor hypoxia-inducible factor-1 (HIF-1). The effects of delayed preconditioning were lost in HIF-1+/- mice [Cai Z, 2003]. The crucial role of the down stream effects of EPO production in delayed preconditioning of brain injury has been demonstrated by the attenuation of protection observed with the use of a soluble EPO receptor, and *in vitro*, medium transfer from hypoxic and glucose-starved astrocytes to untreated neurons induced protection against hypoxia in neuronal cells, which was attenuated strongly by the application of a soluble EPO receptor and anti-EPO receptor antibodies [Ruscher K, 2002]. The main difference is that, unlike treatment at reperfusion, preconditioning with the pre-treatment protocol enables increased protein synthesis and not simply activation of existing protein messengers.

Fourth, the recent findings that bone marrow–derived stem cells contribute to the regeneration of proximal tubule epithelial cells following I/R injury also creates an attractive hypothesis that the protection observed with EPO pretreatment is partially due to an increase

in the mobilization and circulation of endothelial progenitor cells and possibly bone marrow–derived stem cells. It has been shown in mice that EPO treatment caused a significant increase in the percentage of proliferating lin-/sca-1+ stem cells in the bone marrow and mobilization of endothelial progenitor cells [Heeschen C, 2003; Bahlmann FH, 2003]. There is evidence that the pretreatment protocol of EPO used here results in enhanced levels of circulating endothelial progenitor cells. Most notably, it has been suggested that the increase in circulating endothelial progenitor cells by EPO contributes to the beneficial effects of EPO in animal models of I/R. It is, however, not known whether enhanced circulating levels of endothelial cell progenitors protect the kidney against I/R injury or improve endothelial repair and hence recovery of renal function after an acute ischaemic event.

The effects of EPO in a mouse model of ischaemia reperfusion described in this chapter have demonstrated that the observed effects in the rat are confirmed in a different species, increasing the likelihood of these effects being applicable to human studies. This is an important observation, as other growth factors such as insulin-like growth factor-1 (IGF-1) that were effective in one animal model have subsequently been not shown similar results in studies in rats or human clinical trials [Hirschberg R, 1999].

The beneficial effect of EPO on the course of ischaemic AKI has now been confirmed in several other studies [Yang CW, 2003; Vesey DA, 2004]. Yang *et al* administered high dose EPO (5000 U/ Kg IP) 24 hrs before the induction of ischaemia, and observed a significant degree of renal protection, and suggested that EPO caused the up-regulation of heat-shock protein 70 (HSP70). Vesey *et al* used a less severe animal model (nephrectomy and unilateral renal ischaemia), and demonstrated a significant reduction in both necrotic and apoptotic cell death, particularly in the region of the cortico-medullary junction

.

Having demonstrated that EPO prevents the renal injury induced by ischaemia reperfusion in an animal model, associated particularly with a significant reduction in the degree of apoptotic cell death, the next step was to determine whether EPO would have a direct effect on proximal tubular cells *in vitro*, using a range of injury models that stimulate the mechanisms of cellular injury induced by ischaemia-reperfusion.

Chapter Five:

Erythropoietin prevents Toxin-induced Apoptosis

5.1 Introduction

Cisplatin is a highly effective chemotherapeutic agent used in the treatment of a wide variety of solid tumours, particularly ovarian, head and neck, and testicular germ cell tumours [Boulikas T, 2003]. However, 25-35% of patients experience a significant decline in renal function after administration [Lebwohl D, 1998]. The nephrotoxicity is a cumulative, dose-dependent effect which may necessitate dose reduction or withdrawal of cisplatin treatment, and hence limiting its effectiveness in many patients. Despite this toxicity, cisplatin remains one of the most commonly used chemotherapy drugs due to its therapeutic efficacy. Several mechanisms have been proposed for cisplatin nephrotoxicity [Arany I, 2003].

In animal models of cisplatin nephrotoxicity, analysis of proximal tubular injury reveals both necrotic and apoptotic mechanisms of cell death [Zhou H, 1999], which predominately affects the S3 segment of the proximal tubule. *In vitro*, the morphological changes of apoptosis have been demonstrated in low-dose cisplatin treated mouse isolated proximal tubules [Lieberthal W, 1996]. In culture, cisplatin induces apoptosis in a porcine renal proximal tubular epithelial cell line (LLC-PK_1 cells) via Bax translocation to the mitochondrial membrane, cytochrome c release, and the activation of caspase-9 and caspase-3 [Park MS, 2002].

In proximal tubule cells in culture, mitochondrial depolarisation leading to the release of mitochondrial pro-apoptotic molecules including cytochrome c, Omi/ HtrA2, Smac/DIABLO and apoptotic inducing factor (AIF) has been shown in response to cisplatin treatment [Seth R, 2005; Cilenti L, 2005]. Mitochondrial depolarisation may be induced through a number of pathways, including oxidative stress, activation of mitogen activated kinases including JNK, and DNA damage, leading to p53-dependent caspase-2 activation [Jiang M, 2004; Seth R, 2005]. However, the importance of DNA damage to cisplatin-induced cell death has been questioned. Cisplatin has been shown to activate the caspase

cascade in enucleated cells (cytoplasts) via the generation of superoxide. Lower doses of cisplatin, insufficient to cause apoptosis, may lead to DNA damage, p53 activation and replicative senescence [Berndttson, 2007].

5.2 Aims

The data presented in the previous chapter shows that EPO induces several signalling pathways, following ligand binding to its specific cell surface receptor, in proximal tubular epithelial cells *in vitro*, and that the activation of these pathways increased the resistance of the cell against apoptosis cell death induced by several different stimuli. The aim of the experiments in this chapter was study the particular mechanisms that mediated this anti-apoptotic effect by utilizing cisplatin-induced apoptosis as a standard model of mitochondrial stress induced caspase-dependent cell death. A rat model of cisplatin nephrotoxicity was used to determine whether the effects observed *in vitro* were confirmed in an animal model.

5.3 Methods and Materials

5.3.1 Fluorescent Microscopy and JC-1 staining of live cells

Quantitative changes in mitochondrial membrane potential ($\Delta\varphi m$) in cells at the early stages of apoptosis were measured using the fluorescent dye JC-1 [De Lisa F, 1995]. This dye exists as a monomer with emission at 530 nm (green fluorescence) at low concentrations but forms J-aggregates with emission at 590 nm (red fluorescence) at high concentrations. Therefore, the relative fluorescence of JC-1 at different wavelengths can be considered as an indicator of a change in mitochondrial membrane polarization.

HK-2 cells were seeded at 1 x 10^5/ mL in 6 well plates in standard medium. Cells were stimulated with cisplatin for 16 hours overnight, in the presence or absence of EPO (50 U/ mL). Cells were washed with 1 mL PBS, and then 1 mL 4% paraformaldehyde was added to each well for 10 minutes. Cells were then washed twice with PBS, then 0.2% Triton-X was added. After a further wash step, 2 drops of signal enhancer was added, and the plate incubated for 30 minutes. The cells were washed in PBS, then the coverslip was transferred and placed in an inverted position on the centre of a microscope slide, and 2 drops of mounting buffer containing DAPI, a fluorescent dye which strongly binds nuclear DNA, was added, and the slides stored in the dark. Slides were examined on a Zeiss fluorescent microscope. Relative intensity of fluorescence was qualitatively determined by 2 independent observers for 3 high-powered fields. Representative images were saved.

5.3.2 JC-1 Quantitative Assay

The medium was removed, and replaced with phenol-red free medium containing JC-1 (10 μM), and incubated in the dark for 30 minutes. Fluorescence was measured at two

frequencies 530nm and 580 nm, and controlled for background reading in a blank (cell-free) well. Cisplatin induced a significant reduction in the ratio of fluorescence at 450/ 510 nm, when compared with control cells, demonstrating a decrease in red fluorescence due to loss of mitochondrial "j-aggregrates" following depolarisation of the mitochondrial membrane Briefly cells were seeded at 1 x 10^6/ mL. After different treatments, the cells were incubated with 10 µM JC-1 at 37 °C for 8 min, washed twice, and resuspended in 100µL PBS. Relative fluorescence intensities were monitored using the FluoroMax-2 fluorescence spectrofluorometer with 490 nm excitation/535 nm emission and 570 nm excitation/610 nm emission. The $\Delta\varphi_m$ was expressed as the ratio of the fluorescence of J-aggregate (570 nm excitation/610 nm emission) to monomer (490 nm excitation/535 nm emission) forms of JC-1, controlled by substracting fluorescence detected from blank wells.

5.3.3 PARP Activity Assay

Poly (ADP-ribose) polymerase (PARP) is a nuclear enzyme with DNA nick sensor function. Upon binding to broken DNA, PARP becomes activated and cleaves NAD+ into nicotinamide and ADP-ribose. PARP then polymerises ADP-ribose on nuclear receptor proteins including histones, transcription factors and PARP itself. PARP has been implicated in DNA repair, cell cycle progression and transcriptional regulation. Excessive PARP activation, induced by oxidative stress, leads to the depletion of cellular NAD and ATP pools and results in cell dysfunction or necrotic cell death, discussed in section 1.3.3.

In a cellular ELISA system, cells grown in 96-well plate are incubated with biotinylated-NAD after permeabilization with digitonin. Activated PARP cleaves bio-NAD into nicotinamide and biotinylated ADP-ribose and hence poly-bio-ADP-ribose polymers that are detected by conjugation with a streptavidin-peroxidase and colorimetric peroxidase

substrate. 50 µL of Biotinylated-NAD+ with was added to all experimental wells of a 96-well plate, and the plate was incubated at 37˚C for 30 minutes. The medium was aspirated and 200 µL of 95% ethanol, chilled to -20˚C, was added to each well and followed by 20 min incubation at -20˚C. The ethanol was aspirated and each well was treated with 200 µl 30% hydrogen peroxide solution in methanol. The plate was incubated for 15 minutes at room temperature. The plate was then washed and 200 µl of streptavidin-peroxidase conjugate added, and incubated for 25 minutes at room temperature. The plate was washed three times and 100 µl TMB substrate was added and incubated in the dark. The development of blue colour was measured on the Dynex II by absorbance at 605nm, compared to blank wells.

5.3.4 Quantification of intracellular reactive oxygen species by FACS

The cell permeable fluorogenic probe 2'7'-dichlordihydrofluorescin diacetate (DCF-DA) was used to detect oxidative stress. DCF-DA diffuses freely across cell membranes and is hydrolyzed by non-specific cellular esterases to the non-fluorescent compound dichlorofluorescin (DCFH), which is predominately trapped within the cell. In the presence of ROS, DCFH rapidly undergoes one-electron oxidation to the highly fluorescent compound dichlorofluorescein (DCF). Cell exposed to experimental conditions were washed once in PBS and then incubated with DCF-DA (20 µM) for 30 minutes at 37 ˚C in the dark. The cells were then trypsinized in 0.25% trypsin and then pelleted by centrifugation at 2000 rpm for 5 minutes. Pellets were washed once in PBS, and after a further centrifugation step, were re-suspended in 500 µL PBS in FACS tubes. Samples were analysed on a Becton-Dickenson flow cytometer. Side and forward scatter were controlled and the cell population was gated. Single dimension histogram at the appropriate wavelength was measured and

gated for 10000 cells per sample. For three individual experiments, samples (n=8) were analysed and median fluorescence shift was calculated and analysed.

5.3.5 Rat Model of Cisplatin Nephrotoxicity

This study was carried out using twenty-four male Wistar rats (Tuck, Rayleigh, Essex, UK) that weighed 250 to 300 g and received standard diet and water *ad libitum*. Animals were cared for in accordance with the Home Office Guidance in the Operation of the Animals (Scientific Procedures) Act 1986 (HMSO, London, UK).

Animals were treated with a single intra-peritoneal bolus of cisplatin (7 mg/Kg) or an identical volume of carrier (DMSO) solution. On day 5, blood was taken from tail vein and the animal sacrificed under general anaesthesia using intraperitoneal injection of sinactin (Inactin®, Suzan Bennett, Natick, USA). The abdomen was opened and both kidneys were removed. They were promptly bisected and fixed in formaldehyde (15%) and then embedded in paraffin; sections were cut at 3 µm and stained with haematoxylin and eosin, PAS, and trichrome Masson with light green.

A pathologist carried out a semiquantitative analysis of the kidney sections in a blinded fashion. Glomeruli and vessels were normal. Changes observed were limited to the tubules, especially to the proximal straight S3 portion, the main site of cisplatin toxicity. Tubular lesions were graded as follows: 0=no damage; 1+=area of tubular epithelial cell swelling, vacuolization, necrosis, desquamation less than 50%; 2+=lesion areas grater than 50% with or without focal involvement of the S3 segment in the medullary rays; 3+=lesion areas 100% with diffuse involvement of the medullary rays.

5.4 Results

5.4.1 Cisplatin induces dose dependent increase in proximal tubular epithelial cell death which is attenuated by pre-administration of EPO

Cisplatin in DMSO was freshly prepared for each set of experiments. Human proximal tubule epithelial (HK-2) cells were incubated with increasing concentrations of cisplatin for 24 hrs, and then DNA fragmentation (Cell Death ELISA) and cell viability assays (MTS assay) were examined.

Cisplatin caused a reduction in cell viability (figure 5.1) which was associated with an increase in DNA fragmentation, as a marker of apoptosis (figure 5.2). These results indicate that the pro-apoptotic effects of cisplatin are dose-dependent, with the greatest amount of DNA fragmentation seen in cells treated with 50 μM cisplatin. Cells were pre-treated with varying concentrations of EPO (10-50 U/ mL) for one hr before being exposed to 25-50 μM cisplatin for 24 hrs. EPO pre-treatment caused a dose-dependent increase in cell viability (when compared to control cells: CP 68% ± 5, CP with EPO 10 U/ml 81% ± 11, CP + EPO 30 86 ± 10, CP + EPO 50 91 ± 11; $P<0.01$) which was associated with a significant decrease in DNA fragmentation (when compared to control cells: CP 7.6 ± 1.2 fold increase in DNA fragmentation, CP + EPO 4.8 ± 0.5; $\boldsymbol{P} < 0.01$).

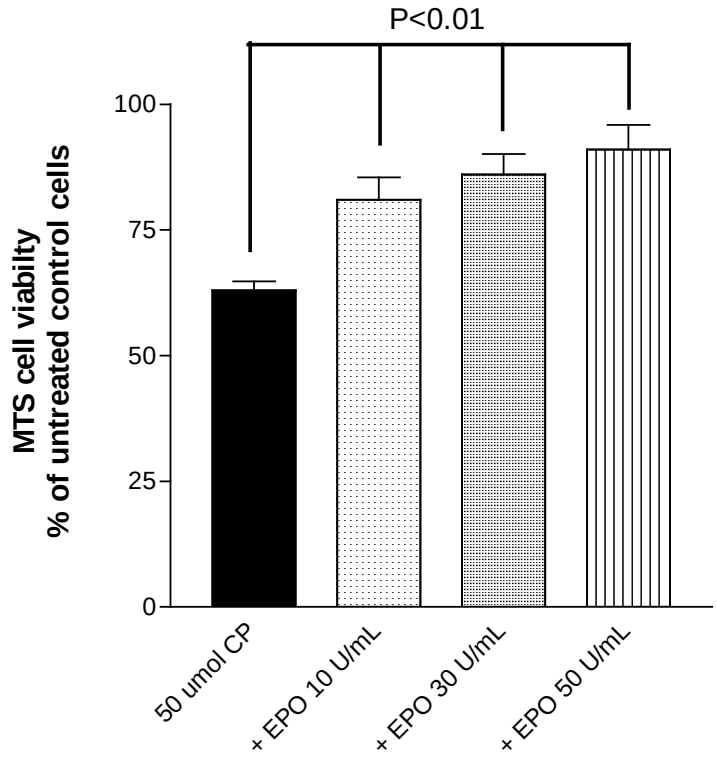

Figure 5.1 Cell Viability is preserved by EPO in dose dependent manner. An MTS assay was performed after 24 hours exposure to cisplatin. Cell viability was expressed relative to the MTS value of control cells (in 3 separate experiments). EPO maintained cell viability when compared to untreated cells (P<0.01 by ANOVA).

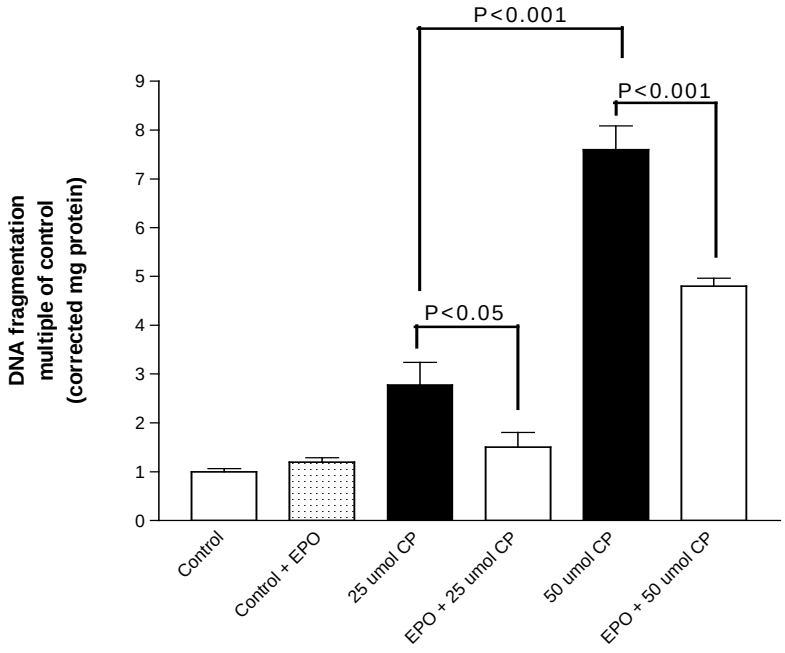

Figure 5.2 EPO pre-treatment reduces Cisplatin induced DNA fragmentation in an ELISA assay. Values for experimental groups were expressed relative to control cells for 3 experiments. EPO significantly abrogated the rise in apoptosis following cisplatin exposure ($p<0.001$ by ANOVA).

5.4.2 Cisplatin induces Apoptosis via the activation of multiple Caspases

To elucidate whether the activation of capase-3 was necessary for cisplatin-induced cell death, HK-2 cells were plated out in a 96-well plate in 100µL phenol-red free standard medium, and a modified *in situ* assay for caspase-3 activation was used. In this assay, total caspase activation at various time points during the experiment was determined by quantification of cumulative AMC fluorescence in small aliquots of experiment medium (see methods section 2.3.4).

Cisplatin (50µM) induced a significant time-dependent increase in caspase-3 activity between 8 and 24 hrs (Figure 5.3). Pre-treatment with EPO (50 U/ mL) for one hr significantly reduced the increase in caspase-3 activity induced by cisplatin at 24 hours (CP 4158 ± 532, CP + EPO 1789 ± 247; $\boldsymbol{P}<0.001$). To determine whether caspase-3 activation was dependent on the mitochondrial stress pathway, lysates previously used to determine DNA fragmentation at 24 hrs were used to assay caspase-9 activity. There was a significant increase in caspase-9 activity induced by cisplatin at 24 hours (Figure 5.4), which was significantly reduced by pre-treatment with EPO (CP 314 ± 71, CP + EPO 165 ± 97, $\boldsymbol{P}<0.05$). Park *et al.* have previously shown no activation of caspase-8 at 24 hours in cisplatin exposed proximal tubular epithelial cells [Park N, 2002]

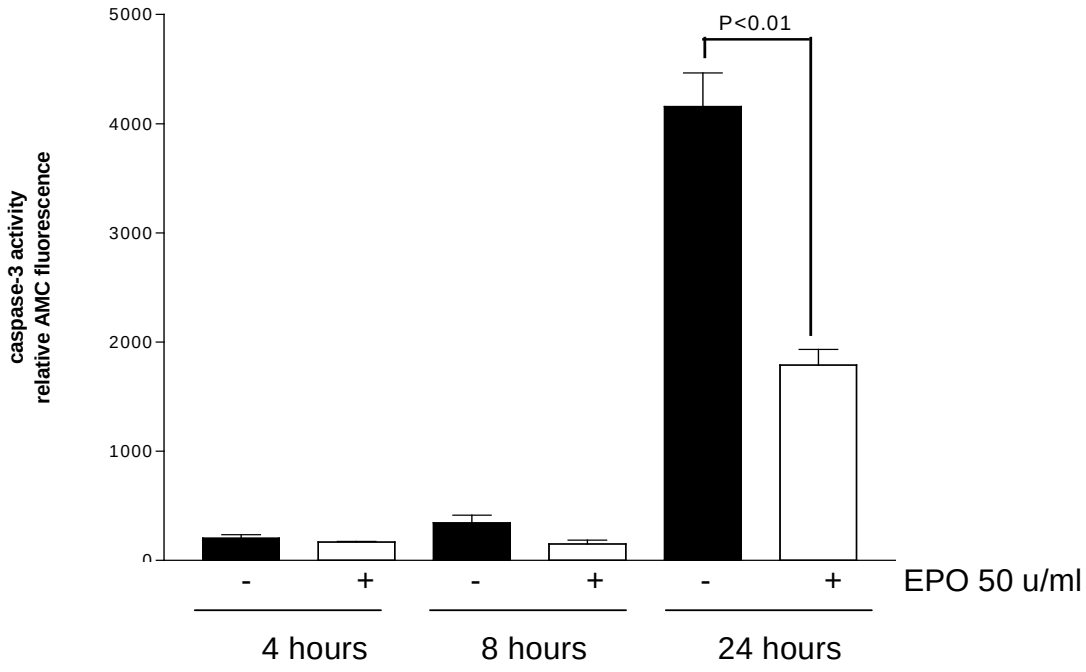

Figure 5.3 Caspase-3 activity was measured at various time points up to 24 hours in cisplatin exposed cells (results from n=6 wells in 3 separate experiments). When compared to early time points, there was significant rise in caspase-3 activity at 24 hours, which was reduced by EPO treatment (P<0.01).

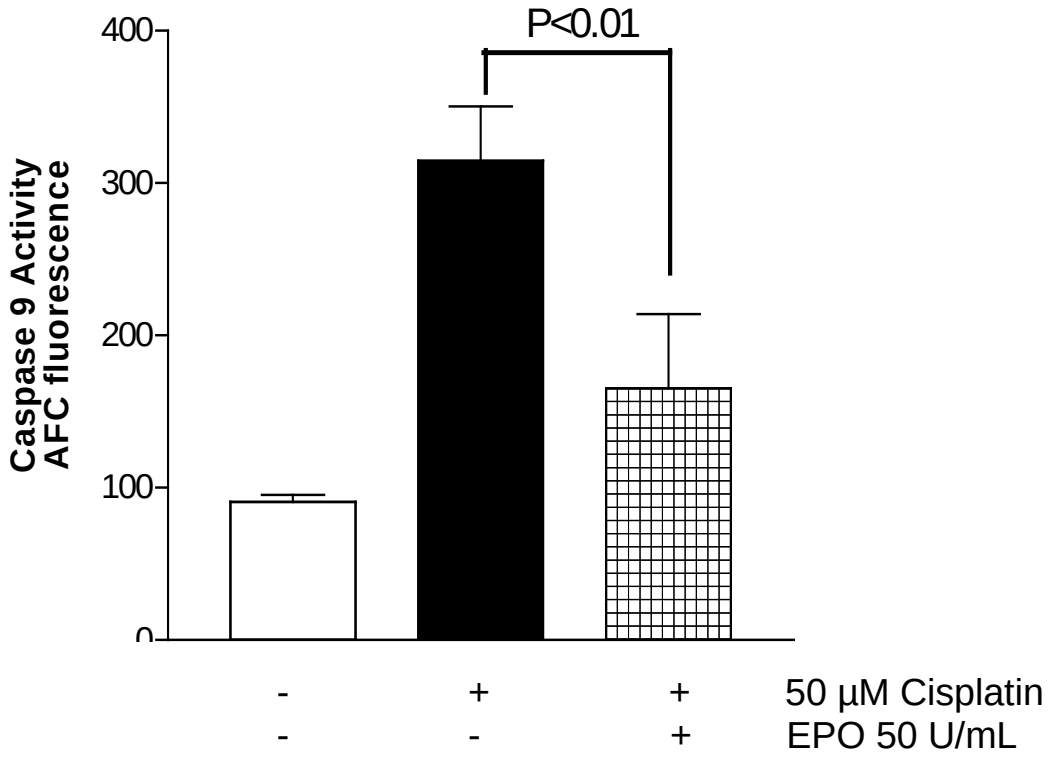

Figure 5.4 EPO reduces caspase-9 activity induced by cisplatin when measured at 24 hours following cisplatin exposure (P<0.01 by ANOVA).

5.4.3 EPO inhibits mitochondrial depolarisation induced by Cisplatin

The activation of caspase-9 requires the release of cytochrome c from depolarised mitochondria. The mitochondrial probe JC-1 was used to study changes in relative mitochondrial membrane potential. Initially, fluorescent microscopy was utilized to examine JC-1 uptake and staining in cisplatin treated cells, as described in 5.3.1. Cells were fixed and stained with JC-1 before microscopy. In a series of experiments (n=3), there was a qualitative difference in JC-1 staining in cisplatin treated cells, with an increase in cells with orange fluorescence in EPO treated cells, indicting preservation of mitochondrial J aggregates (figure 5.5).

In order to quantitatively assess the observed findings in these initial experiments, an *in situ* assay was developed, described in section 5.3.2. HK-2 cells, plated in a 96-well plate (16 wells for each experimental group), were incubated with cisplatin (50 μM) with and without pre-treatment with EPO (50 U/ mL), for 24 hours. Pre-treatment with EPO caused significant preservation of JC-1 ratio (Figure 5.6), indicating preservation of mitochondrial membrane potential (control cells 11.4 ± 0.8, CP 10.3 ± 1.3, CP + EPO 9.0 ± 1.7; $\boldsymbol{P} < 0.05$).

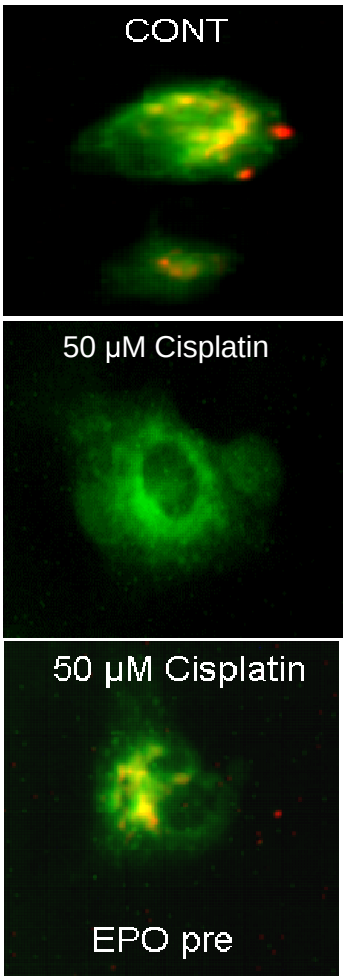

Figure 5.5 JC-1 staining by microscopy in Cisplatin exposed HK-2 cells

Cells incubated with Cisplatin demonstrated reduced orange fluorescence in polarised mitochondria with a predominance of green fluorescence indicating dimerised cytoplasmic JC-1. EPO pre-treatment was associated with preservation of orange fluorescence activity from monomeric JC-1 in mitochondria.

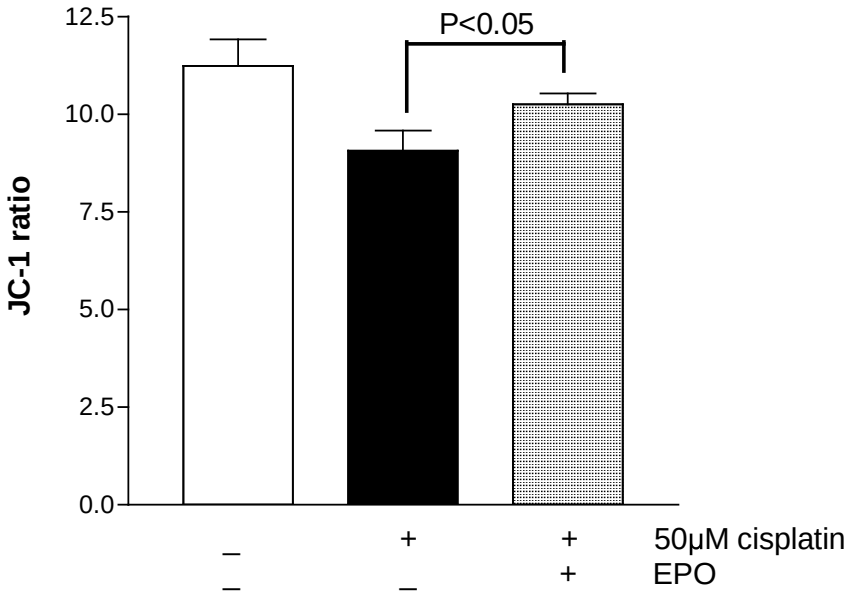

Figure 5.6 EPO pre-treatment was associated with preserved JC-1 ratio when compared to Cisplatin exposed cells. JC-1 was added to cells at the end of the experiment and fluorescence measured at two wavelengths. The ratio was calculated from the difference between intensity at different wavelengths for n=8 wells per experiment (P<0.05 by ANOVA).

5.4.4 Cisplatin induced apoptosis is dependent on the translocation of pro-apoptotic Bax to mitochondria with down-regulation of Bcl-X_L

Changes in mitochondrial membrane potential are dependent on the balance of pro- and anti-apoptotic proteins. HK-2 cells were exposed to cisplatin for 24 hours with and without pre-treatment with EPO. Cells were lysed in RIPA buffer and 20 μg cellular protein was electrophoresed on a pre-cast 4-12% graduated gel (Invitrogen, UK). After electroblotting, membranes were probed with specific antibody to Bcl-X_L (Santa-Cruz). Cisplatin down-regulated the expression of Bcl-X_L, but pre-incubation with EPO prevented the reduction in expression (Figure 5.7a representative blot). Cell fractionation was also performed, and cytoplasmic and mitochondrial expression of Bax was examined by western blotting. Cisplatin induced the translocation of Bax to the mitochondrial fraction (Figure 5.7b).

In order to confirm the role of Bax in cisplatin induced apoptosis, RNA interference was used to knock-down Bax expression in HK-2 cells before cisplatin exposure. HK-2 cells were plated at 1 x 10^5 cells/ mL in 6 well plates, and transfected with Bax and control non-targeted siRNAs, as described in section 2.6. After 24 hrs, the medium was replaced with standard medium with cisplatin (50 μM) for a further 24 hrs. Western immunoblotting with a Bax polyclonal antibody was performed to determine total Bax levels and hence confirm reduced expression in siRNA knock-down.

Knock-down of Bax expression by transfection with Bax siRNA abrogated DNA fragmentation induced by cisplatin (Figure 5.8) to a similar degree to the cellular protection observed with EPO treated cells (control 15 ± 6, CP 70 ± 16, CP + EPO 40 ± 14, CP in Bax siRNA treated cells 33 ± 11; $\boldsymbol{P}$ <0.01), confirming that Bax is a vital mediator of the mitochondrial mechanism of apoptotic cell death induced by cisplatin.

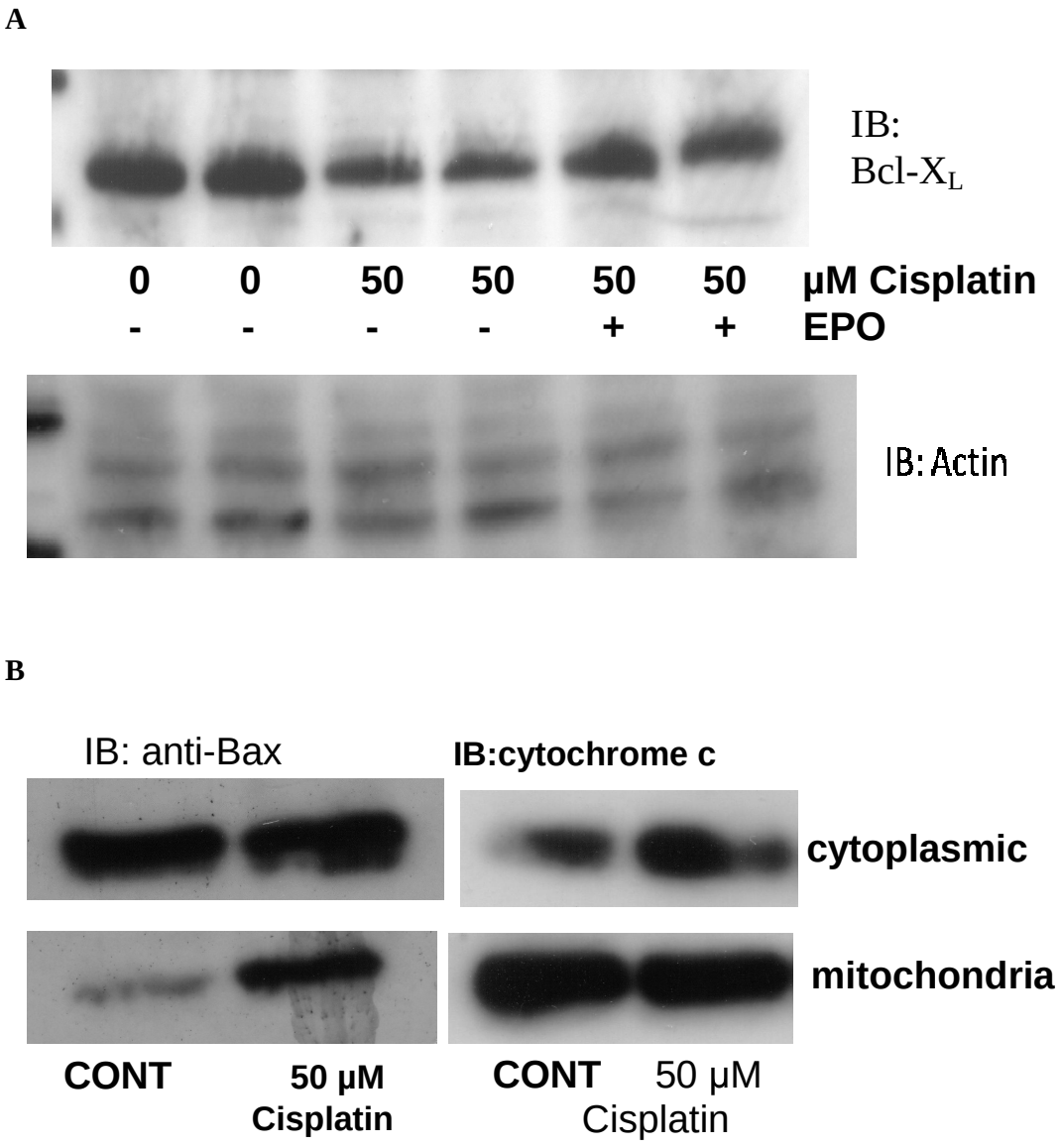

Figure 5.7 Immunoblotting for pro- and anti-apoptotic molecules.

A Immunoblot with Bcl-X_L antibody. Representative blot from n=3 experiments. Cisplatin exposure reduced expression of Bcl-X_L, which was maintained in EPO treated cells.

B Individual blots with specific Bax antibody from cellular fractions. Cisplatin induced Bax shift into mitochondrial fraction when compared to control cells.

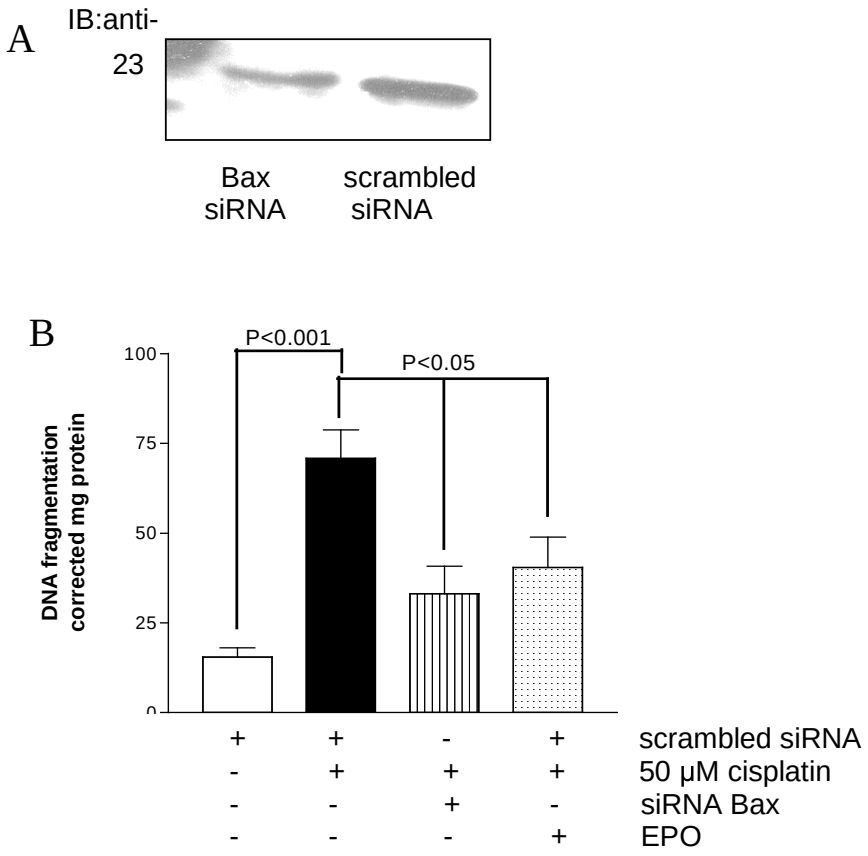

Figure 5.8 Inhibition of Bax prevents cisplatin induced apoptosis.

A Immunoblot with Bax antibody confirms reduction in expression with siRNA.

B DNA fragmentation ELISA as measure of cell death shows significant increase in DNA fragmentation with cisplatin exposure, which was reduced by siRNA Bax knockdown and by EPO treatment (P<0.05, by ANOVA).

5.4.5 EPO maintains the expression of the inhibitor of apoptosis, XIAP

The expression of XIAP by western blotting was decreased after 24 hours exposure to cisplatin. This reduction is expression was prevented in EPO treated cells, shown in Figure 5.9, suggesting that maintenance of NFκB dependent anti-apoptotic signalling via XIAP is important to the anti-apoptotic effects of EPO in this model.

To confirm this, we transfected cells with XIAP siRNA, and then examined the amount of DNA fragmentation induced by cisplatin (50μM) in three separate experiments. Compared to cells transfected with non-targeted control siRNA (control 23 ± 1.9, CP 50 ± 0.4, EPO + CP 34 ± 5, $P<0.01$), there was a small increase in DNA fragmentation in control cells transfected with XIAP siRNA (control 27 ± 4, P=ns). There was significantly more apoptosis in cells exposed to cisplatin in which XIAP had been knocked down (CP 61 ± 2.6) (Figure 5.10). The protective effects of EPO pre-treatment were abrogated by transfection with XIAP siRNA (57 ± 4, P=ns when compared to CP), confirming this pathway as vital to the anti-apoptotic effects of EPO in proximal tubular epithelial cells.

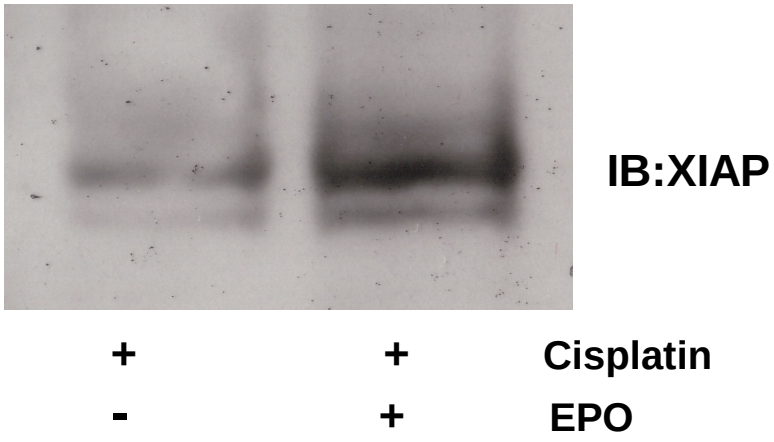

Figure 5.9 Immunoblot of XIAP from lysates of cells exposed to cisplatin and EPO. Representative image from n=3 experiments. Equal protein loading was confirmed by re-probing with housekeeper protein.

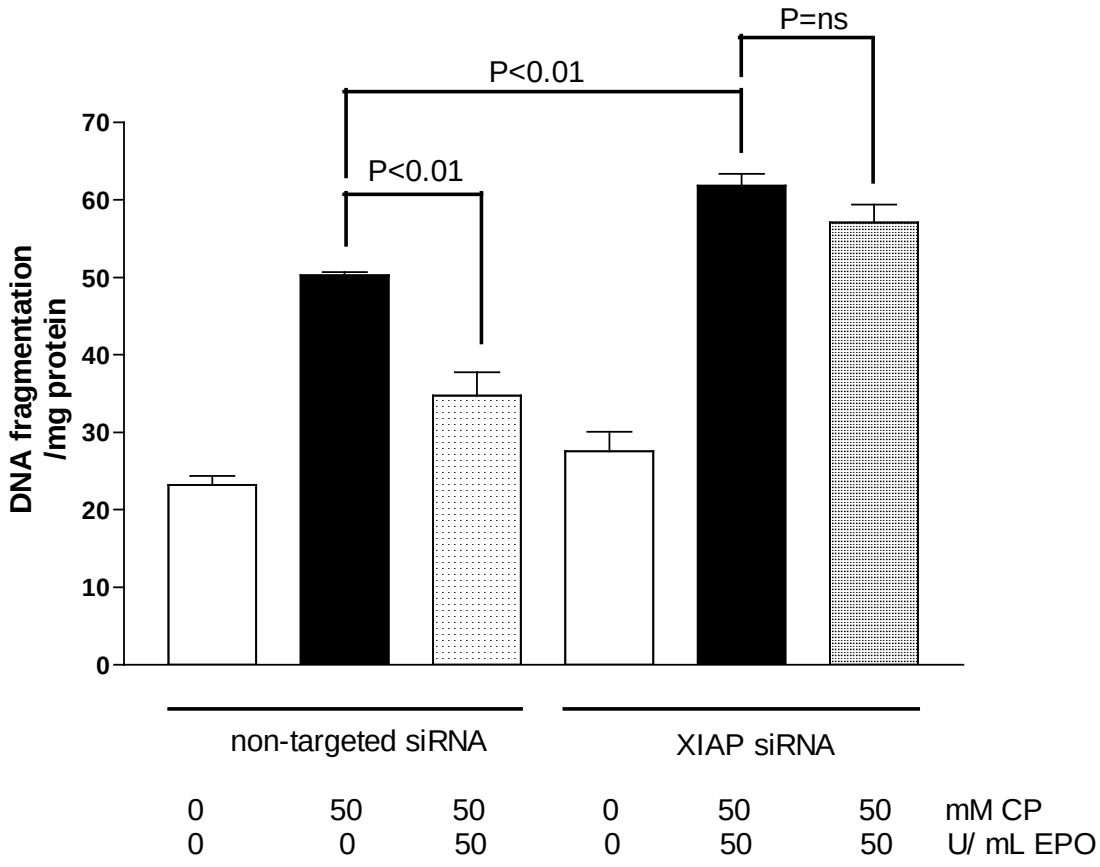

Figure 5.10 Inhibition of XIAP prevents the beneficial effect of EPO in cisplatin induced apoptosis. A DNA fragmentation ELISA assay was used to determine cell death relative to control cells. Transfection with XIAP siRNA induced an increase in DNA fragmentation in control cells when compared to controls. The protection observed with EPO treatment in control transfected cells (P<0.01, ANOVA) was lost in XIAP siRNA transfected cells.

5.4.6 EPO reduces cisplatin induced oxidative stress and PARP activation

Incubation with cisplatin (10 μM-50 μM) caused a significant increase in DCF fluorescence, shown in Figure 5.11, indicating an increase in the generation of reactive oxygen species. Pre-incubation with EPO attenuated the mean increase in oxidative stress induced by cisplatin (control 26 ± 0.7 , 10 μM cisplatin 47± 0.3, 10 μM + EPO 38 ± 3, 25 μM cisplatin 47.5 ± 0.2 , 25 μM cisplatin + EPO 40.5 ±1.5, P< 0.01).

DNA damage induces the activity of PARP-1, which contributes to ATP depletion and secondary necrosis cell death. PARP activity is increased in oxidative stress, and may contribute to the development of lethal cellular injury. PARP-1 activation in live cells was determined as described in 5.3.3. HK-2 cells were seeded in a 96-well plate in standard medium. Cells were pre-treated with EPO (50 U/ mL) for one hour, then the medium was removed and replaced by 100 μL standard medium containing cisplatin (50 μM). Cisplatin exposed cells showed marked activation of PARP-1 (control 0.24 ± 0.07, CP 0.84 ± 0.4; ***P***<0.01), which was significantly reduced by EPO pre-treatment (CP + EPO 0.27 ± 0.04, ***P***<0.01 when compared to CP), shown in Figure 5.12.

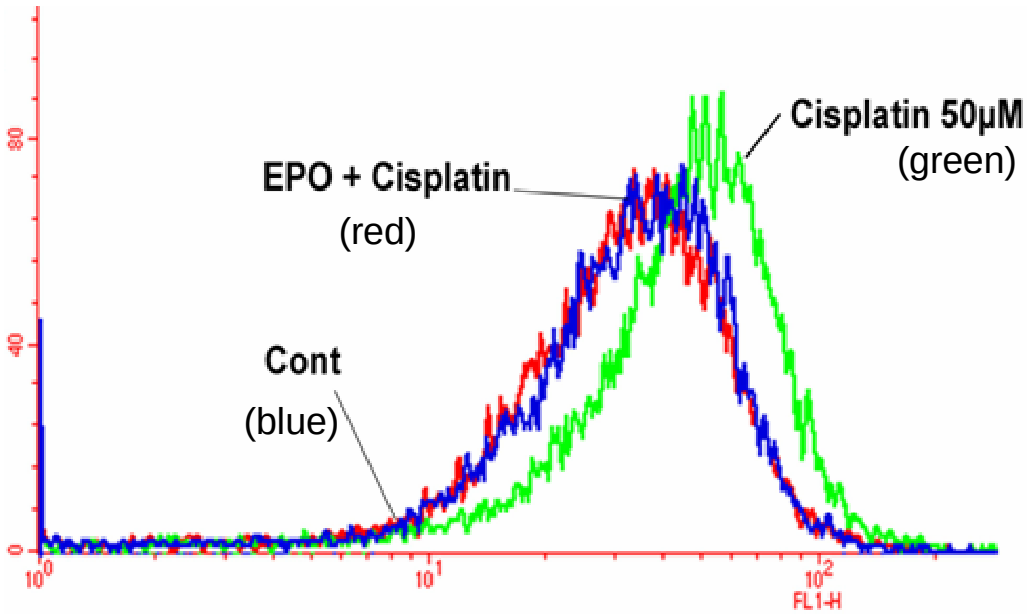

Figure 5.11 DCF staining in cisplatin treated HK-2 cells caused a right-shift due to an increase in oxidative radical production which is reversed by EPO. Image downloaded from flow cytometry representative of n=4 experiments.

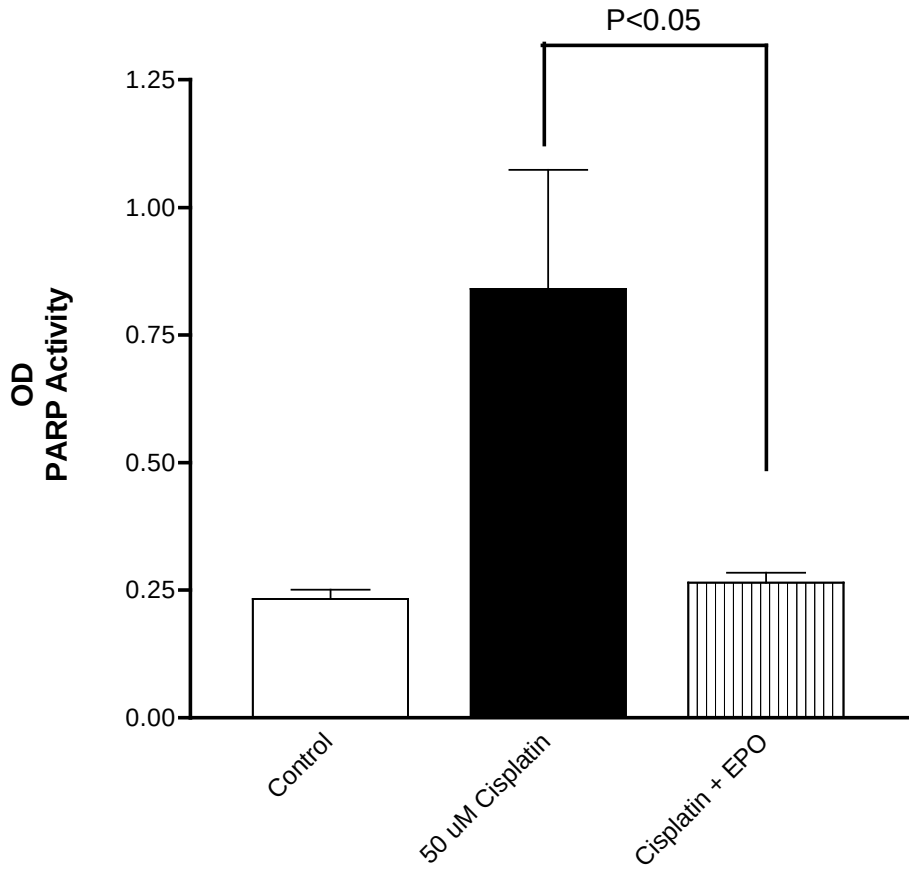

Figure 5.12 EPO reduces PARP-1 activation induced by cisplatin administration. PARP activity was measured by measurement of utilization of biotinylated NAD. When compared to control cells, cisplatin caused significant increase in PARP-1 activity, which was abrogated by EPO pre-treatment (P<0.01 by ANOVA).

5.4.7 EPO reduces Renal dysfunction in a model of cisplatin Nephrotoxicity

Cisplatin (7 mg/ Kg) IP induced significant renal dysfunction in male wistar rats (n=9) on day 5 (creatinine 115 ± 52 umol/l). Animals pre-administered EPO (1000 U/Kg) 24 hours before cisplatin exposure (n=8) showed significant reduction in serum creatinine at day 5 (creatinine 61 ± 36, $\boldsymbol{P}<0.05$). Daily EPO administration (300 U/Kg) commenced after cisplatin exposure did not demonstrate any significant improvement in serum creatinine at day 5 (n=6), consistent with previously published observations [Variza ND, 2004], shown in Figure 5.13.

EPO pre-administration was associated with preservation of normal kidney architecture on histological examination, shown in Figure 5.14, with reduced histological injury scored by two pathologists blinded to experimental grouping (sham animals 0; cisplatin + vehicle 145 ± 1; EPO pre-treatment + cisplatin 45 ± 4, $\boldsymbol{P}<0.01$).

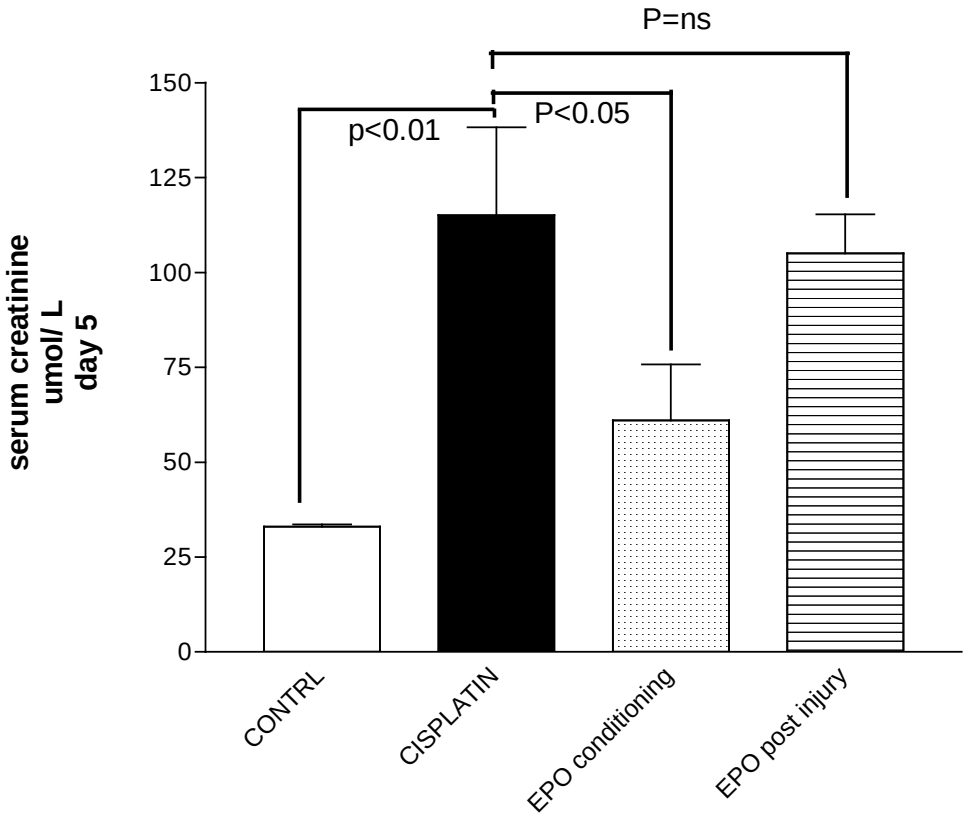

Figure 5.13 Serum creatinine at day 5 following Cisplatin exposure in male Wistar Rats. Cisplatin caused renal dysfunction with a significant increase in serum creatinine at day 5 (P<0.01). Pre-treatment with EPO (n=8) reduced the degree of dysfunction at day 5 (P<0.05, ANOVA), whereas daily administration of EPO post-cisplatin exposure had no effect.

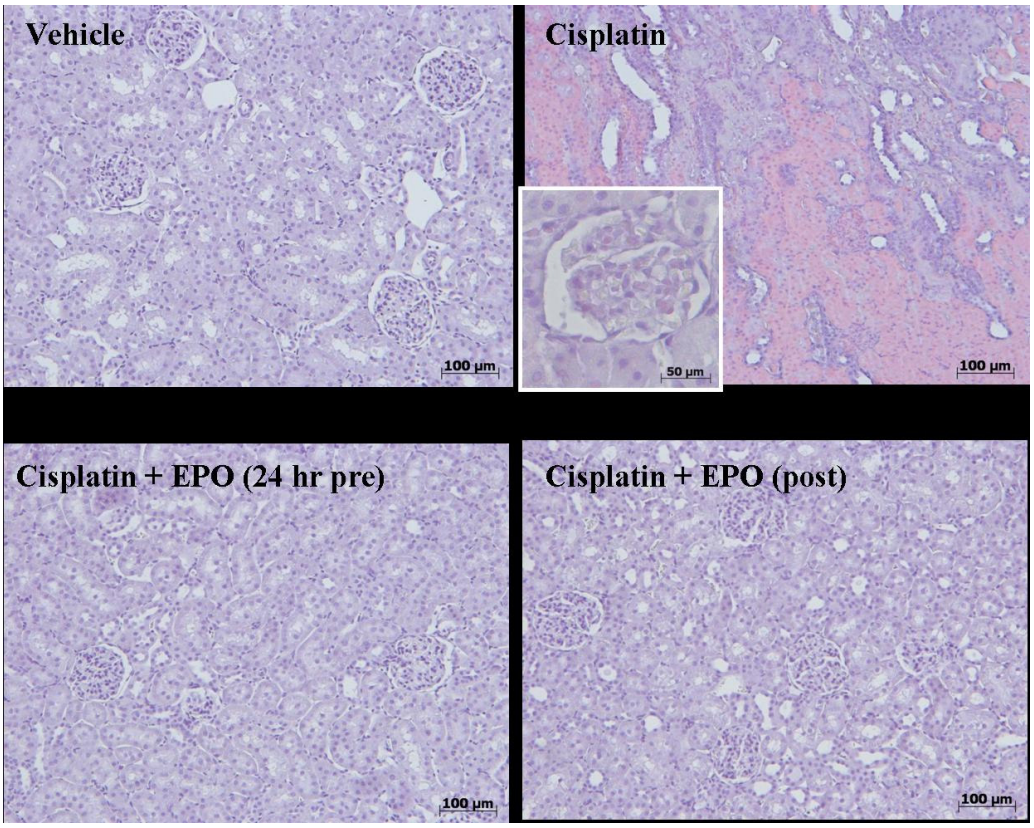

Figure 5.14 Histological assessment of Renal Injury induced by Cisplatin was assessed by two blinded pathologists. Histological severity scoring, described in 5.3.5, showed that cisplatin induced widespread changes in the kidney when compared to control sham animals (P<0.01), and this was reduced by pre-treatment with EPO (P<0.01, by ANOVA). Representative images from each group are shown.

5.5 Discussion

The evidence presented in this chapter confirmed the findings described in chapter four, demonstrating that EPO significantly abrogated the induction of apoptotic cell death. EPO prevented cisplatin induced tubular epithelial cell toxicity through the activation of a number of important cell survival pathways. The reduction in apoptosis, measured by DNA fragmentation, was accompanied by a reduction in caspase-9 and caspase-3 activity, and preservation of mitochondrial membrane potential.

Cisplatin induced the translocation of bax to the mitochondrial fraction, and associated with the down-regulation of the Bcl-2 family member Bcl-X_L, promotes mitochondrial depolarisation. In healthy cells, bax is sequestered in the cytoplasm via an interaction with 14-3-3 proteins, but following cellular stress, activation of the mitogen-activated protein kinase c-jun N-terminal kinase (JNK) phosphorylates 14-3-3 protein, leading to dissociation of Bax and mitochondrial depolarisation [Tsuruta F, 2004]. Cisplatin has been shown to cause a sustained activation of JNK and p38 in cancer cells lines and proximal tubular epithelial cells in culture. Inhibition of JNK activation by either kinase inhibitors or transfection of dominant negative MEKK1 has been shown to reduce apoptotic cell death after 24 hours, although there is some conflicting evidence [Krillele D, 2003; Arany I, 2004].

A major pathway for the protective effects of EPO in cisplatin induced apoptosis in these experiments was the preservation of anti-apoptotic molecules including XIAP and Bcl-X_L. XIAP expression was maintained by EPO, which may be due to several mechanisms, including increased transcription through NF-κB activation, and AKT-dependent

phosphorylation of XIAP which renders it more resistant to ubiquitin-dependent degradation [Dan HC, 2004].

These studies have provided further elucidation of the molecular mechanisms by which EPO exerts its anti-apoptotic effects in the kidney. EPO binds to its cell surface receptor, leading to activation of two major signalling pathways – the non-genomic activation of the PI-3 K /AKT pathway, which leads to inactivation of a number of apoptotic mediators, and activation and nuclear translocation of the transcription factor NF-κB, which induces genomic expression of a wide range of anti-apoptotic mediators, particularly XIAP, which inhibit apoptosis at several levels through the inhibition of caspase-3, -7 and -9, and contributes to the down-regulation of JNK signalling.

When administered as a pre-treatment, EPO exerted a significant effect on the course of cisplatin nephrotoxicity in a rat model. These observations were consistent with previous work, which demonstrated that EPO given after exposure to cisplatin did not affect the degree of injury seen, but induces a more rapid recovery in kidney function with tubular regeneration and mitosis occurring earlier than in untreated animals [Varizi ND, 2001]. Following on from the findings in models of ischaemia reperfusion injury in the kidney described in chapters three and four, these experiments confirm that EPO upregulates signalling pathways that alter the physiological resistance to an ischaemic or toxin insult.

The beneficial effect of EPO demonstrated in these experiments has been confirmed in two recent studies using animal models of cisplatin nephrotoxicity [Salahudeen AK, 2008; Choi DE, 2009]. Salahudeen et al used an in vitro model of cisplatin induced apoptosis, and the protective effect was abrogated by the use of an inactive form of human EPO, and by the inhibition of JAK2 signalling with the inhibitor AG490. Darbopoietin (25 µg/ Kg) reduced apoptotic and necrotic cell death in a in vivo model of cisplatin toxicity, and this benefit was not reduced in control group that underwent venesection to control for changes in haemocrit.

Chapter Six:

Effects of Erythropoietin in the Heart

6.1 Introduction

Cardiovascular disease is the number one cause of mortality in the developed world, and is fast becoming the main global health concern. In the United Kingdom, 105842 people died as a result of coronary artery disease in 2005, of which 36323 were attributed to acute myocardial infarction [Government Statistics, 2008]. Coronary atherosclerosis is a chronic disease with stable and unstable periods. During unstable periods with activated inflammation in the vascular wall, myocardial ischaemia and infarction may be a consequence of an arterial occlusion, reduced flow within a stenosed vessel or acute thrombosis related to plaque rupture.

Coronary artery occlusion and resulting myocardial ischaemia can be reversed by surgical or pharmacological strategies to remove the obstruction and restore myocardial blood supply. Cell death occurs after a period of as little as twenty minutes, although it may take several hours before myocardial necrosis can be identified by macroscopic post-mortem examination. Long term outcome has been correlated with the degree of recannulation of the coronary artery lumen [Clements IP, 1993], and hence the degree of restoration of normal arterial blood flow and myocardial perfusion and oxygenation. Successful examples include the administration of thrombolytic agents, streptokinase and tissue plasminogen activator, which lyse the platelet thrombus, and percutaneous transluminal angioplasty, in which the artery is selectively cannulated with a wire and a balloon inflated across the occlusion to mechanically restore patency, which evidence has suggested is the superior primary therapy [Weaver WD, 1997]. Large clinical trials investigating the use of thrombolytics have shown reduction in infarct size and mortality, and improvement in left ventricular function, if carried out within 6 hours of the onset of symptoms [GISSI 1986, ISIS-2 1988]. Restoration

of blood flow or reperfusion is absolutely essential for the survival of the ischaemic myocardium. However, reperfusion is not without its own consequences, as animal models suggest that reperfusion injury accounts for up to 50% of the final size of a myocardial insult [Bolli R, 2004].

Myocardial reperfusion injury was first described by Jennings *et al* in a canine model with histological features of cell swelling, contracture of myofibrils, and disruption of the sarcolemma [Jennings RB, 1960]. The injury to the heart during reperfusion causes several types of cardiac dysfunction, which are analogous to the early phases of acute kidney injury; initially "myocardial stunning" denotes mechanical dysfunction that persists after reperfusion despite the absence of irreversible damage and despite restoration of normal or near-normal coronary artery flow [Braunwald E, 1982]. The myocardium usually recovers from this reversible form of injury after several days or weeks, with ventricular remodelling around the area of infarction.

At a cellular level, myocardial cell death occurs through mechanisms that are similar to those in the kidney, including changes in intracellular calcium, oxidative stress and mitochondrial dysfunction and interruption of normal cellular metabolic processes. Recently, attention has been focused on the phenomenon of ischaemic preconditioning, in which repeated short periods of myocardial ischaemia lead to physiological changes which limit the degree of injury induced by subsequent prolonged ischaemia. Ischaemic late pre-conditioning is dependent on HIF-α signalling, and has been associated with increased circulating EPO produced in the kidney and reduction in infarction size [Cai Z, 2003].

6.2 Aims

In view of the protective effects observed with EPO in a rat model of renal ischaemia reperfusion, it was important to extend these observations into another organ, and the heart is an ideal model to study. Previous studies have suggested a role for EPO in foetal cardiac development [Wu H, 1999], and the receptor is present on foetal and neonatal ventricular myocytes [Juul SE, 1998], although the expression of the receptor in adult tissues is not known. However, cardiac tissue has a very large amount of endothelium which does express the EPO-R [Chong ZZ, 2003], which could be an important site of action of EPO during the physiological response to ischaemia reperfusion injury in the heart.

6.3 Methods

6.3.1 Rat ventricular myoblast cell (H9c2) culture

The H9c2 embryonal rat heart-derived cell line (Kimes and Brandt, 1976; Hescheler *et al.*, 1991) was obtained from the American Type Culture Collection (CRL 1446) and cultured in growth medium comprising DMEM (containing 1000 mg/l D-glucose and 110 mg/l sodium pyruvate) supplemented with 10% heat-inactivated newborn calf serum, 100 U/ml penicillin and 100 µg/ml streptomycin. Cells were grown in an air/CO_2 (49:1) humidified incubator at 37°C. Sub-confluent (80 %) cells were harvested and seeded into six-well tissue culture plates in 2 mL growth medium. The cells were allowed to adhere for 18 hours in an incubator at 37°C with 5% CO_2 in 95% air.

6.3.2 Myocardial Infarction in the anaesthetised rat

Male Wistar rats (200-250 g, Tuck, Rayleigh, Essex, U.K.) were anaesthetised with thiopentone sodium (Intraval®, 120 mg/kg i.p.; Rhone-Merrieux, Essex, U.K.). The rats were tracheotomised, intubated and ventilated with a Harvard ventilator (30% inspiratory oxygen concentration, 70 strokes/min, tidal volume: 8-10 ml/kg). Body temperature was maintained at 38±1ºC. The right carotid artery was cannulated and connected to a pressure transducer (Spectramed, P23XL) to monitor mean arterial blood pressure (MAP). The right jugular vein was cannulated for the administration of drugs.

Subsequently, a lateral thoracotomy was performed and the heart was suspended in a temporary pericardial cradle. A snare occluder was placed around the left anterior

descending coronary artery (LAD). After completion of the surgical procedure the animals were allowed to stabilise for 30 min before LAD ligation. The coronary artery was occluded at time 0 by tightening of the occluder. This was associated with the typical haemodynamic (fall in MAP) changes of myocardial ischemia. After 25 min of acute myocardial ischaemia, the occluder was re-opened to allow reperfusion for 2 h. Heart rate (HR) and MAP were continuously recorded on a 4-channel Grass 7D polygraph recorder (Grass, Mass., U.S.A.).

6.3.3 Determination of infarction size and area of risk

The coronary artery was re-occluded at the end of the reperfusion period, and Evans Blue dye (1 ml of 2% w/v) was injected into the left ventricle, via the right carotid artery cannula, to distinguish between perfused and non-perfused sections of the heart. The Evans Blue solution stains the perfused myocardium, while the occluded vascular bed remains uncoloured, and defines the area at risk (AR). The animals were killed with an overdose of anaesthetic and the heart excised. It was sectioned into slices of 3-4 mm, the right ventricular wall was removed, and the AR (unstained) was separated from the non-ischaemic (blue) area.

The identified AR tissue was cut into small pieces and incubated with *p*-nitroblue tetrazolium (NBT, 0.5mg/ml) for 40 min at 37°C. In the presence of functioning dehydrogenase enzyme systems in surviving viable myocardium, NBT forms a dark blue formazan, whilst areas of necrosis lack dehydrogenase activity and therefore fail to stain. Pieces were separated according to staining and weighed to determine the amount of myocardial infarction as a percentage of the weight of the total AR tissue.

6.3.4 Experimental design for *in vivo* experiments

The experimental groups outlined below were studied according the protocol described in 6.2.2.

(1) MI - control group: (n=8) Animals subjected to 15 min LAD occlusion and at 1 min prior to reperfusion received vehicle control (saline, 1 mg/ Kg bolus iv)

(2) MI - EPO group: (n=12) Animals subjected to 15 min LAD occlusion at at 1 min prior to reperfusion received EPO (300 U/ Kg in saline bolus iv)

(3) Sham Group: (n=6) Animals were subjected to the surgical procedure, without coronary artery occlusion and reperfusion, treated with vehicle control (saline 1mg/ Kg bolus iv)

6.4 Results

6.4.1 Effect of EPO on H9C2 cell proliferation

Preliminary experiments were aimed at confirming that the EPO/ EPO-R system was functional in H9C2 cells. After harvesting and counting, H9C2 cells were plated at a density of 0.5 x 10^6 in a clear 96-well plate with 100 μL phenol-red free standard medium containing 10% FCS. EPO was added to a final concentration of 10 U/mL – 30 U/mL. After 24 hrs incubation, 20 μL of MTS solution was added to each well and the plate returned to the incubator for 30 min. Optical density was measured in the colorimeter after 30 minutes incubation, and results were calculated as percentage of value of control cell minus blank well correction. In each of 3 experiments, twelve wells were used for each experimental group.

When compared to control cells cultured in standard medium with 10% FCS, there was a significant increase in cell number in response to administration of EPO (when compared to control cells, EPO 10U/mL 25 % ± 7, EPO 30 U/mL 33 % ± 8, $P<0.001$). The response to erythropoietin was also dose-dependent, being maximal at 30 U/ mL (Figure 6.1).

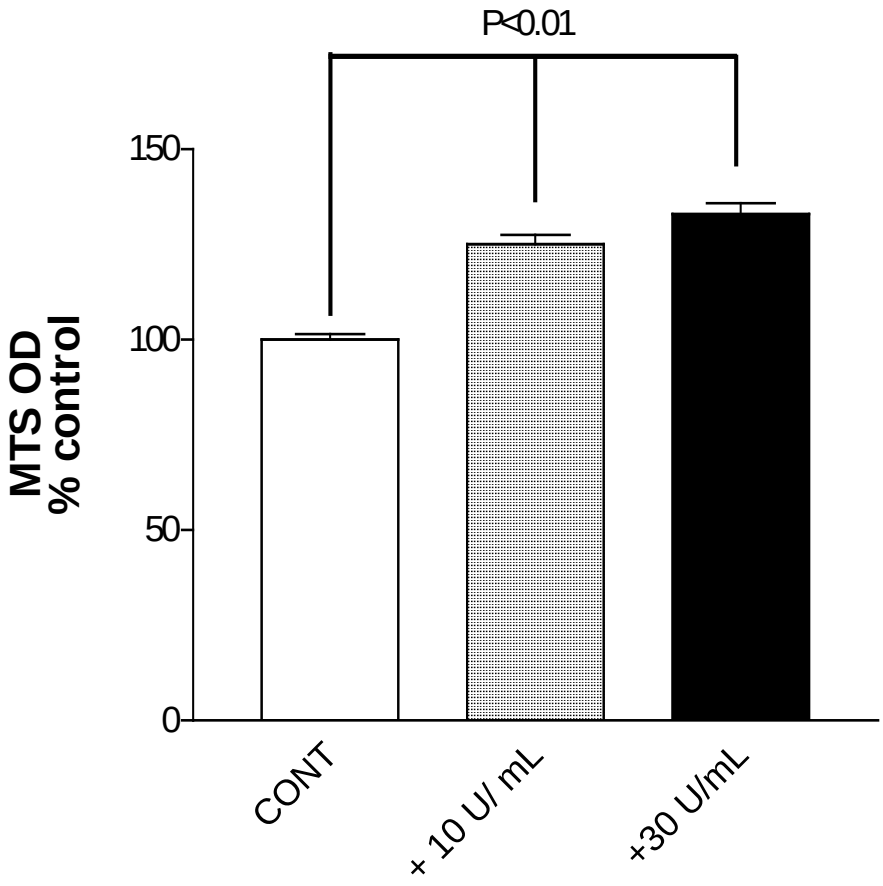

Figure 6.1 EPO induces proliferation above control in H9c2 cells. The MTS assay was used as an indirect measure of cellular proliferation. When compared to control cells, EPO caused an increase in cellular metabolism, consistent with an increase in cell number, in a dose-dependent manner (P<0.01 by ANOVA).

6.4.2 EPO maintains cell viability in serum deprived H9c2 cells

H9C2 cells were plated at a density of 0.5 x 10^6 in a clear 96-well plate with 100 μL phenol-red free standard medium in the absence of FCS. EPO was added in increasing concentrations (1 U/mL – 10 U/mL – 30 U/mL – 100 U/mL). Cells were incubated for 24 hours, and then 20 μL MTS solution was added to each well. After 30 minutes, the plate was read, and cell viability calculated as a percentage of control value.

H9C2 cells deprived of FCS showed significant reduction in cell number after 24 hrs (figure 6.2). EPO significantly maintained cell viability in all doses above that observed in serum deprived conditions (serum free 0.37 ± 0.03, +EPO 10 U/ml 0.46 ± 0.04, +EPO 30 U/ml 0.48 ± 0.03, +EPO 50 U/ml 0.51 ± 0.026, +EPO 100 U/ml 0.50 ± 0.026, all $P<0.001$). The protection observed with EPO increased in a dose-dependent manner, although with highest dose (100 U/mL) there was no appreciable increase in effect over that seen in cells treated with 50 U/mL EPO.

The decrease in cell viability seen in serum deprived culture conditions was due to loss of cell numbers by apoptotic cell death, which is associated with an increase in activity of the serine protease caspase-3 (figure 6.3). Cell lysates were used to examine caspase-3 activity, as described in 2.2.4, to confirm that erythropoietin inhibits caspase-3 activation from a variety of insults. Serum deprivation induced a significant increase in caspases-3 activity (control 125 ± 83, serum deprivation 3068 ± 756, $P<0.001$), which was attenuated by EPO (30 U/ mL) pre-administration (973 ± 599, $P<0.01$ when compared to serum deprivation).

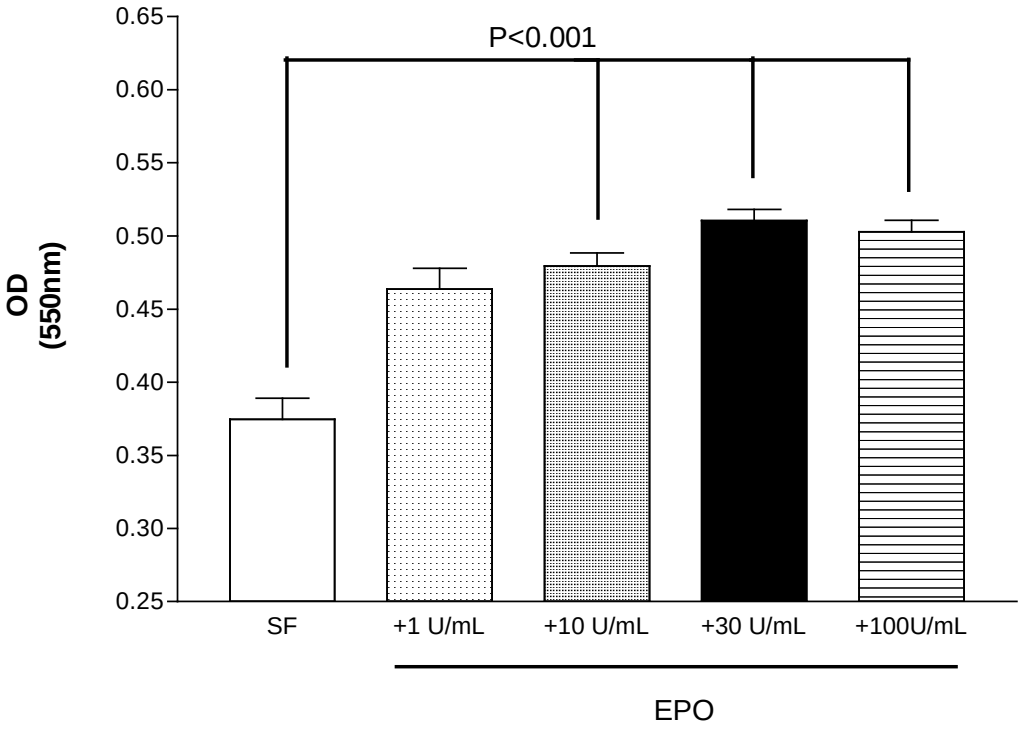

Figure 6.2 EPO preserves cell numbers in serum deprived conditions, measured by MTS assay. Measurement of cell viability was calculated by optical density minus blank well scores. EPO improved cell viability in a dose-dependent manner (P<0.01 by ANOVA).

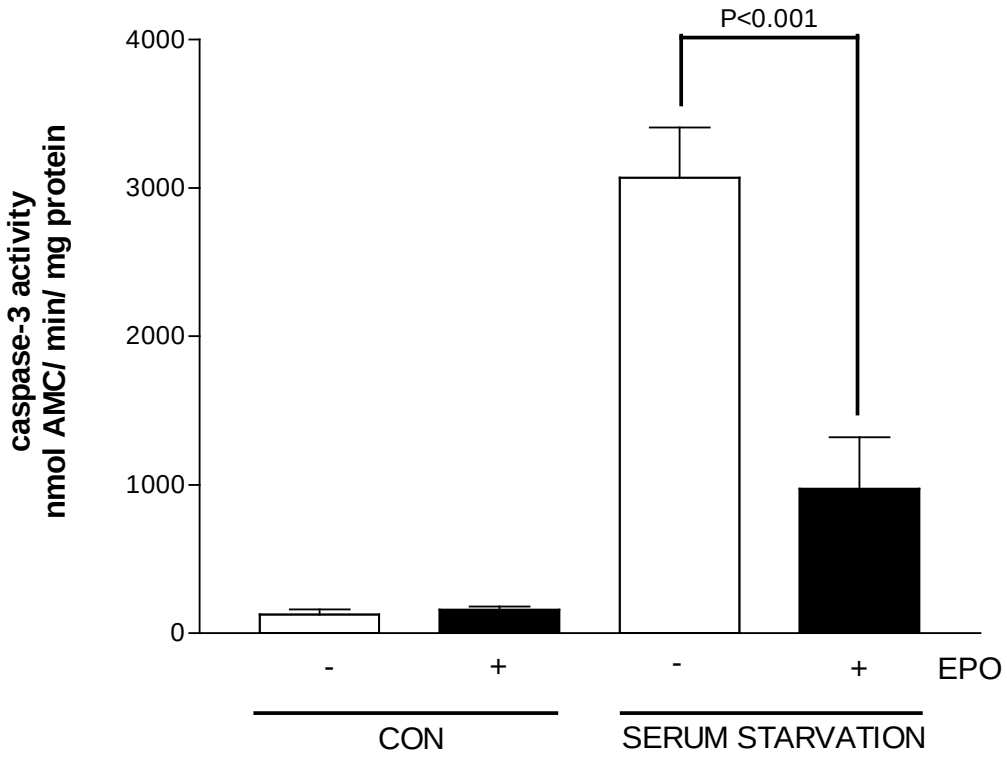

Figure 6.3 EPO inhibits caspase-3 activation in serum deprived conditions, measured by a end-point caspase assay. Serum starvation caused an increase in caspase-3 activity when compared to control (P<0.0001), which was significantly reduced by treatment with EPO (P<0.001).

6.4.4 EPO prevents oxidative stress induced apoptosis in H9C2 cells.

In order to mimic the type of injury observed during reperfusion, hydrogen peroxide was used as a model of oxidative stress in H9c2 cells. After harvesting and counting, H9C2 cells were plated at a density of 1 x 10^6 in a clear 6-well plate with 1 mL standard medium without FCS. Erythropoietin was added in final concentrations of 10 U/mL – 30 U/mL of medium and after 1 hr, hydrogen peroxide (final concentration 200 μM) was added, and the plates returned to the incubator for 24 hrs. The medium was removed and cells washed with 1 mL ice-cold PBS. The cells were scraped with Teflon cell scraper, and centrifuged at 400 g for 5 minutes at 4˚C. Pellets were lysed in digitonin buffer, and DNA fragmentation was assessed in lysates using cell death detection ELISA, described in 2.3.10.

Hydrogen peroxide (200 μM) induced significant DNA fragmentation after 24 hrs in serum-starved H9C2 cells (Figure 6.4). Pre-incubation with EPO (30 U/mL) for 1 hr prior to hydrogen peroxide significantly reduced DNA fragmentation (control 1.0 ± 0.18, H2O2 1.97 ± 0.6, EPO + H2O2 1.1 ± 0.4, $P<0.01$).

The lysates from the previous experiment were subsequently used to examine caspase-3 activation. Hydrogen peroxide (200 μM) induced a significant increase in caspases-3 activity (Figure 6.5), consistent with the observed increase in DNA fragmentation (Figure 6.4). Pre-incubation with EPO (30 IU/mL) for 1hr was associated with a significant reduction of the increase in caspase-3 activity induced by hydrogen peroxide (control 126 ± 83, H2O2 1890 ± 304, EPO + H_2O_2 1333 ± 287, $P<0.01$).

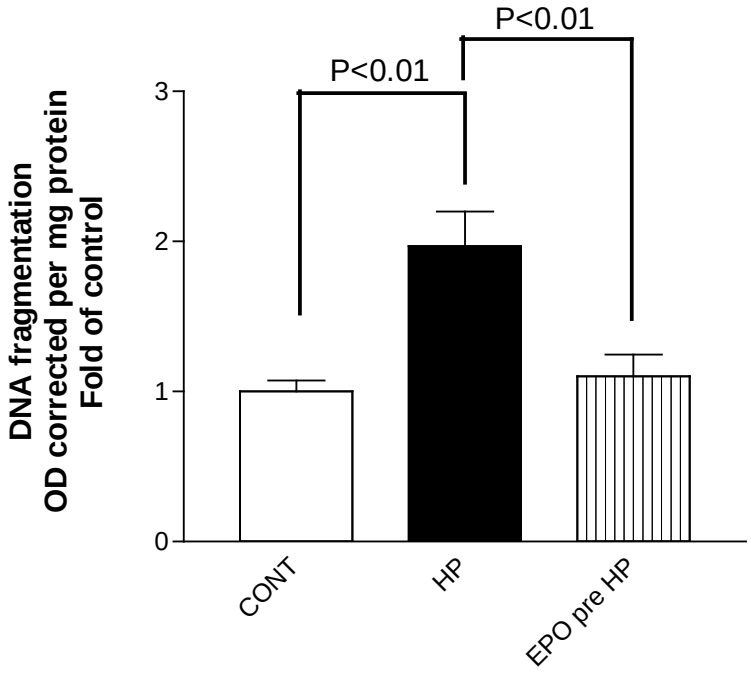

Figure 6.4 EPO reduces Oxidative stress induced cell death, measured with DNA fragmentation ELISA. Hydrogen peroxide caused an increase in cell death, which was reduced by EPO treatment (P<0.01, by ANOVA).

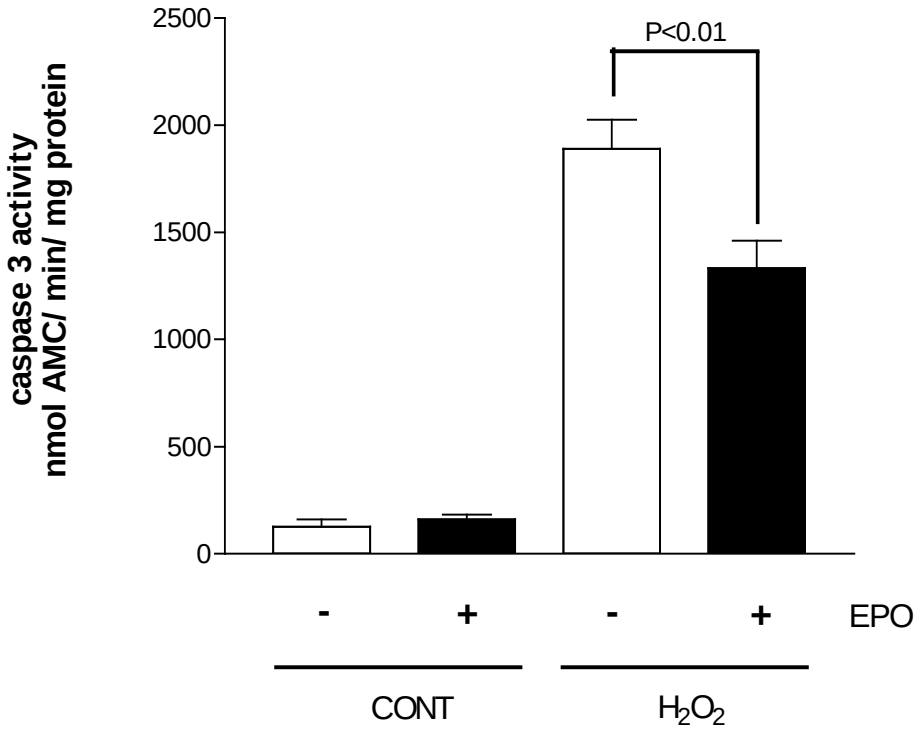

Figure 6.5 Caspase-3 activity in hydrogen peroxide treated H9c2 cells was measured with an end-point caspase 3 assay. When compared to control cells, hydrogen peroxide induced caspase-3 activity (P<0.001), which was reduced by EPO treatment (P<0.01 by ANOVA).

6.4.6 Administration of EPO upon reperfusion reduces myocardial infarction size in the rat

The mean values for area at risk (AR) were similar in all animal groups studied and ranged from 49 ± 2 to 52 ± 2 % (P>0.05). In rats, which received vehicle alone, occlusion of the LAD for 25 min followed by reperfusion for 2 hours resulted in an infarct size of 64 ± 3% (n=9) of the AR, show in Figure 6.6.

When compared with vehicle, administration of EPO (300 IU/kg i.v. bolus administration at 1 min prior to the onset of reperfusion) caused a significant reduction in myocardial infarct size (Figure 6.7). Sham operation alone did not result in a significant degree of infarction in any of the animal groups studied (< 1 % of the AR). It should be noted that coronary artery occlusion and reperfusion caused a progressive fall in mean arterial blood pressure (from a baseline MAP of 111 ± 6 mm/Hg to 77 ± 5 mm/Hg at the end of the 2 hr reperfusion period), (when compared with sham-operated animals). Administration of EPO had no significant effect on blood pressure.

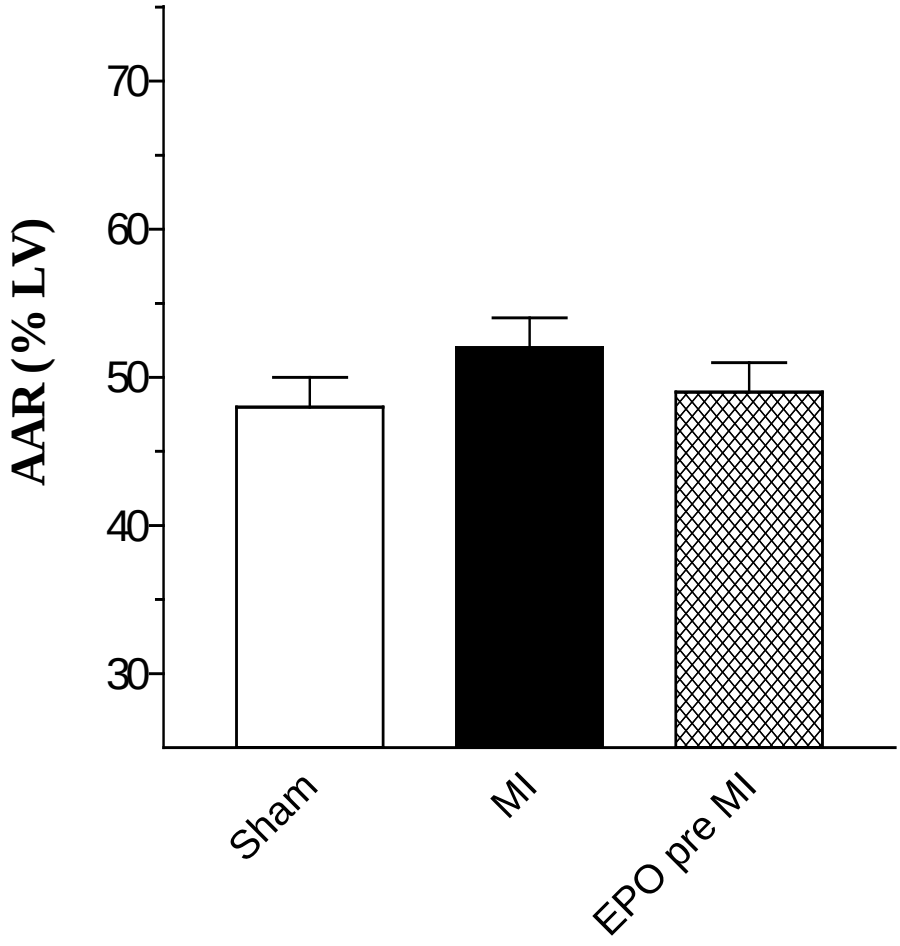

Figure 6.6 There was no difference in the Area at Risk in Myocardial infarction in the rat between the experimental groups, confirming that ischaemia was restricted to myocardium perfused via a single vessel.

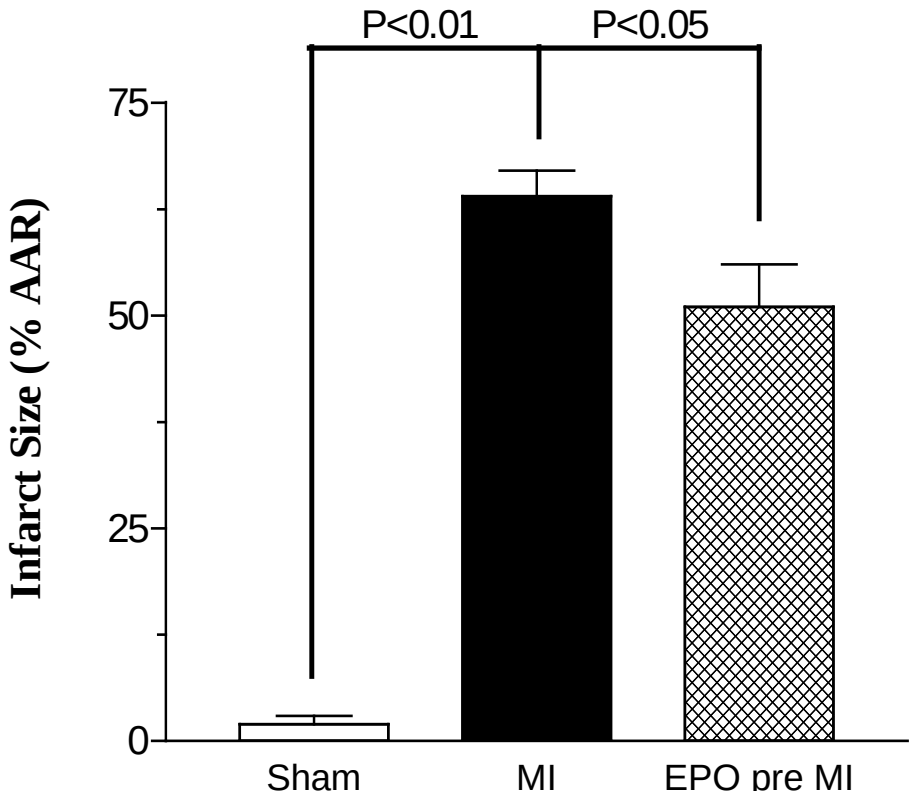

Figure 6.7 EPO reduces infarction size in a rat model of myocardial infarction. The area of infarction was measured by NBT staining, and the percentage of the area at risk stained was calculated. Treatment with EPO significantly reduced the percentage area of infarction (P<0.05)

6.5 Discussion

Having shown that EPO was protective in a short term model of renal ischaemia-reperfusion injury, shown in Chapter three, and that this protection may be mediated by direct effects on intrinsic kidney cells, it was important to examine whether this effect was organ-specific, or whether EPO would also be effective in a broader spectrum of organs, particularly the heart.

For EPO to exert direct actions on cardiac myocytes, these cells must express the appropriate receptor. The EPO receptor has been demonstrated in cardiac tissues as shown in a recent study of adult mouse hearts [Cai Z, 2003]. The potential disadvantage of examining whole organ preparations is that it this does not exclude expression on non-myocytic cells of the heart, particularly the endothelium, and cardiac fibroblasts. These issues are partially addressed by immunohistochemical staining and immunoblotting of neonatal rat ventricular cardiac myocytes, which has shown that these cells, at least, express the EPO receptor. A functional assessment was used in H9c2 cells, and there was a significant dose-dependent increase in cell number induced by EPO administration.

In the simplest experimental system showing cardioprotection by EPO, H9C2 cells were exposed to EPO and subjected to *in vitro* conditions that mimic the stresses experienced either during or following infarction. EPO reduced apoptotic cell death induced by growth factor withdrawal and oxidative stress. This was associated with a significant decrease in caspase-3 activity, demonstrating that these injury models in different cell types are dependent on similar signal transduction pathways.

In an established model of myocardial infarction, EPO administration at the time of reperfusion in a dose similar to that successfully utilized in the kidney injury model, described in chapter three, reduced the area of myocardial infarction significantly.

Several studies have been published, subsequent to our experiments, which confirm our finding that EPO protects the heart in animal models of ischaemia-reperfusion [Cai Z, 2003; Moon C, 2003; Calvillo L, 2003; Parsa CJ, 2004; Wright GL, 2004].

Parsa *et al* evaluated the actions of EPO (5000 units/kg body weight, intraperitoneal injection) in the adult rabbit heart. EPO was delivered at the time of coronary artery ligation and its effects studied at 3 days. Cardiac function was measured *in vivo* by micro-manometry both under basal conditions and in response to β-adrenergic stimulation. Whilst EPO treated hearts did not completely retain global function, peak left ventricular pressures and left ventricular relaxation were significantly improved when compared to non-EPO-treated animals subjected to infarct. Closer examination of the area at risk showed that EPO decreased the area of infarcted tissue.

Calvillo *et al* and Moon *et al* have also followed recovery *in vivo* for longer periods of time following EPO treatment. These studies have examined adult male rats. Calvillo *et al* delivered EPO (5000 units/kg body weight, intraperitoneal injection) in two protocols. First, the effects of EPO pre-treatment were evaluated by administration at 24 and 0.5 hrs prior to a 30 min ligation of the left anterior descending coronary artery. In the alternative protocol, EPO administration was initiated at the time of reperfusion when the suture was removed. In both protocols, animals subsequently received repeat doses of EPO every 24 hrs for the following 7 days, then haemodynamic measurements were made of cardiac function, and the hearts were examined histologically. Cell death was measured together with cardiac myocyte cross-sectional area as an estimate of the hypertrophic response following increased workload.

These studies showed less cardiac myocyte loss and a smaller increase in myocyte size in those animals treated with EPO prior to ischaemia reperfusion. These differences appeared sufficient to normalise haemodynamic function, specifically with ventricular wall stress

remaining normal. In all of these studies, it would appear that the initial actions of EPO to reduce the degree of apoptotic cell death was the major contributor to the reduction in initial infarct areas and would therefore the decrease in left ventricular dilatation.

Chapter Seven:

Summary

7.1 General Summary

The haematopoietic growth hormone EPO plays an essential but tightly regulated role in maintaining basal erythropoiesis, with the ability to increase production many times over in response to stress stimuli. The EPO gene is exquisitely controlled by the hypoxia inducible factor HIF in response to oxygen tension in the renal interstitium. Originally it was thought that EPO had a sole function in the survival, maturation and differentiation of erthyroid progenitors. It has now been established that EPO is also present in many sites outside the bone marrow, including the vasculature, brain, and kidney and plays an important physiological role in the response of different tissues to ischaemia.

This thesis attempts to provide evidence to extend the effect of EPO to the response of the kidney and the heart to ischaemic injury, which is mediated by the interaction between EPO and its cell surface receptor, and the signalling pathways activated. The series of experiments described in these chapters show that EPO reduces apoptotic cell death and organ dysfunction in several models of kidney injury. Several approaches were made in an attempt to elucidate the mediators of this survival signal, and how this applies to organ systems *in vivo*. Whilst this thesis does not provide a complete picture of these mechanisms, it demonstrates that the growth hormone EPO is a potential therapeutic tool to lessen the degree of organ damage caused by ischaemia and other toxic insults.

The major findings of this thesis are:

- EPO administered either before the onset of ischaemia, or at the point of reperfusion, significantly reduced the degree of renal dysfunction observed in a standard model of severe ischaemia reperfusion in the rat by (i) biochemical analysis, (ii) preservation of urine volume and (iii) creatinine clearance.

- The reduction of functional injury was mirrored by preservation of (i) normal renal tubular architecture and (ii) tubular function and (iii) reduced markers of tubular and reperfusion injury.

- EPO reduced the activity of multiple caspases, and the quantity of apoptotic tubular cell death. Apoptosis was measured by the presence of classic histological changes of nuclear blebbing and condensation, and was accurately quantified by the use of immunohistochemistry with an antibody specific to the cleaved active fragment of the executioner caspase-3.

- The EPO-receptor was shown to be expressed on human proximal tubular epithelial cells by immunoblotting, and ligand binding and receptor activation was associated with a proliferative response and a dose-dependent increase in cell numbers. This response was dependent on the presence of the known EPO-receptor and its associated JAK2 kinase, as inhibition of expression by RNA interference completely abrogated the observed cellular responses.

- EPO activates several signalling pathways that contribute to the observed inhibition of apoptosis, including STATs and AKT. EPO was effective in preventing cell death in a number of injury models. In particular, cisplatin-induced apoptosis was utilized to show that EPO altered the development of oxidative stress and prevented PARP-1 activation. The effect on cisplatin induced injury was also confirmed in an animal model with improvements in biochemical and histological parameters at day five after a single dose of erythropoietin was administered as a pre-conditioning therapy.

- The final chapter of this thesis showed that EPO also had signalling effects and prevented cell death in cardiac cells in culture, and, importantly, significantly

reduced myocardial infarction size in a rat model of coronary artery occlusion. This demonstrated that EPO is functional in a number of cell types and organ systems.

These findings are important and act as compelling evidence to consider the extension of studies in clinical practice to the use of EPO in trials of acute kidney injury. Translation of early successes in animal studies to positive outcomes in human clinical trials in AKI has proven difficult, but EPO is an attractive agent, particularly as it is widely established as a highly effective therapeutic tool in the management of anaemia.

It is important to further elucidate the mechanism by which EPO exerts these observed effects. The development of EPO related peptides, and modified EPO molecules such as carbamylated EPO (CEPO), which appear to have similar effects to EPO on cell death in ischaemia reperfusion injury in several organ systems, have suggested that these effects are mediated by a different cell surface receptor. Future work to continue the work described in this thesis would include:

- Receptor interaction studies using fluorescent-labelled EPO receptor and CD131 to determine whether ligand binding with EPO and CEPO cause direct proximity and interaction of these receptor chains.

- Dose ranging studies to determine the optimum dose of EPO that is effective in animal models. This would allow for planning of human clinical trials with the smallest effective dose.

- Investigation of the regulation of EPO-receptor expression in health and post-injury. There is some evidence that EPO-receptor expression is upregulated early following ischaemia that might act to amplify the anti-apoptotic signal.

- Clinical studies in specific clinical areas with predictable degrees of renal injury, such as kidney transplantation, renal injury following cardiac surgery or contrast nephropathy.

References

Abdelrahman,M. *et al.* Erythropoietin attenuates the tissue injury associated with hemorrhagic shock and myocardial ischemia. *Shock* **22**, 63-69 (2004).

Abuelo JG. Normotensive ischaemic acute renal failure. *N Eng J Med* **357**: 797-805 (2007).

Acehan D, Jiang X, Morgan DG, Heuser JE, Wang X, Akey CW. Three-dimensional structure of the apoptosome: implications for assembly, procaspase-9 binding, and activation. *Mol Cell.* **9**: 423-432 (2002).

Aiello, L.P. Angiogenic pathways in diabetic retinopathy. *N. Engl. J. Med.* **353**, 839-841 (2005).

Anders, H.J., Vielhauer,V. & Schlondorff,D. Chemokines and chemokine receptors are involved in the resolution or progression of renal disease. *Kidney Int.* **63**, 401-415 (2003).

Anderson JL, Marshall HW, White RS, Datz F. Streptokinase thrombolysis for acute myocardial infarction in young adults with normal coronary arteries. *Am Heart J* **106**: 1437-1438 (1983)

Annuk,M., Linde,T., Lind,L. & Fellstrom,B. Erythropoietin Impairs Endothelial Vasodilatory Function in Patients with Renal Anemia and in Healthy Subjects. *Nephron Clin. Pract.* **102**, c30-c34 (2005).

Arany,I. & Safirstein,R.L. Cisplatin nephrotoxicity. *Semin. Nephrol.* **23**, 460-464 (2003).

Arcasoy MO, Harris KW, Forget BG. A human erythropoietin receptor gene mutant causing familial erythrocytosis is associated with deregulation of the rates of Jak2 and Stat5 inactivation. *Exp Hematol.* **27**: 63-74(1999)

Arriero,M., Brodsky,S.V., Gealekman,O., Lucas,P.A. & Goligorsky,M.S. Adult skeletal muscle stem cells differentiate into endothelial lineage and ameliorate renal dysfunction after acute ischemia. *Am. J. Physiol Renal Physiol* **287**, F621-F627 (2004).

Ascon DB, Lopez-Briones S, Liu M, Ascon M, Savransky V, Colvin RB, Soloski MJ, Rabb H. Phenotypic and functional characterization of kidney-infiltrating lymphocytes in renal ischemia reperfusion injury. *J Immunol*. **177**: 3380-3387 (2006).

Auer J, Simon G, Stevens J, Griffiths P, Howarth D, Anastassiades E, Gokal R, Oliver D. Quality of life improvements in CAPD patients treated with subcutaneously administered erythropoietin for anemia. *Perit Dial Int.* **12**: 40-42 (1992)

Avasarala,J.R. & Konduru,S.S. Recombinant erythropoietin down-regulates IL-6 and CXCR4 genes in TNF-alpha-treated primary cultures of human microvascular endothelial cells: implications for multiple sclerosis. *J. Mol. Neurosci.* **25**, 183-189 (2005).

Awad A, Rouse M, Huang L, Vergis A, Reutershan J, Cathro H, Linden J, Okusa M. Compartmentalizatoin of neutrophils in the kidney and lung following acute ischaemic kidney injury. *Kidney Int* **75**: 689-698 (2009).

Bahlmann,F.H. *et al.* Endothelial progenitor cell proliferation and differentiation is regulated by erythropoietin. *Kidney Int.* **64**, 1648-1652 (2003).

Bahlmann,F.H. *et al.* Erythropoietin regulates endothelial progenitor cells. *Blood* **103**, 921-926 (2004).

Bahlmann,F.H. *et al.* Low-dose therapy with the long-acting erythropoietin analogue darbepoetin alpha persistently activates endothelial Akt and attenuates progressive organ failure. *Circulation* **110**, 1006-1012 (2004).

Baker,J.E. Erythropoietin mimics ischemic preconditioning. *Vascul. Pharmacol.* **42**, 233-241 (2005).

Basile,D.P., Donohoe,D., Roethe,K. & Osborn,J.L. Renal ischemic injury results in permanent damage to peritubular capillaries and influences long-term function. *Am. J. Physiol Renal Physiol* **281**, F887-F899 (2001).

Baylis C, Brenner BM. Modulation by prostaglandin synthesis inhibitors of the action of exogenous angiotensin II on glomerular ultrafiltration in the rat. *Circ Res* **43**: 889-898 (1978).

Bazan JF. *et al.* Structural design and molecular evolution of a cytokine receptor superfamily. *Proc Natl Acad Sci U S A.* **87**:6934-6938 (1990)

Belayev, L. *et al.* Neuroprotective effect of darbepoetin alfa, a novel recombinant erythropoietic protein, in focal cerebral ischemia in rats. *Stroke* **36**, 1071-1076 (2005).

Belenkov,A.I. *et al.* Erythropoietin induces cancer cell resistance to ionizing radiation and to cisplatin. *Mol. Cancer Ther.* **3**, 1525-1532 (2004).

Belenkov,A.I. et al. Erythropoietin induces cancer cell resistance to ionizing radiation and to cisplatin. *Mol. Cancer Ther.* **3:** 1525-1532 (2004).

Benohr,P., Harsch,S., Proksch,B. & Gleiter,C.H. Does angiotensin II modulate erythropoietin production in HepG2 cells? *Nephron Exp. Nephrol.* **98**, e124-e131 (2004).

Bernaudin M, Marti HH, Roussel S, Divoux D, Nouvelot A, MacKenzie ET, Petit E. A potential role for erythropoietin in focal permanent cerebral ischemia in mice. *J Cereb Blood Flow Metab.* **19**: 643-651 (1999).

Berndtsson M, Hägg M, Panaretakis T, Havelka AM, Shoshan MC, Linder S. Acute apoptosis by cisplatin requires induction of reactive oxygen species but is not associated with damage to nuclear DNA. *Int J Cancer*. **120**:175-180 (2007)

Bolli R, Manchikalapudi S, Tang XL, Takano H, Qiu Y, Guo Y, Zhang Q, Jadoon AK. The protective effect of late preconditioning against myocardial stunning in conscious rabbits is mediated by nitric oxide synthase. Evidence that nitric oxide acts both as a trigger and as a mediator of the late phase of ischemic preconditioning. *Circ Res.* **81**:1094-1107 (1997)

Bommer J, Kugel M, Schoeppe W, Brunkhorst R, Samtleben W, Bramsiepe P, Scigalla P. Dose-related effects of recombinant human erythropoietin on erythropoiesis. Results of a multicenter trial in patients with end-stage renal disease. *Contrib Nephrol.* **66**: 85-93 (1998)

Bonventre,J.V. Dedifferentiation and proliferation of surviving epithelial cells in acute renal failure. *J. Am. Soc. Nephrol.* **14 S1**, S55-S61 (2003).

Bosomworth MP, Aparicio S, Hay A. Urine N-acetyl-β-D-glucosaminidase – a marker of tubular damage ?. *Nephrol Dialysis Transplant* **14**: 620-626 (1999).

Boulikas T, Vougiouka M. Cisplatin and platinum drugs at the molecular level. (Review). *Oncol Rep*. **10**:1663-1682 (2003).

Boyer SH, Bishop TR, Rogers OC, Noyes AN, Frelin LP, Hobbs S. Roles of erythropoietin, insulin-like growth factor 1, and unidentified serum factors in promoting maturation of purified murine erythroid colony-forming units. *Blood*. **80**: 2503-2012 (1992)

Braunwald E, Kloner RA. The stunned myocardium: prolonged, post-ischaemic ventricular dysfunction. *Circulation* **66**: 1146-1149 (1982).

Brezis,M. & Rosen,S. Hypoxia of the renal medulla--its implications for disease. *N. Engl. J. Med.* **332**, 647-655 (1995).

Brines M, Grasso G, Fiordaliso F, Sfacteria A, Ghezzi P, Fratelli M, Latini R,Xie QW, Smart J, Su-Rick CJ, Pobre E, Diaz D, Gomez D, Hand C, Coleman T, Cerami A. Erythropoietin mediates tissue protection through an erythropoietin and common beta-subunit heteroreceptor. *Proc Natl Acad Sci U S A.* **101**: 14907-14912 (2004).

Brines,M. & Cerami,A. Emerging biological roles for erythropoietin in the nervous system. *Nat. Rev. Neurosci.* **6**, 484-494 (2005).

Brodsky,S.V. *et al.* Endothelial dysfunction in ischemic acute renal failure: rescue by transplanted endothelial cells. *Am. J. Physiol Renal Physiol* **282**, F1140-F1149 (2002).

Brooks C, Wang J, Yang T, Dong Z. Characterization of cell clones isolated from hypoxia-selected renal proximal tubular cells. *Am J Physiol Renal Physiol.* **292**: F243-252 (2007).

Buemi,M. *et al.* Recombinant human erythropoietin stimulates angiogenesis and healing of ischemic skin wounds. *Shock* **22**, 169-173 (2004).

Buemi M, Grasso G, Corica F, Calapai G, Salpietro FM, Casuscelli T, Sfacteria A, Aloisi C, Alafaci C, Sturiale A, Frisina N, Tomasello F. In vivo evidence that erythropoietin has a neuroprotective effect during subarachnoid haemorrhage. *Eur J Pharmacol.* **392**: 31-34 (2000)

Buhl,M.R. The predictive value of 5'-adenine nucleotide depletion and replenishment in ischaemic rabbit kidney tissue. *Int. Urol. Nephrol.* **11**, 325-333 (1979).

Bullard,A.J., Govewalla,P. & Yellon,D.M. Erythropoietin protects the myocardium against reperfusion injury in vitro and in vivo. *Basic Res. Cardiol.* **100**, 397-403 (2005).

Cai,Z. *et al.* Hearts from rodents exposed to intermittent hypoxia or erythropoietin are protected against ischemia-reperfusion injury. *Circulation* **108**, 79-85 (2003).

Calvillo L, Latini R, Kajstura J, Leri A, Anversa P, Ghezzi P, Salio M, Cerami A, Brines M. Recombinant human erythropoietin protects the myocardium from ischemia-reperfusion injury and promotes beneficial remodeling. *Proc Natl Acad Sci U S A.* **100**: 4802-4806 (2003)

Campana WM, Myers RR. Exogenous erythropoietin protects against dorsal root ganglion apoptosis and pain following peripheral nerve injury. *Eur J Neurosci*.**18**: 1497-1506 (2003).

Carlini RG, Dusso AS, Obialo CI, Alvarez UM, Rothstein M. Recombinant human erythropoietin (rHuEPO) increases endothelin-1 release by endothelial cells. *Kidney Int.* **43**: 1010-1014 (1993)

Castaneda,M.P. *et al.* Activation of mitochondrial apoptotic pathways in human renal allografts after ischemiareperfusion injury. *Transplantation* **76**, 50-54 (2003).

Cecconi F, Alvarez-Bolado G, Meyer BI, Roth KA, Gruss P. Apaf1 (CED-4 homolog) regulates programmed cell death in mammalian development. *Cell*. **94**: 727-737 (1998).

Celik M, Gökmen N, Erbayraktar S, Akhisaroglu M, Konakc S, Ulukus C, Genc S, Genc K, Sagiroglu E, Cerami A, Brines M. Erythropoietin prevents motor neuron apoptosis and neurologic disability in experimental spinal cord ischaemic injury. *Proc Natl Acad Sci U S A*. **99**: 2258-2263 (2002)

Chakravorty,S.J., Cockwell,P., Girdlestone,J., Brooks,C.J. & Savage,C.O. Fractalkine expression on human renal tubular epithelial cells: potential role in mononuclear cell adhesion. *Clin. Exp. Immunol.* **129**, 150-159 (2002).

Chatterjee PK, Brown PA, Cuzzocrea S, Zacharowski K, Stewart KN, Mota-Filipe H, McDonald MC, Thiemermann C. Calpain inhibitor-1 reduces renal ischemia/reperfusion injury in the rat. *Kidney Int.* **59**: 2073-2078 (2001)

Chatterjee PK, Cuzzocrea S, Thiemermann C. Inhibitors of poly (ADP-ribose) synthetase protect rat proximal tubular cells against oxidant stress. *Kidney Int.* **56**: 973-984 (1999).

Chatterjee PK, Todorovic Z, Sivarajah A, Mota-Filipe H, Brown PA, Stewart KN, Cuzzocrea S, Thiemermann C. Differential effects of caspase inhibitors on the renal dysfunction and injury caused by ischemia-reperfusion of the rat kidney. *Eur J Pharmacol*. **503**:173-183 (2004).

Chatterjee PK, Zacharowski K, Cuzzocrea S, Otto M, Thiemermann C: Inhibitors of poly (ADP-ribose) synthetase reduce renal ischemia-reperfusion injury in the anesthetized rat in vivo. *FASEB J* **14**: 641–651 (2000)

Chatterjee,P.K. & Thiemermann,C. An in vivo model of ischemia/reperfusion and inflammation of the kidneys of the rat. *Methods Mol. Biol.* **225**, 223-237 (2003).

Chatterjee,P.K. Pleiotropic renal actions of erythropoietin. *Lancet* **365**, 1890-1892 (2005).

Chen N, Chen X, Huang R, Zeng H, Gong J, Meng W, Lu Y, Zhao F, Wang L, Zhou Q. BCL-xL is a target gene regulated by hypoxia inducible factor-1{alpha}. *J Biol Chem*. **284**: 10004-10012 (2009).

Chertow GM, Burdick E, Honour M, Bonventre JV, Bates DW. Acute kidney injury, mortality, length of stay, and costs in hospitalized patients. *J Am Soc Nephrol* **16**: 3365-3370 (2005).

Chien CT, Lee PH, Chen CF, Ma MC, Lai MK, Hsu SM. De novo demonstration and co-localization of free-radical production and apoptosis formation in rat kidney subjected to ischemia/reperfusion. *J Am Soc Nephrol*. **12**: 973-982 (2001).

Chien CT, Shyue SK, Lai MK. Bcl-xL augmentation potentially reduces ischemia/reperfusion induced proximal and distal tubular apoptosis and autophagy. *Transplantation*. **84**:1183-1190 (2007).

Chin H, Nakamura N, Kamiyama R, Miyasaka N, Ihle JN, Miura O. Physical and functional interactions between Stat5 and the tyrosine-phosphorylated receptors for erythropoietin and interleukin-3. *Blood.* **88**: 4415-4425 (1996)

Choi DE, Jeong JY, Lim BJ, Lee KW, Shin YT, Na KR. Pretreatment with darbepoetin attenuates renal injury in a rat model of cisplatin-induced nephrotoxicity. *Korean J Intern Med*. **24**: 238-246 (2009).

Chong ZZ, Li F, Maiese K. Activating Akt and the brain's resources to drive cellular survival and prevent inflammatory injury. *Histol Histopathol*. **20**(1):299-315 (2005)

Chong ZZ, Lin SH, Kang JQ, Maiese K. Erythropoietin prevents early and late neuronal demise through modulation of Akt1 and induction of caspase 1, 3, and 8. *J Neurosci Res* **71**: 659-669 (2003).

Chong ZZ, Kang JQ, Maiese K. Erythropoietin is a novel vascular protectant through activation of Akt1 and mitochondrial modulation of cysteine proteases. *Circulation*. **106**: 2973-2979 (2002)

Chrétien S, Varlet P, Verdier F, Gobert S, Cartron JP, Gisselbrecht S, Mayeux P, Lacombe C. Erythropoietin-induced erythroid differentiation of the human erythroleukemia cell line TF-1 correlates with impaired STAT5 activation. *EMBO J*. **15**: 4174-4181 (1996)

Cilenti L, Kyriazis GA, Soundarapandian MM, Stratico V, Yerkes A, Park KM,Sheridan AM, Alnemri ES, Bonventre JV, Zervos AS. Omi/HtrA2 protease mediates cisplatin-induced cell death in renal cells. *Am J Physiol Renal Physiol*. **288**: F371-379 (2005)

Clements IP, Christian TF, Higano ST, Gibbons RJ, Gersh BJ. Residual flow to the infarct zone as a determinant of infarct size after direct angioplasty. *Circulation* **88**: 1527-1533 (1993).

Clements IP, Christian TF, Higano ST, Gibbons RJ, Gersh BJ. Residual flow to the infarct zone as a determinant of infarct size after direct angioplasty. *Circulation*. **88**:1527-1533 (1993)

Conger,J.D. & Weil,J.V. Abnormal vascular function following ischemia-reperfusion injury. *J. Investig. Med.* **43**, 431-442 (1995).

Coussons,P.J., Baig,S., Fanutti,C. & Grant,R. Novel tissue remodelling roles for human recombinant erythropoietin. *Biochem. Soc. Trans.* **33**, 1129-1130 (2005).

Daemen,M.A. *et al.* Inhibition of apoptosis induced by ischemia-reperfusion prevents inflammation. *J. Clin. Invest* **104**, 541-549 (1999).

Daemen,M.A., de Vries,B. & Buurman,W.A. Apoptosis and inflammation in renal reperfusion injury. *Transplantation* **73**, 1693-1700 (2002).

Daemen,M.A., de Vries,B., van't Veer,C., Wolfs,T.G. & Buurman,W.A. Apoptosis and chemokine induction after renal ischemia-reperfusion. *Transplantation* **71**, 1007-1011 (2001).

Dagher,P.C. Apoptosis in ischemic renal injury: roles of GTP depletion and p53. *Kidney Int.* **66**, 506-509 (2004).

Dagher,P.C. Modeling ischemia in vitro: selective depletion of adenine and guanine nucleotide pools. *Am. J. Physiol Cell Physiol* **279**, C1270-C1277 (2000).

Dagnon,K. *et al.* Expression of erythropoietin and erythropoietin receptor in non-small cell lung carcinomas. *Clin. Cancer Res.* **11**, 993-999 (2005).

Dame,C. & Fahnenstich,H. Don't give up on erythropoietin as a neuroprotective agent. *Pediatrics* **116**, 521-522 (2005).

Damen JE, Wakao H, Miyajima A, Krosl J, Humphries RK, Cutler RL, Krystal G. Tyrosine 343 in the erythropoietin receptor positively regulates erythropoietin-induced cell proliferation and Stat5 activation. *EMBO J*. **14**: 5557-5568 (1995)

Damen,J.E., Cutler,R.L., Jiao,H., Yi,T. & Krystal,G. Phosphorylation of tyrosine 503 in the erythropoietin receptor (EpR) is essential for binding the P85 subunit of phosphatidylinositol (PI) 3-kinase and for EpR-associated PI 3-kinase activity. *J. Biol. Chem.* **270**, 23402-23408 (1995).

Dan HC, Sun M, Kaneko S, Feldman RI, Nicosia SV, Wang HG, Tsang BK, Cheng JQ. Akt phosphorylation and stabilization of X-linked inhibitor of apoptosis protein (XIAP). *J Biol Chem.* **279**: 5405-5412. (2004)

Dan HC, Sun M, Kaneko S, Feldman RI, Nicosia SV, Wang HG, Tsang BK, Cheng JQ. Akt phosphorylation and stabilization of X-linked inhibitor of apoptosis protein (XIAP). *J Biol Chem*. **279**: 5405-5412 (2004)

D'Andrea AD, Lodish HF, Wong GG. Expression cloning of the murine erythropoietin receptor. *Cell.* **57**: 277-285 (1989)

D'Andrea AD, Szklut PJ, Lodish HF, Alderman EM. Inhibition of receptor binding and neutralization of bioactivity by anti-erythropoietin monoclonal antibodies. *Blood.* **75**: 874-880 (1990).

Davidman,M., Olson,P., Kohen,J., Leither,T. & Kjellstrand,C. Iatrogenic renal disease. *Arch. Intern. Med.* **151**, 1809-1812 (1991).

De Greef,K.E. *et al.* Neutrophils and acute ischemia-reperfusion injury. *J. Nephrol.* **11**, 110-122 (1998).

De Greef,K.E., Ysebaert,D.K., Persy,V., Vercauteren,S.R. & De Broe,M.E. ICAM-1 expression and leukocyte accumulation in inner stripe of outer medulla in early phase of ischemic compared to HgCl2-induced ARF. *Kidney Int.* **63**, 1697-1707 (2003).

de Murcia JM, Niedergang C, Trucco C, Ricoul M, Dutrillaux B, Mark M, Oliver FJ, Masson M, Dierich A, LeMeur M, Walztinger C, Chambon P, de Murcia G. Requirement of poly(ADP-ribose) polymerase in recovery from DNA damage in mice and in cells. *Proc Natl Acad Sci U S A.* **94**: 7303-7307 (1997).

Dean,B.B. *et al.* Erythropoiesis-stimulating protein therapy and the decline of renal function: a retrospective analysis of patients with chronic kidney disease. *Curr. Med. Res. Opin.* **21**, 981-987 (2005).

Depping, R. *et al.* Expression of the erythropoietin receptor in human heart. *J. Thorac. Cardiovasc. Surg.* **130**, 877-878 (2005).

Devarajan P. Cellular and molecular derangements in acute tubular necrosis. *Curr Opin Pediatr.* **17**: 193-199 (2005).

Deveraux QL, Roy N, Stennicke HR, Van Arsdale T, Zhou Q, Srinivasula SM, Alnemri ES, Salvesen GS, Reed JC. IAPs block apoptotic events induced by caspase-8 and cytochrome c by direct inhibition of distinct caspases. *EMBO J.* **17**: 2215-2223 (1998).

Deveraux QL, Stennicke HR, Salvesen GS, Reed JC. Endogenous inhibitors of caspases. *J Clin Immunol.* **19**:388-398 (1999).

Deyoung,P., Kapur,A., Lichtman,M., Kling,P. & Carlton,D. Effects of erythropoietin on respiratory epithelial cell growth and function.: 9. *Pediatr. Res.* **58**, 817 (2005).

Di Lisa F, Blank PS, Colonna R, Gambassi G, Silverman HS, Stern MD, Hansford RG. Mitochondrial membrane potential in single living adult rat cardiac myocytes exposed to anoxia or metabolic inhibition. *J Physiol*. **486**: 1-13 (1995)

Digicaylioglu M, Bichet S, Marti HH, Wenger RH, Rivas LA, Bauer C, Gassmann M. Localization of specific erythropoietin binding sites in defined areas of the mouse brain. *Proc Natl Acad Sci U S A.* **92**: 3717-3720 (1995)

Digicaylioglu M. & Lipton,S.A. Erythropoietin-mediated neuroprotection involves cross-talk between Jak2 and NF-kappaB signalling cascades. *Nature* **412**, 641-647 (2001).

Dong Z, Venkatachalam MA, Wang J, Patel Y, Saikumar P, Semenza GL, Force T, Nishiyama J. Up-regulation of apoptosis inhibitory protein IAP-2 by hypoxia. Hif-1 -independent mechanisms. *J Biol Chem*. **276**: 18702-18709 (2001).

Dong Z, Wang JZ, Yu F, Venkatachalam MA. Apoptosis-resistance of hypoxic cells: multiple factors involved and a role for IAP-2. *Am J Pathol*. **163**: 663-671 (2003).

Downward J. Mechanisms and consequences of activation of protein kinase B/Akt. *Curr Opin Cell Biol*. **10**: 262-267 (1998)

Driscoll M. Molecular genetics of cell death in the nematode Caenorhabditis elegans. *J Neurobiol*. **23**: 1327-1351 (1992)

Du C, Fang M, Li Y, Li L, Wang X. Smac, a mitochondrial protein that promotes cytochrome c-dependent caspase activation by eliminating IAP inhibition. *Cell*. **102**: 33-42 (2000)

Dusanter-Fourt I, Casadevall N, Lacombe C, Muller O, Billat C, Fischer S, Mayeux P. Erythropoietin induces the tyrosine phosphorylation of its own receptor in human erythropoietin-responsive cells. *J Biol Chem.* **267**: 10670-10675(1992)

Dworkin LD, Ichikawa I, Brenner BM. Hormonal modulation of glomerular function. *Am J Physio* **244**: F95-104 (1983)

Edelstein CL, Alkhunaizi AA, Schrier RW. The role of calcium in the pathogenesis of acute renal failure. *Ren Fail.* **19**: 199-207 (1997).

Edelstein CL, Yaqoob MM, Alkhunaizi AM, Gengaro PE, Nemenoff RA, Wang KK, Schrier RW. Modulation of hypoxia-induced calpain activity in rat renal proximal tubules. *Kidney Int.* **50**: 1150-1157 (1996)

Elbashir SM, Harboth J, Lendeckel W, Yalcin A. Duplexes of 21-nucleotide RNAs mediate RNA interference in cultured mammalian cells. *Nature* **411**:494-498 (2001)

Elliott S, Busse L, Bass MB, Lu H, Sarosi I, Sinclair AM, Spahr C, Um M, Van G, and Begley CG. Anti-Epo receptor antibodies do not predict Epo receptor expression. *Blood*. **107**: 1892-1895 (2006).

Emir,M. *et al.* Effect of erythropoietin on bcl-2 gene expression in rat cardiac myocytes after traumatic brain injury. *Transplant. Proc.* **36**, 2935-2938 (2004).

Erslev AJ, Besarab A. Erythropoietin in the pathogenesis and treatment of the anemia of chronic renal failure. *Kidney Int.* **51**: 622-630 (1997)

Eschbach JW, Egrie JC, Downing MR, Browne JK, Adamson JW. Correction of the anemia of end-stage renal disease with recombinant human erythropoietin. Results of a combined phase I and II clinical trial. *N Engl J Med*. **316**: 73-78 (1987)

Feldenberg,L.R., Thevananther,S., del Rio,M., de Leon,M. & Devarajan,P. Partial ATP depletion induces Fas- and caspase-mediated apoptosis in MDCK cells. *Am. J. Physiol* **276**, F837-F846 (1999).

Feldman,L. *et al.* Erythropoietin stimulates growth and STAT5 phosphorylation in human prostate epithelial and prostate cancer cells. *Prostate* **66**: 135-145 (2005)

Fiordaliso,F. *et al.* A nonerythropoietic derivative of erythropoietin protects the myocardium from ischemia-reperfusion injury. *Proc. Natl. Acad. Sci. U. S. A* **102**, 2046-2051 (2005).

Fisher,J.W. Erythropoietin: physiology and pharmacology update. *Exp. Biol. Med. (Maywood.)* **228**, 1-14 (2003).

Friedewald,J.J. & Rabb,H. Inflammatory cells in ischemic acute renal failure. *Kidney Int.* **66**, 486-491 (2004).

George,J. *et al.* Erythropoietin promotes endothelial progenitor cell proliferative and adhesive properties in a PI 3-kinase-dependent manner. *Cardiovasc. Res.* **68**, 299-306 (2005).

Goligorsky,M.S. Whispers and shouts in the pathogenesis of acute renal ischaemia. *Nephrol. Dial. Transplant.* **20**, 261-266 (2005).

Gorio A, Gokmen N, Erbayraktar S, Yilmaz O, Madaschi L, Cichetti C, Di Giulio AM, Vardar E, Cerami A, Brines M. Recombinant human erythropoietin counteracts secondary injury and markedly enhances neurological recovery from experimental spinal cord trauma. *Proc Natl Acad Sci U S A.* **99**: 9450-9455 (2002).

Grasso G, Buemi M, Alafaci C, Sfacteria A, Passalacqua M, Sturiale A, Calapai G, De Vico G, Piedimonte G, Salpietro FM, Tomasello F. Beneficial effects of systemic administration of recombinant human erythropoietin in rabbits subjected to subarachnoid hemorrhage. *Proc Natl Acad Sci U S A.* **99**: 5627-5631 (2002)

Grasso,G. *et al.* Erythropoietin and erythropoietin receptor expression after experimental spinal cord injury encourages therapy by exogenous erythropoietin. *Neurosurgery* **56**, 821-827 (2005).

Grigoryev D, Liu M, Hassoun H, Cheadle C, Barnes K, Rabb H. The local and systemic transcriptome after acute kidney injury. *J Am Soc Nephrol* **19**: 547-558 (2008).

Grimm C. *et al.* Neuroprotection by hypoxic preconditioning: HIF-1 and erythropoietin protect from retinal degeneration. *Semin. Cell Dev. Biol.* **16** , 531-538 (2005).

Groopman JE, Molina JM, Scadden DT. Hematopoietic growth factors: Biology and clinical applications. *N Engl J Med*. **321**(21):1449-1459 (1989).

Gross A, McDonnell JM, Korsmeyer SJ. BCL-2 family members and the mitochondria in apoptosis. *Genes Dev.* **13**: 1899-1911 (1999)

Gruppo Italiano per lo Studio della Streptochinasi nell'Infarto miocardico (GISSI). Effectiveness of intravenous thrombolytic treatment in acute myocardial infarction. *Lancet* i: 397-402 (1986)

Hale, S.A., Wong,C. & Lounsbury,K.M. Erythropoietin disrupts hypoxia-inducible factor signaling in ovarian cancer cells. *Gynecol. Oncol.* 100: 14-19 (2006).

Haller H, de Groot K, Bahlmann F, Elger M & Fliser D. Stem cells and progenitor cells in renal disease. *Kidney Int.* **68**, 1932-1936 (2005).

Hamadmad,S.N., Henry,M.K. & Hohl,R.J. Erythropoietin Receptor Signal Transduction Requires Protein Geranylgeranylation. *J. Pharmacol. Exp. Ther.* **316**: 403-409 (2005).

Hamilton AJ, Baulcombe DC. A species of small antisense RNA in post translational gene silencing in plants. *Science* **286:** 950-952 (1999).

Hanlon,P.R. *et al.* Mechanisms of erythropoietin-mediated cardioprotection during ischemia-reperfusion injury: role of protein kinase C and phosphatidylinositol 3-kinase signaling. *FASEB J.* **19**, 1323-1325 (2005).

Harriman JF, Waters-Williams S, Chu DL, Powers JC, Schnellmann RG. Efficacy of novel calpain inhibitors in preventing renal cell death. *J Pharmacol Exp Ther*. **294**: 1083-1087 (2000)

Haseyama Y, Sawada K, Oda A, Koizumi K, Takano H, Tarumi T, Nishio M, Handa M, Ikeda Y, Koike T. Phosphatidylinositol 3-kinase is involved in the

protection of primary cultured human erythroid precursor cells from apoptosis. *Blood.* **94**: 1568-1577 (1999)

Haseyama,Y. *et al.* Phosphatidylinositol 3-kinase is involved in the protection of primary cultured human erythroid precursor cells from apoptosis. *Blood* **94**, 1568-1577 (1999).

Hill P, Shukla D, Tran MG, Aragones J, Cook HT, Carmeliet P, Maxwell PH. Inhibition of hypoxia inducible factor hydroxylases protects against renal ischemia-reperfusion injury. *J Am Soc Nephrol.* **19**: 39-46 (2008)

Hirata,A. *et al.* Erythropoietin just before reperfusion reduces both lethal arrhythmias and infarct size via the phosphatidylinositol-3 kinase-dependent pathway in canine hearts. *Cardiovasc. Drugs Ther.* **19**, 33-40 (2005).

Hollenberg NK, Epstein M, Rosen SM, Basch RI, Oken DE, Merrill JP. Acute oliguric renal failure in man: evidence for preferential renal cortical ischemia. *Medicine (Baltimore).* **47**: 455-474 (1968)

Hou,S.H., Bushinsky,D.A., Wish,J.B., Cohen,J.J. & Harrington,J.T. Hospital-acquired renal insufficiency: a prospective study. *Am. J. Med.* **74**, 243-248 (1983).

Hsu CY, Ordonez J, Chertow G, Fan D, McCulloch C, Go A. The risk of acute renal failure in patients with chronic kidney disease. *Kidney Int* **74**: 101-107 (2008).

Huang C, Davis G, Johns EJ. Study of the actions of human recombinant erythropoietin on rat renal haemodynamics. *Clin Sci (Lond).* **83**: 453-459 (1992)

Iiyama,M., Kakihana,K., Kurosu,T. & Miura,O. Reactive oxygen species generated by hematopoietic cytokines play roles in activation of receptor-mediated signaling and in cell cycle progression. *Cell Signal.* **18**: 174-182 (2006).

ISIS-2 (Second International Study of Infarct Survival) Collaborative Group. Randomised trial of intravenous streptokinase, oral aspirin, both, or neither among 17,187 cases of suspected acute myocardial infarction: ISIS-2. *Lancet*; **ii:** 349-360 (1988).

Iyer NV, Kotch LE, Agani F, Leung SW, Laughner E, Wenger RH, Gassmann M, Gearhart JD, Lawler AM, Yu AY, Semenza GL. Cellular and developmental control of O2 homeostasis by hypoxia-inducible factor 1 alpha. *Genes Dev.* **12**: 149-162 (1998)

Jaakkola P, Mole DR, Tian YM, Wilson MI, Gielbert J, Gaskell SJ, Kriegsheim Av, Hebestreit HF, Mukherji M, Schofield CJ, Maxwell PH, Pugh CW, Ratcliffe PJ. Targeting of HIF-alpha to the von Hippel-Lindau ubiquitylation complex by O2-regulated prolyl hydroxylation. *Science*. **292**: 468-472 (2001).

Jacobs K, Shoemaker C, Rudersdorf R, Neill SD, Kaufman RJ, Mufson A, Seehra J, Jones SS, Hewick R, Fritsch EF, et al. Isolation and characterization of genomic and cDNA clones of human erythropoietin. *Nature*. **313**: 806-810 (1985).

Jennings RB, Sommers HM, Smyth GA, Flack HA, Linn H. Myocardial necrosis induced by temporary occlusion of a coronary artery in the dog. *Arch Path* **70**: 68-78 9 (1960)

Jiang M, Yi X, Hsu S, Wang CY, Dong Z. Role of p53 in cisplatin-induced tubular cell apoptosis: dependence on p53 transcriptional activity. *Am J Physiol Renal Physiol.* **287**: F1140-1147 (2004)

Jin Z, El-Deiry WS. Overview of cell death signaling pathways. *Cancer Biol Ther*. **4**: 139-163 (2005).

Junk AK, Mammis A, Savitz SI, Singh M, Roth S, Malhotra S, Rosenbaum PS, Cerami A, Brines M, Rosenbaum DM. Erythropoietin administration protects retinal neurons from acute ischemia-reperfusion injury. *Proc Natl Acad Sci U S A.* **99**: 10659-10664 (2002)

Juul SE, Yachnis AT, Christensen RD. Tissue Distribution of erythropoietin and erythropoietin receptor in the developing human fetus. *Early Hum Dev* **52**: 235-249 (1998).

Juul SE. Nonerythropoietic roles of erythropoietin in the fetus and neonate. *Clin Perinatol.* **27**: 527-541 (200)

Kadri,Z. *et al.* Phosphatidylinositol 3-kinase/Akt induced by erythropoietin renders the erythroid differentiation factor GATA-1 competent for TIMP-1 gene transactivation. *Mol. Cell Biol.* **25**, 7412-7422 (2005).

Katsura,Y. *et al.* Erythropoietin is highly elevated in vitreous fluid of patients with proliferative diabetic retinopathy. *Diabetes Care* **28**, 2252-2254 (2005).

Katz,O. *et al.* Erythropoietin induced tumour mass reduction in murine lymphoproliferative models. *Acta Haematol.* **114**, 177-179 (2005).

Kaufman J, Dhakal M, Patel B, Hamburger R. Community-acquired acute renal failure. *Am J Kid Dis* **17**: 191-198 (1991).

Kaushal GP, Kaushal V, Hong X, Shah SV. Role and regulation of activation of caspases in cisplatin-induced injury to renal tubular epithelial cells. *Kidney Int.* **60**:1726-1736 (2001).

Kaushal GP, Singh AB, Shah SV. Identification of gene family of caspases in rat kidney and altered expression in ischemia-reperfusion injury. *Am J Physiol*. **274**: F587-595 (1998)

Kaushansky K. Lineage-specific hematopoietic growth factors. *N Engl J Med*.**354**: 2034-2045 (2006)

Kellum JA, Levin N, Bouman C, Lameire N. Developing a consensus classification system for Acute renal Failure. *Curr Opin Crit Care* **8**: 509-514 (2002).

Kelly KJ, Plotkin Z, Dagher PC. Guanosine supplementation reduces apoptosis and protects renal function in the setting of ischaemic injury. *J Clin Invest.* **108**: 1291-1298 (2001)

Kelly KJ, Plotkin Z, Vulgamott SL, Dagher PC. P53 mediates the apoptotic response to GTP depletion after renal ischemia-reperfusion: protective role of a p53 inhibitor. *J Am Soc Nephrol.* **14**: 128-138 (2003).

Kelly KJ, Sandoval RM, Dunn KW, Molitoris BA, Dagher PC. A novel method to determine specificity and sensitivity of the TUNEL reaction in the quantitation of apoptosis. *Am J Physiol Cell Physiol*. **284**: C1309-1318 (2003).

Kelly KJ. Distant effects of experimental renal ischemia/reperfusion injury. *J Am Soc Nephrol.* **14**:1549-1558 (2003)

Kelly,K.J., Williams,W.W., Jr., Colvin,R.B. & Bonventre,J.V. Antibody to intercellular adhesion molecule 1 protects the kidney against ischemic injury. *Proc. Natl. Acad. Sci. U. S. A* **91**, 812-816 (1994).

Kennedy,J. & Buchan,A.M. C-EPO: ready for prime-time preconditioning? *Cerebrovasc. Dis.* **19**, 272-273 (2005).

Kerr JF, Wyllie AH, Currie AR. Apoptosis: a basic biological phenomenon with wide-ranging implications in tissue kinetics. *Br J Cancer*. **26**: 239-257 (1972).

Kivirikko KI, Pihlajaniemi T. Collagen hydroxylases and the protein disulfide isomerase subunit of prolyl 4-hydroxylases. *Adv Enzymol Relat Areas Mol Biol*. **72**: 325-398 (1998).

Klingmüller U, Lorenz U, Cantley LC, Neel BG, Lodish HF. Specific recruitment of SH-PTP1 to the erythropoietin receptor causes inactivation of JAK2 and termination of proliferative signals. *Cell*. **80**:729-738 (1995)

Kobayashi T, Yanase H, Iwanaga T, Sasaki R, Nagao M. Epididymis is a novel site of erythropoietin production in mouse reproductive organs. *Biochem Biophys Res Commun.* **296**: 145-151 (2002)

Kotanko P, Margreiter R, Pfaller W. Urinary N-Acetyl--D-Glucosaminidase and Neopterin Aid in the Diagnosis of Rejection and Acute Tubular Necrosis in Initially Nonfunctioning Kidney Grafts. *Nephron* **84**: 228-235 (2000).

Kretz,A., Happold,C.J., Marticke,J.K. & Isenmann,S. Erythropoietin promotes regeneration of adult CNS neurons via Jak2/Stat3 and PI3K/AKT pathway activation. *Mol. Cell Neurosci.* **29**, 569-579 (2005).

Krilleke D, Ucur E, Pulte D, Schulze-Osthoff K, Debatin KM, Herr I. Inhibition of JNK signaling diminishes early but not late cellular stress-induced apoptosis. *Int J Cancer*. **107**: 520-527 (2003).

Kröning R, Katz D, Lichtenstein AK, Nagami GT. Differential effects of cisplatin in proximal and distal renal tubule epithelial cell lines. *Br J Cancer*. **79**: 293-299 (1999)

Kumar SM, Acs G, Fang D, Herlyn M, Elder DE, Xu X. Functional erythropoietin autocrine loop in melanoma. *Am J Pathol*. **166**: 823-830 (2005)

Kumral,A. *et al.* Protective effects of erythropoietin against ethanol-induced apoptotic neurodegeneration and oxidative stress in the developing C57BL/6 mouse brain. *Brain Res. Dev. Brain Res*. **160**: 146-156 (2005).

Lameire N, Van Biesen W, Vanholder R Acute renal failure. *Lancet* **365**: 417-430 (2005).

Lavrik IN, Golks A, Krammer PH. Caspases: pharmacological manipulation of cell death. *J Clin Invest.* **115**: 2665-2672 (2005).

Lebwohl D, Canetta R: Clinical development of platinum complexes in cancer therapy: An historical perspective and an update. *Eur J Cancer* **34** : 1522 –1534 (1998)

Lee,Y.S. *et al.* Coexpression of erythropoietin and erythropoietin receptor in von Hippel-Lindau disease-associated renal cysts and renal cell carcinoma. *Clin. Cancer Res.* **11**, 1059-1064 (2005).

Leist M, Ghezzi P, Grasso G, Bianchi R, Villa P, Fratelli M, Savino C, Bianchi M, Nielsen J, Gerwien J, Kallunki P, Larsen AK, Helboe L, Christensen S, Pedersen LO, Nielsen M, Torup L, Sager T, Sfacteria A, Erbayraktar S, Erbayraktar Z, Gokmen N, Yilmaz O, Cerami-Hand C, Xie QW, Coleman T, Cerami A, Brines M. Derivatives of erythropoietin that are tissue protective but not erythropoietic. *Science.* **305**: 239-242 (2004).

Lester,R.D., Jo,M., Campana,W.M. & Gonias,S.L. Erythropoietin promotes MCF-7 breast cancer cell migration by a ERK/MAP kinase-dependent pathway and is primarily responsible for the increase in migration observed in hypoxia. *J. Biol. Chem.* **280**: 39273-39277 (2005).

Levy E, Viscoli CM, Horwitz R. The effect of acute renal failure on mortality: a cohort analysis. *JAMA* **15**: 1489-1494 (1996).

Li,F., Chong,Z.Z. & Maiese,K. Erythropoietin on a tightrope: balancing neuronal and vascular protection between intrinsic and extrinsic pathways. *Neurosignals.* **13**, 265-289 (2004).

Liangos O, Wald R, O'Bell JW, Price L, Pereira B, Jaber BL. Epidemiology and Outcomes of Acute Renal Failure in Hospitalised Patients: A National Survey. *Clin J AM Soc Nephrol* **1**: 43-51 (2006).

Lieberthal W, Levine JS. Mechanisms of apoptosis and its potential role in renal tubular epithelial cell injury. *Am J Physiol*. **271**: F477-488 (1996).

Lieberthal W, Menza SA, Levine JS. Graded ATP depletion can cause necrosis or apoptosis of cultured mouse proximal tubular cells. *Am J Physiol*. **274**: F315-327 (1998)

Lieberthal,W., Triaca,V. & Levine,J. Mechanisms of death induced by cisplatin in proximal tubular epithelial cells: apoptosis vs. necrosis. *Am. J. Physiol* **270**, F700-F708 (1996).

Lieberthal,W., Wolf,E.F., Rennke,H.G., Valeri,C.R. & Levinsky,N.G. Renal ischemia and reperfusion impair endothelium-dependent vascular relaxation. *Am. J. Physiol* **256**, F894-F900 (1989).

Lin,F. *et al.* Hematopoietic stem cells contribute to the regeneration of renal tubules after renal ischemia-reperfusion injury in mice. *J. Am. Soc. Nephrol.* **14**, 1188-1199 (2003).

Liu X, Rainey JJ, Harriman JF, Schnellmann RG. Calpains mediate acute renal cell death: role of autolysis and translocation. *Am J Physiol Renal Physiol*. **281**: F728-738 (2001).

Liu,J., Narasimhan,P., Yu,F. & Chan,P.H. Neuroprotection by hypoxic preconditioning involves oxidative stress-mediated expression of hypoxia-inducible factor and erythropoietin. *Stroke* **36**, 1264-1269 (2005).

Lu,D. *et al.* Erythropoietin enhances neurogenesis and restores spatial memory in rats after traumatic brain injury. *J. Neurotrauma* **22**, 1011-1017 (2005).

Macdougall,I.C. CERA (Continuous Erythropoietin Receptor Activator): A New Erythropoiesis-Stimulating Agent for the Treatment of Anemia. *Curr. Hematol. Rep.* **4**, 436-440 (2005).

Macedo E, Abdulkader R, Castro I, Sobrinho AC, Yu L, Vieira JM Jr. Lack of protection of N-acetylcysteine (NAC) in acute renal failure related to elective aortic aneurysm repair-a randomized controlled trial. *Nephrol Dial Transplant.* **21**: 1863-1869 (2006).

Maeshima,A., Yamashita,S. & Nojima,Y. Identification of renal progenitor-like tubular cells that participate in the regeneration processes of the kidney. *J. Am. Soc. Nephrol.* **14**, 3138-3146 (2003).

Maiese,K., Li,F. & Chong,Z.Z. New avenues of exploration for erythropoietin. *JAMA* **293**, 90-95 (2005).

Manolis,A.S. *et al.* Erythropoietin in heart failure and other cardiovascular diseases: hematopoietic and pleiotropic effects. *Curr. Drug Targets. Cardiovasc. Haematol. Disord.* **5**, 355-375 (2005).

Marrero MB, Venema RC, Ma H, Ling BN, Eaton DC. Erythropoietin receptor-operated Ca^{2+} channels: activation by phospholipase C-gamma 1. *Kidney Int*. **53**: 1259-1268 (1998)

Marsden VS, O'Connor L, O'Reilly LA, Silke J, Metcalf D, Ekert PG, Huang DC, Cecconi F, Kuida K, Tomaselli KJ, Roy S, Nicholson DW, Vaux DL, Bouillet P, Adams JM, Strasser A. Apoptosis initiated by Bcl-2-regulated caspase activation independently of the cytochrome c/Apaf-1/caspase-9 apoptosome. *Nature*. **419**: 634-637 (2002).

Marti HH, Wenger RH, Rivas LA, Straumann U, Digicaylioglu M, Henn V, Yonekawa Y, Bauer C, Gassmann M. Erythropoietin gene expression in human, monkey and murine brain. *Eur J Neurosci*. **8**: 666-676 (1996).

Masuda S, Okano M, Yamagishi K, Nagao M, Ueda M, Sasaki R. A novel site of erythropoietin production. Oxygen-dependent production in cultured rat astrocytes. *J Biol Chem*. **269**: 19488-19493 (1994)

Matsui Y, Kyoi S, Takagi H, Hsu CP, Hariharan N, Ago T, Vatner SF, Sadoshima J. Molecular mechanisms and physiological significance of autophagy during myocardial ischemia and reperfusion. *Autophagy*. **4**: 409-415 (2008).

Matsumoto M, Makino Y, Tanaka T, Tanaka H, Ishizaka N, Noiri E, Fujita T, Nangaku M. Induction of renoprotective gene expression by cobalt ameliorates ischemic injury of the kidney in rats. *J Am Soc Nephrol*. **14**: 1825-1832 (2003)

Matsushita H, Johnston MV, Lange MS, Wilson MA. Protective effect of erythropoietin in neonatal hypoxic ischemia in mice. *Neuroreport.* **14**: 1757-1761 (2003)

Matthews DJ, Topping RS, Cass RT, Giebel LB. A sequential dimerization mechanism for erythropoietin receptor activation. *Proc Natl Acad Sci U S A.* **93**: 9471-9476 (1996)

Maxwell PH, Osmond MK, Pugh CW, Heryet A, Nicholls LG, Tan CC, Doe BG, Ferguson DJ, Johnson MH, Ratcliffe PJ. Identification of the renal erythropoietin-producing cells using transgenic mice. *Kidney Int.* **44**: 1149-1162 (1993)

Maxwell,P. HIF-1: an oxygen response system with special relevance to the kidney. *J. Am. Soc. Nephrol.* **14**, 2712-2722 (2003).

McDonald MC, Mota-Filipe H, Wright JA, Abdelrahman M, Threadgill MD, Thompson AS, Thiemermann C. Effects of 5-aminoisoquinolinone, a water-soluble, potent inhibitor of the activity of poly (ADP-ribose) polymerase on the organ injury and dysfunction caused by haemorrhagic shock. *Br J Pharmacol.* **130**: 843-850 (2000).

Melnikov VY, Ecder T, Fantuzzi G, Siegmund B, Lucia MS, Dinarello CA, Schrier RW, Edelstein CL. Impaired IL-18 processing protects caspase-1-deficient mice from ischemic acute renal failure. *J Clin Invest.* **107**: 1145-1152 (2001)

Megyesi,J., Andrade,L., Vieira,J.M., Jr., Safirstein,R.L. & Price,P.M. Positive effect of the induction of p21WAF1/CIP1 on the course of ischemic acute renal failure. *Kidney Int.* **60**: 2164-2172 (2001).

Mehta,R.L. *et al.* Spectrum of acute renal failure in the intensive care unit: the PICARD experience. *Kidney Int.* **66**, 1613-1621 (2004).

Miller CP, Liu ZY, Noguchi CT, Wojchowski DM. A minimal cytoplasmic subdomain of the erythropoietin receptor mediates erythroid and megakaryocytic cell development. *Blood*. **94**: 3381-3387 (1999)

Miura M, Zhu H, Rotello R, Hartwieg EA, Yuan J. Induction of apoptosis in fibroblasts by IL-1 beta-converting enzyme, a mammalian homolog of the C. elegans cell death gene ced-3. *Cell.* **75**: 653-660 (1993)

Miyake T, Kung CK, Goldwasser E. Purification of human erythropoietin. *J Biol Chem.* **252**: 5558-5564 (1977).

Mizutani,A., Okajima,K., Uchiba,M. & Noguchi,T. Activated protein C reduces ischemia/reperfusion-induced renal injury in rats by inhibiting leukocyte activation. *Blood* **95**, 3781-3787 (2000).

Molina A, Ubeda M, Escribese MM, García-Bermejo L, Sancho D, Pérez de Lema G, Liaño F, Cabañas C, Sánchez-Madrid F, Mampaso F. Renal ischemia/reperfusion injury: functional tissue preservation by anti-activated {beta}1 integrin therapy. *J Am Soc Nephrol*. **16**: 374-382 (2005)

Molitoris,B.A. & Sutton,T.A. Endothelial injury and dysfunction: role in the extension phase of acute renal failure. *Kidney Int.* **66**, 496-499 (2004).

Molitoris,B.A., Dahl,R. & Geerdes,A. Cytoskeleton disruption and apical redistribution of proximal tubule Na(+)-K(+)-ATPase during ischemia. *Am. J. Physiol* **263**, F488-F495 (1992).

Molitoris,B.A., Sandoval,R. & Sutton,T.A. Endothelial injury and dysfunction in ischemic acute renal failure. *Crit Care Med.* **30**, S235-S240 (2002).

Moon,C., Krawczyk,M., Ahn D, Ahmet I, Paik,D., Lakatta,E.G. & Talan,M.I. Eythropoietin reduces myocardial infaerction and left ventricular functional decline after coronary artery ligation in rats.*Proc Natl Acad Sci USA* **100**: 11612-11617 (2003).

Morishita E, Masuda S, Nagao M, Yasuda Y, Sasaki R. Erythropoietin receptor is expressed in rat hippocampal and cerebral cortical neurons, and erythropoietin prevents in vitro glutamate-induced neuronal death. *Neuroscience*. **76**: 105-116 (1997)

Mortality statistics Review by Registrar general, Office of national statistics, 2008.

Moucadel,V. & Constantinescu,S.N. Differential STAT5 signaling by ligand-dependent and constitutively active cytokine receptors. *J. Biol. Chem.* **280**, 13364-13373 (2005).

Munugalavadla,V. *et al.* Repression of c-kit and its downstream substrates by GATA-1 inhibits cell proliferation during erythroid maturation. *Mol. Cell Biol.* **25**, 6747-6759 (2005).

Murry CE, Jennings RB, Reimer KA. Preconditioning with ischemia: a delay of lethal cell injury in ischemic myocardium. *Circulation.* 1986 Nov;**74**(5):1124-1136 (1986)

Myers,B.D. & Moran,S.M. Hemodynamically mediated acute renal failure. *N. Engl. J. Med.* **314**, 97-105 (1986).

Namiuchi,S. *et al.* High serum erythropoietin level is associated with smaller infarct size in patients with acute myocardial infarction who undergo successful primary percutaneous coronary intervention. *J. Am. Coll. Cardiol.* **45**, 1406-1412 (2005).

Nash,K., Hafeez,A. & Hou,S. Hospital-acquired renal insufficiency. *Am. J. Kidney Dis.* **39**, 930-936 (2002).

Nemoto T, Yokota N, Keane WF, Rabb H. Recombinant erythropoietin rapidly treats anemia in ischemic acute renal failure. *Kidney Int.* **59**: 246-251 (2001).

Noiri E, Peresleni T, Miller F, Goligorsky MS. In vivo targeting of inducible NO synthase with oligodeoxynucleotides protects rat kidney against ischemia. *J Clin Invest.* **97**: 2377-2383 (1996)

O'Connor PM. Renal oxygen delivery: matching delivery to metabolic demand. *Clin Exp Pharmacol Physiol* **33**: 961-967 (2006).

Oberbauer R, Rohrmoser M, Regele H, Mühlbacher F, Mayer G. Apoptosis of tubular epithelial cells in donor kidney biopsies predicts early renal allograft function. *J Am Soc Nephrol*. **10**: 2006-2013 (1999)

Ohsumi Y. Molecular dissection of autophagy: two ubiquitin-like systems. *Nat Rev Mol Cell Biol*. **2**: 211-216 (2001).

Oliver,J.A., Maarouf,O., Cheema,F.H., Martens,T.P. & Al Awqati,Q. The renal papilla is a niche for adult kidney stem cells. *J. Clin. Invest* **114**, 795-804 (2004).

O'Valle F, Benítez MC, Gómez-Morales M, Bravo J, Osuna A, Martin-Oliva D, Oliver FJ, Del Moral RG. Role of poly (ADP-ribose) polymerase in kidney

transplant and its relationship with delayed renal function: multivariate analysis. *Transplant Proc*. **37**: 3684-3687 (2005).

Park,M.S., De Leon,M. & Devarajan,P. Cisplatin induces apoptosis in LLC-PK1 cells via activation of mitochondrial pathways. *J. Am. Soc. Nephrol.* **13**, 858-865 (2002).

Park,P. *et al.* Injury in renal ischemia-reperfusion is independent from immunoglobulins and T lymphocytes. *Am. J. Physiol Renal Physiol* **282**, F352-F357 (2002).

Parsa CJ, Kim J, Riel RU, Pascal LS, Thompson RB, Petrofski JA, Matsumoto A, Stamler JS, Koch WJ. Cardioprotective effects of erythropoietin in the reperfused ischemic heart: a potential role for cardiac fibroblasts. *J Biol Chem*. **279**: 20655-20662 (2004).

Plotnikov EY, Kazachenko AV, Vyssokikh MY, Vasileva AK, Tcvirkun DV, Isaev NK, Kirpatovsky VI, Zorov DB. The role of mitochondria in oxidative and nitrosative stress during ischemia/reperfusion in the rat kidney. *Kidney Int*. **72**: 1493-1502 (2007)

Rana A, Sathyanarayana P, Lieberthal W. Role of apoptosis of renal tubular cells in acute renal failure: therapeutic implications. **Apoptosis**. **6**: 83-102 (2001)

Ratcliffe PJ. HIF-1 and HIF-2: working alone or together in hypoxia? *J Clin Invest*. **117**: 862-865 (2007).

Reid CD, Fidler J, Oliver DO, Cotes PM, Pippard MJ, Winearls CG. Erythroid progenitor cell kinetics in chronic haemodialysis patients responding to treatment with recombinant human erythropoietin. *Br J Haematol*. **70**: 375-380 (1988)

Rice JC, Spence JS, Yetman DL, Safirstein RL. Monocyte chemoattractant protein-1 expression correlates with monocyte infiltration in the post-ischemic kidney. *Ren Fail.* **24**: 703-723 (2004)

Richmond,T.D., Chohan,M. & Barber,D.L. Turning cells red: signal transduction mediated by erythropoietin. *Trends Cell Biol.* **15**, 146-155 (2005).

Roberto Bolli, Lance Becker, Garrett Gross, Robert Mentzer, Jr, David Balshaw and David A. Lathrop. Myocardial Protection at a Crossroads: The Need for Translation Into Clinical Therapy. *Circ Res* **95**: 125-134 (2004)

Rodriguez J, Lazebnik Y. Caspase-9 and APAF-1 form an active holoenzyme. *Genes Dev*. **13**: 3179-3184 (1999).

Rosen S, Stillman I. Acute Tubular Necrosis Is a Syndrome of Physiologic and Pathologic Dissociation. *J Am Soc Nephrol* **19**: 871-875 (2008).

Rossert,J. & Eckardt,K.U. Erythropoietin receptors: their role beyond erythropoiesis. *Nephrol. Dial. Transplant.* **20**, 1025-1028 (2005).

Rui,T. *et al.* Erythropoietin prevents the acute myocardial inflammatory response induced by ischemia/reperfusion via induction of AP-1. *Cardiovasc. Res.* **65**, 719-727 (2005).

Ruscher,K. *et al.* Erythropoietin is a paracrine mediator of ischemic tolerance in the brain: evidence from an in vitro model. *J. Neurosci.* **22**, 10291-10301 (2002).

Ryan MJ, Johnson G, Kirk J, Fuerstenberg S, Zager R, Torok-Storb. HK-2: An immortalized proximal tubule epithelial cell line from normal adult human Kidney. *Kidney Inter* **45**: 48-57 (1994).

Sadamoto Y, Igase K, Sakanaka M, Sato K, Otsuka H, Sakaki S, Masuda S, Sasaki R. Erythropoietin prevents place navigation disability and cortical infarction in rats with permanent occlusion of the middle cerebral artery. *Biochem Biophys Res Commun.* **253**: 26-32 (1998).

Sakanaka M, Wen TC, Matsuda S, Masuda S, Morishita E, Nagao M, Sasaki R. In vivo evidence that erythropoietin protects neurons from ischemic damage. *Proc Natl Acad Sci U S A.* **95**: 4635-4640 (1998)

Sakanaka,M. *et al.* In vivo evidence that erythropoietin protects neurons from ischemic damage. *Proc. Natl. Acad. Sci. U. S. A* **95**, 4635-4640 (1998).

Salahudeen AK, Haider N, Jenkins J, Joshi M, Patel H, Huang H, Yang M, Zhe H. Antiapoptotic properties of erythropoiesis-stimulating proteins in models of cisplatin-induced acute kidney injury. *Am J Physiol Renal Physiol*. **294**: F1354-1365 (2008)

Salahudeen AK, Haider N, Jenkins J, Joshi M, Patel H, Huang H, Yang M, Zhe H. Antiapoptotic properties of erythropoiesis-stimulating proteins in models of cisplatin-induced acute kidney injury. *Am J Physiol Renal Physiol*. **294**: F1354-1365 (2008).

Sawyer ST, Hankins WD. The functional form of the erythropoietin receptor is a 78-kDa protein: correlation with cell surface expression, endocytosis, and phosphorylation. *Proc Natl Acad Sci U S A.* **90**: 6849-6853 (1993)

Scalera,F. *et al.* Erythropoietin increases asymmetric dimethylarginine in endothelial cells: role of dimethylarginine dimethylaminohydrolase. *J. Am. Soc. Nephrol.* **16**, 892-898 (2005).

Schumer M, Colombel MC, Sawczuk IS, Gobé G, Connor J, O'Toole KM, Olsson CA, Wise GJ, Buttyan R. Morphologic, biochemical, and molecular evidence of apoptosis during the reperfusion phase after brief periods of renal ischemia. *Am J Pathol.* **140**: 831-838 (1992)

Scortegagna,M. *et al.* HIF-2alpha regulates murine hematopoietic development in an erythropoietin-dependent manner. *Blood* **105**, 3133-3140 (2005).

Scott AM, Saleh M. The inflammatory caspases: guardians against infections and sepsis. *Cell Death Differ.* **14**: 23-31 (2007).

Sekiguchi,N., Inoguchi,T., Kobayashi,K., Sonoda,N. & Nawata,H. Erythropoietin attenuated high glucose-induced apoptosis in cultured human aortic endothelial cells. *Biochem. Biophys. Res. Commun.* **334**, 218-222 (2005).

Seth R, Yang C, Kaushal V, Shah SV, Kaushal GP. p53-dependent caspase-2 activation in mitochondrial release of apoptosis-inducing factor and its role in renal tubular epithelial cell injury. *J Biol Chem*.;**280**: 31230-31239 (2005)

Shanley PF, Brezis M, Spokes K, Silva P, Epstein F, Rosen S. Hypoxic injury in the proximal tubule of the isolated perfused rat kidney. *Kid Inter* **29**, 1021–1032 (1986).

Shannon,K. & Van Etten,R.A. JAKing up hematopoietic proliferation. *Cancer Cell* **7**, 291-293 (2005).

Sharples,E.J. *et al.* Erythropoietin protects the kidney against the injury and dysfunction caused by ischemia-reperfusion. *J. Am. Soc. Nephrol.* **15**, 2115-2124 (2004).

Silva M, Grillot D, Benito A, Richard C, Nuñez G, Fernández-Luna JL. Erythropoietin can promote erythroid progenitor survival by repressing apoptosis through Bcl-XL and Bcl-2. *Blood*. **88**: 1576-1582 (1996)

Singh AB, Kaushal V, Megyesi JK, Shah SV, Kaushal GP. Cloning and expression of rat caspase-6 and its localization in renal ischemia/reperfusion injury *Kidney Int.* **62**: 106-115 (2002)

Smith KJ, Bleyer AJ, Little WC, Sane DC. The cardiovascular effects of erythropoietin. *Cardiovasc Res*. **59**: 538-548 (2003)

Smith PK, Krohn RI, Hermanson GT, Mallia AK, Gartner FH, Provenzano MD, Fujimoto EK, Goeke NM, Olson BJ, Klenk DC. Measurement of protein using bicinchoninic acid. *Anal Biochem*. **150**: 76-85 (1985)

Sola,A., Rogido,M., Lee,B.H., Genetta,T. & Wen,T.C. Erythropoietin after focal cerebral ischemia activates the Janus kinase-signal transducer and activator of transcription signaling pathway and improves brain injury in postnatal day 7 rats. *Pediatr. Res.* **57**, 481-487 (2005).

Spandou,E. *et al.* Erythropoietin prevents long-term sensorimotor deficits and brain injury following neonatal hypoxia-ischemia in rats. *Brain Res.* **1045**, 22-30 (2005).

Spivak JL, Fisher J, Isaacs MA, Hankins WD. Protein kinases and phosphatises are involved in erythropoietin-mediated signal transduction. *Exp Hematol*. **20**: 500-504 (1992)

Stennicke HR, Salvesen GS. Catalytic properties of the caspases. *Cell Death Differ*. **6**: 1054-1059 (1999).

Stokman,G., Leemans,J.C., Claessen,N., Weening,J.J. & Florquin,S. Hematopoietic Stem Cell Mobilization Therapy Accelerates Recovery of Renal Function Independent of Stem Cell Contribution. *J. Am. Soc. Nephrol* **16**: 1684-1692 (2005).

Sun C, Cai M, Gunasekera AH, Meadows RP, Wang H, Chen J, Zhang H, Wu W, Xu N, Ng SC, Fesik SW. NMR structure and mutagenesis of the inhibitor-of-apoptosis protein XIAP. *Nature* **401**: 818-822 (1999).

Sundal E, Businger J, Kappeler A. Treatment of transfusion-dependent anaemia of chronic renal failure with recombinant human erythropoietin. A European multicentre study in 142 patients to define dose regimen and safety profile. *Nephrol Dial Transplant*. **6**: 955-965 (1991)

Sutton,T.A. & Molitoris,B.A. Mechanisms of cellular injury in ischemic acute renal failure. *Semin. Nephrol.* **18**, 490-497 (1998).

Sutton,T.A., Fisher,C.J. & Molitoris,B.A. Microvascular endothelial injury and dysfunction during ischemic acute renal failure. *Kidney Int.* **62**, 1539-1549 (2002).

Suwa,T., Hogg,J.C., Quinlan,K.B. & Van Eeden,S.F. The effect of interleukin-6 on L-selectin levels on polymorphonuclear leukocytes. *Am. J. Physiol Heart Circ. Physiol* **283**, H879-H884 (2002).

Suzuki C, Isaka Y, Takabatake Y, Tanaka H, Koike M, Shibata M, Uchiyama Y, Takahara S, Imai E. Participation of autophagy in renal ischemia/reperfusion injury. *Biochem Biophys Res Commun*. **368**: 100-106 (2008).

Suzuki Y, Imai Y, Nakayama H, Takahashi K, Takio K, Takahashi R. A serine protease, HtrA2, is released from the mitochondria and interacts with XIAP, inducing cell death. *Mol Cell*. **8**: 613-621 (2001)

Terragni J, Graham JR, Adams KW, Schaffer ME, Tullai JW, Cooper GM. Phosphatidylinositol 3-kinase signaling in proliferating cells maintains an anti-apoptotic transcriptional program mediated by inhibition of FOXO and non-canonical activation of NFkappaB transcription factors. *BMC Cell Biol*. **28**: 9-16 (2008).

Thadhani,R., Pascual,M. & Bonventre,J.V. Acute renal failure. *N. Engl. J. Med.* **334**, 1448-1460 (1996).

Thakar,C.V. *et al.* ARF after open-heart surgery: Influence of gender and race. *Am. J. Kidney Dis.* **41**, 742-751 (2003).

Togel,F. *et al.* Administered mesenchymal stem cells protect against ischemic acute renal failure through differentiation-independent mechanisms. *Am. J. Physiol Renal Physiol* **289**: F31-42 (2005).

Togel,F., Isaac,J., Hu,Z., Weiss,K. & Westenfelder,C. Renal SDF-1 signals mobilization and homing of CXCR4-positive cells to the kidney after ischemic injury. *Kidney Int.* **67**: 1772-1784 (2005).

Tong,W., Zhang,J. & Lodish,H.F. Lnk inhibits erythropoiesis and Epo-dependent JAK2 activation and downstream signaling pathways. *Blood* **105**, 4604-4612 (2005).

Tovari,J. *et al.* Recombinant human erythropoietin alpha targets intratumoral blood vessels, improving chemotherapy in human xenograft models. *Cancer Res.* **65**, 7186-7193 (2005).

Tsujimoto Y, Shimizu S. Another way to die: autophagic programmed cell death. *Cell Death Differ*. **12 S2**: 1528-1534 (2005).

Tsuruta F, Sunayama J, Mori Y, Hattori S, Shimizu S, Tsujimoto Y, Yoshioka K, Masuyama N, Gotoh Y. JNK promotes Bax translocation to mitochondria through phosphorylation of 14-3-3 proteins. *EMBO J*. **23**: 1889-1899 (2004)

Um M, Gross AW, Lodish HF. A "classical" homodimeric erythropoietin receptor is essential for the antiapoptotic effects of erythropoietin on differentiated neuroblastoma SH-SY5Y and pheochromocytoma PC-12 cells. *Cell Signal*. **19**: 634-645 (2007).

Vaziri,N.D., Zhou,X.J. & Liao,S.Y. Erythropoietin enhances recovery from cisplatin-induced acute renal failure. *Am. J. Physiol* **266**, F360-F366 (1994).

Venkatachalam MA, Bernard DB, Donohoe JF, Levinsky NG. Ischemic damage and repair in the rat proximal tubule: differences among the S1, S2, and S3 segments. *Kidney Int.* **14**: 31-49 (1978)

Verdier F, Chrétien S, Billat C, Gisselbrecht S, Lacombe C, Mayeux P. Erythropoietin induces the tyrosine phosphorylation of insulin receptor substrate-2. An alternate pathway for erythropoietin-induced phosphatidylinositol 3-kinase activation. *J Biol Chem*. **272**: 26173-26178 (1997)

Verdier F, Walrafen P, Hubert N, Chretien S, Gisselbrecht S, Lacombe C, Mayeux P. Proteasomes regulate the duration of erythropoietin receptor activation by controlling down-regulation of cell surface receptors. *J Biol Chem*. **275**: 18375-18381 (2000).

Vesey,D.A. *et al.* Erythropoietin protects against ischaemic acute renal injury. *Nephrol. Dial. Transplant.* **19**, 348-355 (2004).

Vittori,D., Pregi,N., Perez,G., Garbossa,G. & Nesse,A. The distinct erythropoietin functions that promote cell survival and proliferation are affected by aluminum exposure through mechanisms involving erythropoietin receptor. *Biochim. Biophys. Acta* **1743** , 29-36 (2005).

Wagner KU, Claudio E, Rucker EB 3rd, Riedlinger G, Broussard C, Schwartzberg PL, Siebenlist U, Hennighausen L. Conditional deletion of the Bcl-gene from erythroid cells results in hemolytic anemia and profound splenomegaly. *Development.* **127**: 4949-4958 (2000)

Wakao H, Harada N, Kitamura T, Mui AL, Miyajima A. Interleukin 2 and erythropoietin activate STAT5/MGF via distinct pathways. *EMBO J.* **14**: 2527-2535 (1995)

Walensky LD. BCL-2 in the crosshairs: tipping the balance of life and death. *Cell Death Differ.* **13**: 1339-1350 (2006).

Wang GL, Semenza GL. General involvement of hypoxia-inducible factor 1 in transcriptional response to hypoxia. *Proc Natl Acad Sci U S A.* **90**: 4304-4308 (1993)

Wang J, Wei Q, Wang CY, Hill WD, Hess DC, Dong Z. Minocycline up-regulates Bcl-2 and protects against cell death in mitochondria. *J Biol Chem.* **279**: 19948-19954 (2004).

Warnecke C, Zaborowska Z, Kurreck J, Erdmann VA, Frei U, Wiesener M, Eckardt KU. Differentiating the functional role of hypoxia-inducible factor (HIF)-1alpha and HIF-2alpha (EPAS-1) by the use of RNA interference: erythropoietin is a HIF-2alpha target gene in Hep3B and Kelly cells. *FASEB J.* **18**: 1462-1464 (2004)

Watanabe,D. *et al.* Erythropoietin as a retinal angiogenic factor in proliferative diabetic retinopathy. *N. Engl. J. Med.* **353**, 782-792 (2005).

Weaver WD, Simes RJ, Betriu A, Grines CL, Zijlstra F, Garcia E, Grinfeld L, Gibbons RJ, Ribeiro EE, DeWood MA, Ribichini F. Comparison of primary coronary angioplasty and intravenous thrombolytic therapy for acute myocardial infarction: a quantitative review. *JAMA.* **278**: 2093-2098 (1997).

Westenfelder C, Baranowski RL. Erythropoietin stimulates proliferation of human renal carcinoma cells. *Kidney Int.* **58**: 647-657 (2001)

Westenfelder,C., Biddle,D.L. & Baranowski,R.L. Human, rat, and mouse kidney cells express functional erythropoietin receptors. *Kidney Int.* **55**, 808-820 (1999).

Wetzels JF, Yu L, Wang X, Kribben A, Burke TJ, Schrier RW. Calcium modulation and cell injury in isolated rat proximal tubules. *J Pharmacol Exp Ther*. **267**: 176-180 (1993)

Williams P, Lopez H, Britt D, Chan C, Ezrin A, Hottendorf R. Characterization of renal ischemia-reperfusion injury in rats. *J Pharmacol Toxicol Methods*. **37**: 1-7 (1997)

Winearls CG, Oliver DO, Pippard MJ, Reid C, Downing MR, Cotes PM. Effect of human erythropoietin derived from recombinant DNA on the anaemia of patients maintained by chronic haemodialysis. *Lancet*. **2**: 1175-1178 (1986)

Witthuhn,B.A. *et al.* JAK2 associates with the erythropoietin receptor and is tyrosine phosphorylated and activated following stimulation with erythropoietin. *Cell* **74**, 227-236 (1993).

Witzgall,R., Brown,D., Schwarz,C. & Bonventre,J.V. Localization of proliferating cell nuclear antigen, vimentin, c-Fos, and clusterin in the postischemic kidney. Evidence for a heterogenous genetic response among nephron segments, and a large pool of mitotically active and dedifferentiated cells. *J. Clin. Invest* **93**, 2175-2188 (1994).

Wright GL, Hanlon P, Amin K, Steenbergen C, Murphy E, Arcasoy MO. Erythropoietin receptor expression in adult rat cardiomyocytes is associated with an acute cardioprotective effect for recombinant erythropoietin during ischemia-reperfusion injury. *FASEB J*. **18**: 1031-1033 (2004)

Woroniecki R, Ferdinand JR, Morrow JS, Devarajan P. Dissociation of spectrin-ankyrin complex as a basis for loss of Na-K-ATPase polarity after ischemia. *Am J Physiol Renal Physiol.* **284**: F358-364 (2003).

Wu H, Lee SH, Gao J, Liu X, Iruela-Arispe ML. Inactivation of erythropoietin leads to defects in cardiac morphogenesis. *Development* **126**: 3597-3605 (1999).

Wu H, Liu X, Jaenisch R, Lodish HF. Generation of committed erythroid BFU-E and CFU-E progenitors does not require erythropoietin or the erythropoietin receptor. *Cell.* **83**: 59-67 (1995)

Yamamoto, T. *et al.* Intravital videomicroscopy of peritubular capillaries in renal ischemia. *Am. J. Physiol Renal Physiol* **282**, F1150-F1155 (2002).

Yamasaki M, Mishima HK, Yamashita H, Kashiwagi K, Murata K, Minamoto A, Inaba T. Neuroprotective effects of erythropoietin on glutamate and nitric oxide toxicity in primary cultured retinal ganglion cells. *Brain Res*. **1050**: 15-26 (2005)

Yang,C.W. *et al.* Preconditioning with erythropoietin protects against subsequent ischemia-reperfusion injury in rat kidney. *FASEB J*. **17**, 1754-1755 (2003).

Yasuda Y, Masuda S, Chikuma M, Inoue K, Nagao M, Sasaki R. Estrogen-dependent production of erythropoietin in uterus and its implication in uterine angiogenesis. *J Biol Chem.* **273**: 25381-25387 (1998)

Yatsiv,I. *et al.* Erythropoietin is neuroprotective, improves functional recovery, and reduces neuronal apoptosis and inflammation in a rodent model of experimental closed head injury. *FASEB J*. **19**, 1701-1703 (2005).

Yildirim, E. *et al.* Protective effect of erythropoietin on type II pneumocyte cells after traumatic brain injury in rats. *J. Trauma* **58**, 1252-1258 (2005).

Yokomizo R, Matsuzaki S, Uehara S, Murakami T, Yaegashi N, Okamura K. Erythropoietin and erythropoietin receptor expression in human endometrium throughout the menstrual cycle. *Mol Hum Reprod*. **8**: 441-446 (2002)

Yoshimura A, Zimmers T, Neumann D, Longmore G, Yoshimura Y, Lodish HF. Mutations in the Trp-Ser-X-Trp-Ser motif of the erythropoietin receptor abolish processing, ligand binding, and activation of the receptor. *J Biol Chem*. **267**: 11619-11625 (1992)

Ysebaert, D.K. *et al.* Identification and kinetics of leukocytes after severe ischaemia/reperfusion renal injury. *Nephrol. Dial. Transplant.* **15**, 1562-1574 (2000).

Ysebaert,D.K. *et al.* T cells as mediators in renal ischemia/reperfusion injury. *Kidney Int.* **66**, 491-496 (2004).

Zager,R.A., Gmur,D.J., Bredl,C.R., Eng,M.J. & Fisher,L. Regional responses within the kidney to ischemia: assessment of adenine nucleotide and catabolite profiles. *Biochim. Biophys. Acta* **1035**, 29-36 (1990).

Zanardo, G. *et al.* Acute renal failure in the patient undergoing cardiac operation. Prevalence, mortality rate, and main risk factors. *J. Thorac. Cardiovasc. Surg.* **107**, 1489-1495 (1994).

Zhang X, Zheng X, Sun H, Feng B, Chen G, Vladau C, Li M, Chen D, Suzuki M, Min L, Liu W, Garcia B, Zhong R, Min WP. Prevention of renal ischemic injury by silencing the expression of renal caspase 3 and caspase 8. *Transplantation*. **82**: 1728-1732 (2006)

Zhao R. *et al.* Identification of an acquired JAK2 mutation in polycythemia vera. *J. Biol. Chem.* **280**, 22788-22792 (2005).

Zhao W, Kitidis C, Fleming MD, Lodish HF, Ghaffari S. Erythropoietin stimulates phosphorylation and activation of GATA-1 via the PI3-kinase-AKT signaling pathway. *Blood* **107**: 907-915 (2006).

Zhou H, Miyaji T, Kato A, Fujigaki Y, Sano K, Hishida A. Attenuation of cisplatin-induced acute renal failure is associated with less apoptotic cell death. *J Lab Clin Med*. **134**: 649-658 (1999)